













Université du Québec  
à Rimouski

**PRODUCTION DE MÉTHANE DANS LES SOLS CÔTIERS  
DE L'ARCTIQUE CANADIEN EN CONTEXTE DE  
SUBMERSION OCÉANIQUE (TUKTOYAKTUK,  
TERRITOIRES DU NORD-OUEST)**

Mémoire présenté

dans le cadre du programme de maîtrise en océanographie  
en vue de l'obtention du grade de maître ès sciences (M. Sc)

PAR

© ALEXIE ROY-LAFONTAINE

**Novembre 2024**



**Composition du jury :**

**Stephanie Kusch, présidente du jury, Université du Québec à Rimouski (UQAR)**

**André Pellerin, directeur de recherche, UQAR**

**Peter Douglas, codirecteur de recherche, McGill University**

**Julie Lattaud, examinatrice externe, Université Basel**

Dépôt initial le 12 août 2024

Dépôt final le 5 novembre 2024



UNIVERSITÉ DU QUÉBEC À RIMOUSKI  
Service de la bibliothèque

Avertissement

La diffusion de ce mémoire ou de cette thèse se fait dans le respect des droits de son auteur, qui a signé le formulaire « *Autorisation de reproduire et de diffuser un rapport, un mémoire ou une thèse* ». En signant ce formulaire, l'auteur concède à l'Université du Québec à Rimouski une licence non exclusive d'utilisation et de publication de la totalité ou d'une partie importante de son travail de recherche pour des fins pédagogiques et non commerciales. Plus précisément, l'auteur autorise l'Université du Québec à Rimouski à reproduire, diffuser, prêter, distribuer ou vendre des copies de son travail de recherche à des fins non commerciales sur quelque support que ce soit, y compris Internet. Cette licence et cette autorisation n'entraînent pas une renonciation de la part de l'auteur à ses droits moraux ni à ses droits de propriété intellectuelle. Sauf entente contraire, l'auteur conserve la liberté de diffuser et de commercialiser ou non ce travail dont il possède un exemplaire.



*À mon grand-papa, Jacques.*





## REMERCIEMENTS

Au cours de ma maîtrise, mon rapport avec la nature et les changements climatiques ont évolué de manière significative grâce à de nombreuses réflexions et observations. Même si un mémoire de maîtrise ne change pas le monde, cette expérience a profondément transformé ma vie. Je suis reconnaissante d'avoir été accompagnée par des personnes exceptionnelles tout au long de ce parcours, et je tiens à les remercier sincèrement.

Tout d'abord, un chaleureux merci à André, mon superviseur de recherche. Merci d'avoir toujours appuyé mes idées. Merci infiniment pour le temps que tu m'as consacré, pour nos nombreuses discussions enrichissantes, tant scientifiques qu'autres, et pour m'avoir fait sentir à ma place dans l'univers parfois intimidant de la recherche scientifique. Merci pour toutes les opportunités de terrain et de conférences, ces expériences ont forgé mon éthique de travail et ont rendu mon expérience à la maîtrise extraordinaire. Merci à Peter mon codirecteur pour l'accueil dans son laboratoire à McGill et pour l'intégration dans son équipe de recherche. Merci de m'avoir accordé du temps de façon généreuse. Merci pour les conseils, les idées et surtout pour les discussions pertinentes sur les différents aspects du projet.

Merci à mes parents et à mon frère de toujours m'avoir soutenue au travers de mes projets. Merci à vous de m'avoir montré dès mon enfance les beautés de la nature qui nous entoure par nos multiples voyages de camping. Je crois vivement que ma passion pour notre environnement est née de cet immersion.

Merci à mon copain Renaud, mon partenaire d'aventures, de m'inspirer quotidiennement à suivre mes passions et mes envies, qui a mené à la complétion d'une maîtrise en océanographie. Merci d'avoir été aussi présent malgré la distance et d'avoir su m'écouter, m'encourager et me conseiller dans les moments plus difficiles. Merci à mes amies de Rimouski, Éléonore, Carole-Anne, Ariane, Jeanne et Charlotte. Je suis chanceuse d'avoir pu trouver des amies comme vous lors de mon passage dans le Bas du fleuve. Merci pour les discussions toujours pertinentes, de m'avoir épaulé lors des moments plus difficiles

et surtout de m’ avoir transmis vos précieuses connaissances R. Merci pour les milles soupers, apéros, couchers de Soleil, courses à pied, sorties à vélo, sorties de ski et sessions de travail. Votre amitié a rendu Rimouski encore plus belle. Merci à mes GoldRush Girls, Rose-Marie, Madeleine et Danielle pour l’ incroyable road trip post-conférence ICOP2024 à bord de notre BigHorn dans le Yukon. Cette dernière aventure avant le dépôt de mon mémoire a su me donner une poussée de motivation pour le sprint final.

Merci à Santiago pour ton aide précieuse lors de ton passage dans notre équipe et à Daniel pour le retour toujours pertinent et constructif sur mes travaux. Merci à toutes les personnes que j’ ai rencontré au cours des missions de terrain à Tuktoyaktuk (Bernardo, Rebecca, Madie, Blanda, Julie, Matt, Angus, Mike et Paul) d’ avoir rendu mon passage dans l’ Arctique canadien plus divertissant, mais surtout enrichissant. Merci à Dustin de nous avoir accueilli dans son équipe et de nous avoir transmis sa passion pour la communauté de Tuk. Merci pour les beaux moments que je n’ oublierai jamais. *Quyanainni* à Noel, Robbie, Obie et Dawson, nos guides et moniteurs de faune, d’ avoir assuré notre sécurité mais, surtout pour le partage de vos connaissances et traditions Inuvialuit. *Quyanainni* à la communauté de Tuk d’ avoir accueilli le projet dans leur magnifique village côtier.

Finalement, je tiens à remercier les diverses institutions financières qui ont contribué à la réalisation de ce projet et à mon parcours académique à la maîtrise. Je remercie le Conseil de Recherche en Sciences Naturelles et en Génie du Canada (CRSNG) d’ avoir financé ce projet. Merci au Centre de Recherche sur la Dynamique du Système Terre (Geotop) pour leur soutien financier par une bourse de mobilité pour la réalisation d’ analyses au McGill Isotope Biogeochemistry Lab ainsi que pour l’ octroi d’ une bourse financière pour ma 2<sup>e</sup> année de maîtrise. Merci à l’ UQAR pour le soutien financier lors d’ ICOP 2024 par l’ octroi d’ une bourse de mobilité. Je remercie également le Programme de Formation Scientifique dans le Nord (PFSN) d’ avoir soutenu deux campagnes de terrain à Tuktoyaktuk en 2022 et 2023 et merci au Geological Survey of Canada (GSC) d’ avoir soutenu financièrement les opérations sur le terrain. Sans le soutien de ces institutions, le projet n’ aurait pas été possible.



## AVANT-PROPOS

Les résultats de cette maîtrise s'insèrent dans le programme *Nuna – Changing ground conditions, Community resilience, technical solutions*, qui a pour objectif de développer des solutions multidisciplinaires afin de prévenir et de mitiger les impacts des changements climatiques à Tuktoyaktuk ainsi que de développer des stratégies d'adaptation adaptées. Les techniques mises d'avant par le programme incluent la co-création, les solutions à faibles coûts et basées sur la Nature afin de créer des écosystèmes résilients et des populations adaptées aux changements environnementaux rapides. Le projet de recherche présenté dans ce mémoire visait à évaluer les dynamiques biogéochimiques de la production de méthane dans les sédiments et sols côtiers de Tuktoyaktuk dans les Territoires du Nord-Ouest.

Ce mémoire est présenté en deux chapitres. Le premier chapitre est présenté sous forme d'article scientifique en anglais intitulé : « *Addition of brackish water to tundra soils does not inhibit methane production : implications for coastal subsidence* ». Cet article sera soumis à la revue *Global Change Biology* lors de la session d'automne 2024. En tant que première auteure, j'ai contribué à l'ensemble de la recherche bibliographique et au développement de la question de recherche, à l'échantillonnage, au développement des méthodes d'échantillonnage et d'analyses, j'ai réalisé et participé à l'ensemble des analyses en laboratoire, à l'interprétation des données ainsi qu'à la rédaction. Rebecca Lee, deuxième auteure, a réalisé les cartes géographiques et les analyses spatiales. Le professeur Peter Douglas a conseillé sur les analyses isotopiques, a participé à l'interprétation des résultats et a participé à la révision de l'article. Dustin Whalen a fourni du soutien technique, logistique et financier lors des missions sur le terrain et a aussi participé à la révision de l'article. Finalement, le professeur André Pellerin a fourni l'idée originale, a participé à l'échantillonnage, au développement de la méthode et a participé à la rédaction de l'article. Une version de l'article a été présentée sous forme d'affiche scientifique à l'International

Conférence on Permafrost à Whitehorse au Yukon, du 16 au 20 juin 2024. Le résumé étendu revu par les pairs de cette conférence, publié dans « *ICOP2024 Proceedings* » est présenté à l'Annexe 1.

Le deuxième chapitre de ce mémoire est également présenté sous forme d'article scientifique rédigé en anglais, intitulé : « *Addition of Brackish Water to Thawed Permafrost does not Inhibit Methane Production* ». Cet article n'est pas destiné à une publication scientifique tel quel, puisque le jeu de données est incomplet. Il sera complété durant les années 2024 et 2025 et sera intégré dans une publication scientifique. En tant que première auteure, j'ai effectué la revue de littérature, j'ai participé au développement de la méthode, j'ai participé à l'échantillonnage, j'ai réalisé et participé à l'ensemble des analyses en laboratoire, à l'interprétation des résultats ainsi qu'à la rédaction. Le professeur Peter Douglas, deuxième auteur, a conseillé sur les analyses isotopiques, a participé à l'interprétation des résultats et a participé à la révision de l'article. Dustin Whalen a fourni du soutien technique, logistique et financier lors des missions sur le terrain. Finalement, le professeur André Pellerin a fourni l'idée originale, a participé à l'échantillonnage, au développement de la méthode et a participé à la rédaction de l'article.

Les données présentées dans ce mémoire sont issues de deux campagnes d'échantillonnage dans la région de Tuktoyaktuk en août 2022 et 2023. Ces campagnes ont permis la préparation de plus de 200 incubations pour les mesures de concentrations en CH<sub>4</sub> et des analyses de la signature isotopique du <sup>13</sup>C-CH<sub>4</sub>. J'ai pu aller effectuer les analyses isotopiques au *McGill Isotope Biogeochemistry Lab* du professeur Peter Douglas. De plus, la quantification du Cl<sup>-</sup>, du SO<sub>4</sub><sup>2-</sup>, du NO<sub>3</sub><sup>-</sup> et les analyses élémentaires (%TOC, %AT, <sup>13</sup>C, <sup>15</sup>N) de plus de 68 échantillons de sols ont été effectués.

Au cours de ma maîtrise, j'ai pu m'impliquer dans d'autres projets connexes en océanographie, qui m'ont permis d'élargir et d'approfondir mes connaissances. D'abord, j'ai pu participer activement à la préparation et à la réalisation de la mission C-2022-01 à bord du Coriolis II du 16 au 22 mai 2022. J'ai participé au carottage et à l'extraction des échantillons à bord du navire pour un projet en lien avec les dynamiques de l'hypoxie dans

l'estuaire du Saint-Laurent. À la suite de la mission, j'ai effectué les analyses de métaux et d'éléments dans les eaux porales des échantillons récoltés. J'ai également fait les analyses de carbone inorganique dissous au laboratoire de géochimie des isotopes stables légers du Geotop-UQAM. Ces résultats sont intégrés au mémoire de maîtrise de Gwenn Duval. Ensuite, j'ai participé à l'ouverture d'environ 10 sections de carottes sédimentaires récoltées lors de la mission PeCabeau 2021 dans la mer de Beaufort. Pour chacune des sections, j'ai procédé à la description visuelle des sédiments et au scan par spectrométrie de fluorescence des rayons X (XRF). Finalement, j'ai eu l'opportunité de participer à une 3<sup>e</sup> campagne de terrain à Tuktoyaktuk dans le cadre du projet FLOCHAR - *Fluxes from Land to Ocean : How Coastal Habitats in the Arctic Respond*, mené par l'Institut de recherche allemande Alfred-Wegener. J'ai participé à la préparation et à l'envoi du matériel d'échantillonnage, j'ai activement participé à la récolte des échantillons ainsi qu'à la préparation et à l'extraction des échantillons sur le terrain.

Le travail lié à mon projet de recherche et à mes implications externes a mené à des présentations par affiche à divers congrès :

**Roy-Lafontaine, A.,** Lee, R., Douglas, PMJ., Whalen, D. et Pellerin, A. *Unlocking Microbial Methane Dynamics in Thawing Coastal Permafrost (Tuktyoaktuk, NWT)*. 16-20 juin 2024, International Conference on Permafrost, Whitehorse (Yukon).

**Roy-Lafontaine, A.,** Lee, R., Douglas, PMJ., Whalen, D. et Pellerin, A. *Unlocking Microbial Methane Dynamics in Thawing Coastal Permafrost (Tuktyoaktuk, NWT)*. 22-24 mars 2024, Congrès Annuel du Geotop, Québec (Québec).

Duval, G., **Roy-Lafontaine, A.,** Chaillou, G., Montero Serrano et Pellerin, A. *Tracing Hypoxia with the Sulfur Cycle: Study of the St. Lawrence Estuary*. 10-12 mars 2023, Congrès annuel du Geotop, Orford (Québec).

**Roy-Lafontaine, A.**, Whalen, D. et Pellerin, A. *Thawing Permafrost in the Coastal Canadian Arctic (Tuktyoaktuk, NWT): Microbial Dynamics Associated with Methane and Carbon Dioxide Production*. 10-12 mars 2023, Congrès annuel du Geotop, Orford (Québec).

Duval, G., **Roy-Lafontaine, A.**, Chaillou, G., Montero Serrano et Pellerin, A. *Évaluation des flux de carbone et d'azote organique dissous le long d'une coupe transversal dans la zone hypoxique de l'estuaire maritime du Saint-Laurent*. 31 janvier au 3 février 2022, Réunion Scientifique Annuelle de Québec Océan, Rivière-du-Loup (Québec).





## RÉSUMÉ

La subsidence du territoire et la dégradation du pergélisol dans la péninsule de Tuktoyaktuk, Territoires du Nord-Ouest (TNO), entraînent des taux de recul côtiers de plus de -4 m/an. Ce processus contribue à l'augmentation des zones terrestres inondées, créant des conditions propices à la dégradation anaérobie de la matière organique (MO). En milieu submergé, les taux de production de méthane (CH<sub>4</sub>) issus de la dégradation biogénique de la MO sont incertains en raison des interactions complexes entre la MO terrestre et l'eau de mer. L'hypothèse principale de cette recherche est que, dans le contexte de submersion, la production de CH<sub>4</sub> est inhibée par la présence de sulfates dans l'eau de mer, favorisant la sulfato-réduction. L'objectif principal du projet est de proposer une approche expérimentale à l'étude des flux de CH<sub>4</sub> en Arctique côtier, en utilisant des techniques d'incubations couplées à des mesures géochimiques et isotopiques. Plus précisément, le projet vise à 1) identifier les impacts de la connectivité continent-océan sur la production de CH<sub>4</sub> dans les sédiments et les sols de la couche active ainsi que de quantifier cette production et 2) quantifier les taux de production de CH<sub>4</sub> et lors du dégel du pergélisol en contexte de submersion océanique. En août 2022 et 2023, des échantillons de sédiments marins et de sols côtiers ainsi que de sols non-côtiers ont été prélevés dans la région de Tuktoyaktuk, afin de représenter une gradation d'influence marine. Les résultats montrent que la méthanogénèse n'est pas inhibée dans les sols côtiers et non-côtiers malgré la présence de sulfates. Certaines incubations de la couche active côtière ont produit jusqu'à 40 nmol cm<sup>-3</sup> j<sup>-1</sup> de CH<sub>4</sub>. Dans les incubations de pergélisol dégelé et submergé d'eau saumâtre, deux sites similaires ont montré une augmentation des taux de production de CH<sub>4</sub> alors que l'autre site n'a produit aucun CH<sub>4</sub>. Ces résultats contrastants sont potentiellement reliés à la conservation des conditions géochimiques spécifiques de chaque environnement en conditions de pergélisol. Cette étude a permis de démontrer le potentiel des écosystèmes côtiers Arctique à soutenir une communauté microbienne capable de produire du CH<sub>4</sub> en conditions de submersion océanique. Elle souligne également l'importance des conditions géochimiques locales dans l'estimation de la contribution de ces écosystèmes dans les émissions de carbone atmosphérique.

**Mots clés :** Arctique côtier, émissions, méthane, méthanogénèse, pergélisol, isotopes stables, sulfate, submersion côtière, érosion, subsidence terrestre

## ABSTRACT

Land subsidence and permafrost degradation in the Tuktoyaktuk Peninsula, Northwest Territories (NWT), result in coastal erosion rates of -4 m/year. This mechanism contributes to an increase in inundated terrestrial soils, creating conditions favorable to the anaerobic degradation of organic matter (OM). Under submerged conditions, the rates of CH<sub>4</sub> production from microbial degradation of OM are uncertain due to the complex interactions between terrestrial OM and seawater. The primary hypothesis of this research project is that, in submerged conditions, CH<sub>4</sub> production is inhibited by the presence of sulfates in seawater, which promotes sulfate reduction. The main objective of the project is to propose an experimental approach to studying CH<sub>4</sub> fluxes in Arctic coastal regions using incubation techniques combined with geochemical and isotopic measurements. Specifically, the project aims to 1) identify the impacts of continent-ocean connectivity on CH<sub>4</sub> production in the active layer, and 2) quantify CH<sub>4</sub> production rates in thawed permafrost during ocean submersion. In August 2022 and 2023, samples of marine sediments, coastal soils, and inland soils were collected from the Tuktoyaktuk region. Results show that methanogenesis is not inhibited in coastal and inland soils despite the presence of sulfates. Some coastal active layer incubations produced up to 40 nmol cm<sup>-3</sup> day<sup>-1</sup> of CH<sub>4</sub>. In incubations of thawed inland permafrost soils submerged in brackish water, two out of three sites showed increased CH<sub>4</sub> production rates, while one site produced no CH<sub>4</sub>, potentially attributed to the preservation of specific geochemical conditions in permafrost conditions. In summary, this study demonstrated the potential of Arctic coastal ecosystems to support a microbial community capable of producing CH<sub>4</sub> under oceanic submersion and highlighted that local geochemical conditions in permafrost environments are important factors in estimating the contribution of Arctic coastal ecosystems to atmospheric carbon emissions.

**Keywords:** Coastal Arctic, emissions, methane, methanogenesis, permafrost, stable isotopes, sulfate, land submersion, erosion, submersion, land subsidence



## TABLE DES MATIÈRES

REMERCIEMENTS .....	ix
AVANT-PROPOS .....	xii
RÉSUMÉ.....	xvii
ABSTRACT .....	xviii
TABLE DES MATIÈRES .....	xx
LISTE DES TABLEAUX.....	xxiii
LISTE DES FIGURES.....	xxiv
LISTE DES ABRÉVIATIONS, DES SIGLES ET DES ACRONYMES .....	xxviii
INTRODUCTION GÉNÉRALE.....	1
CHAPITRE 1 - L'ADDITION D'EAU SAUMÂTRE N'INHIBE PAS LA PRODUCTION DE MÉTHANE DANS LES SOLS DE LA TOUNDRA ARCTIQUE : IMPLICATIONS POUR LA SUBSIDENCE CÔTIÈRE.....	18
1.1 RESUME EN FRANÇAIS DU PREMIER ARTICLE .....	19
1.2 ADDITION OF BRACKISH WATER TO TUNDRA SOILS DOES NOT INHIBIT METHANE PRODUCTION: IMPLICATIONS FOR COASTAL SUBSIDENCE IN THE ARCTIC.....	20
1.3 INTRODUCTION.....	20
1.4 METHODOLOGY.....	23
1.4.1 Site description and sampling .....	23
1.4.2 Methane production rates in incubations .....	26
1.4.3 Elemental and isotope composition of the sediment.....	27
1.4.4 Stable carbon isotopic composition of methane .....	28
1.4.5 Sulfates and chlorine concentrations in sediments .....	29
1.5 RESULTS.....	29
1.5.1 Soil description and composition.....	29

1.5.2 Methane production.....	32
1.5.3 Isotopic composition of <sup>13</sup> C-CH <sub>4</sub> .....	35
1.6 DISCUSSION .....	36
1.6.1 Addition of brackish water to anoxic incubations did not strongly suppress methanogenesis.....	36
1.6.2 CH <sub>4</sub> production pathways depend on hydrology and organic matter lability.....	40
1.6.3 Active layer methane production rates are comparable to the net CH <sub>4</sub> fluxes measured in similar environments .....	42
1.7 CONCLUSIONS.....	45
1.8 ACKNOWLEDGEMENTS.....	45
1.9 SUPPLEMENTAL INFORMATION .....	46
<b>CHAPITRE 2 – LA PRODUCTION DE MÉTHANE DANS LE PERGÉLISOL DÉGELÉ N’EST PAS INHIBÉE PAR L’AJOUT D’EAU SAUMÂTRE .....</b>	<b>51</b>
2.1 RESUME EN FRANÇAIS DU DEUXIEME ARTICLE.....	52
2.2 ADDITION OF BRACKISH WATER TO THAWED PERMAFROST DOES NOT INHIBIT METHANE PRODUCTION .....	53
2.3 INTRODUCTION .....	53
2.4 METHODOLOGY .....	55
2.4.1 Site description and sampling.....	55
2.4.2 Methane production rates in incubation experiment .....	57
2.4.3 Geochemical analyses on soil samples.....	57
2.4.4 Stable carbon isotopic composition of methane.....	58
2.5 RESULTS .....	58
2.5.1 Soil characterization and geochemical composition .....	58
2.5.2 Incubations methane production rates.....	61
2.5.3 Isotopic composition of <sup>13</sup> C-CH <sub>4</sub> produced in incubations .....	63
2.6 DISCUSSION .....	64
2.6.1 Addition of brackish water to incubations .....	64
2.6.2 A contrasting correlation between TOC and CH <sub>4</sub> production rates .....	65
2.7 CONCLUSION.....	69

2.8 ACKNOWLEDGEMENTS .....	69
CONCLUSION GÉNÉRALE .....	71
PERSPECTIVES.....	73
ANNEXE 1: Methane production in a coastal permafrost region of the Canadian Arctic (Tuktoyaktuk, NWT).....	76
RÉFÉRENCES BIBLIOGRAPHIQUES .....	80

## LISTE DES TABLEAUX

- Table 1.** Séquence des réactions de minéralisation de la MO associées à l'enthalpie libre respective. La méthanogénèse est décrite par deux réactions à substrats distincts. Selon Canfield, 1993 et Leclerc et al., 1995. ....8
- Table 2.** Total methane active layer production in a context of marine submersion from high-centered polygons, low-centered polygons and throughs during growing season applied to the spatial scale of the polygonal landscape of RP. Two samples were taken for the the high-polygon form. The mean active layer depth of the region is 35 cm. The error represents the propagation of the analytical uncertainty. ....44

## LISTE DES FIGURES

<b>Figure 1.</b> Distribution des zones de pergélisol et leurs côtes. Les côtes canadiennes bordant l’océan Arctique sont entièrement constituées de pergélisol (Tirée de Lantuit et al., 2013).....	3
<b>Figure 2.</b> Profil vertical du pergélisol défini par la température (tirée de Palangi et Abyaneh, 2017).....	4
<b>Figure 3.</b> Cycle du carbone dans un environnement de pergélisol (tirée de Margesin, 2008).....	11
<b>Figure 4.</b> Sites d’études de la synthèse pan-Arctique de Treat et al. (2015) sur les études d’incubations anaérobiques dans les biomes boréal et tundra. Les points jaunes correspondent aux localisations géographiques des études (tirée de Treat et al., 2015).....	13
<b>Figure 5.</b> Distribution spatiale des structures de glace massive sur les côtes canadiennes. La péninsule de Tuktoyaktuk est située dans l'encadré rouge (modifiée de Manson et al., 2019).....	14
<b>Figure 6.</b> Variabilité spatiale des processus dominants du recul du trait de côte dans la péninsule de Tuktoyaktuk (tirée de Costa, 2022). ....	15
<b>Figure 7.</b> Schematic representation of polygonal tundra with peat accumulation as seen in continuous permafrost environments. High-centered polygons are associated with drier conditions, while low-centered polygons, troughs and pondlets are associated with humid or water-saturated conditions. Vegetation cover and OM reflect the hydrology of sites. Not to scale.....	21
<b>Figure 8.</b> Map of study area indicating the sampled sites with yellow dots. Harbor site is located in the marine zone, Toker Point site is located in the coastal zone and Reindeer Point site is located in the inland zone.....	24
<b>Figure 9.</b> Total organic carbon and sulfate concentration in sediment or soil from the active layer of different sites in this study. The datasets are separated into two for clarity. The upper part of the figure (panels A and B) displays the data of the marine site Harbor (profile 01 and 02), and the coastal site, Toker Point (profile 07, 08 and 09). The lower part of the figure (panel C	



and D) displays the data from the inland site Reindeer Point (profile 10A, 10B, 10C and 10D). The black horizontal dotted line in each graph represents the permafrost-active layer interface except for the Harbor site, where the active layer is much deeper but not measured. TOC data from Harbor site is not available. A uniform color pattern is used throughout this article.....30

**Figure 10.** CH<sub>4</sub> production in incubations of soil and sediment with brackish water from (a) TP and (b) RP. Each datapoint represent the mean value of three incubations. The error bars equal to the standard deviation of the three separate incubations. Each profile corresponds to a specific landform. At Toker Point (panel A), profile 07 is from a low-centered polygon, profile 08 is from a trough and profile 09 is from a high-centered polygon. At Reindeer point (panel B), profile 10A is from a high-centered polygon, profile 10B is from a trough, profile 10C is from a low-centered polygon and profile 10D is from a high-centered polygon. ....32

**Figure 11.** Total active layer production rates at Toker Point (Coastal) and Reindeer Point (Inland) organized by geomorphological forms of high-centered polygons, low-centered polygons and troughs. High-centered polygons at RP is the mean of two profiles. All other landforms at RP and TP are one profile. The uncertainty on total active layer production rate is propagated from the uncertainty of individual CH<sub>4</sub> production rates, not averages from replicate sites.....34

**Figure 12.** Isotopic composition of CH<sub>4</sub> produced in brackish water incubations from (a) TP and (b) RP. Each datapoint corresponds to the mean value of two or three measurements done on one incubation, depending on the headspace concentration. The dashed vertical lines correspond to in situ ebullition CH<sub>4</sub> collected in pondlets at each sampling site (n=1). These values give information on the pathways used by the soil microbes to produce CH<sub>4</sub>. δ<sup>13</sup>C between -65‰ and -50‰ is typically associated with acetoclastic methanogenesis, while δ<sup>13</sup>C between -110‰ and -60‰ is associated with hydrogenotrophic methanogenesis (Hornibrook et al., 1997, 2000). The error bar on each point represents the analytical uncertainty on the measured value.....35

**Figure 13.** Temporal variability of the lake surrounding RP polygonal ground (North of lake), showcasing stability since 1947.....46

**Figure 14.** Map of Reindeer Point sampling site with delimitation of geomorphological polygonal forms. Forms were drawn based on aerial imagery from 2022.....47

<b>Figure 15.</b> Cl <sup>-</sup> concentrations in (a) Harbor + Toker Point and (b) Reindeer Point sediments used in the incubation experiment. ....	48
<b>Figure 16.</b> δ <sup>13</sup> C of (a) Harbor + Toker Point and (b) Reindeer Point sediments used in the incubation experiment. Values measured within the range of terrestrial OM (Fu et al., 1993). ....	49
<b>Figure 17.</b> CH <sub>4</sub> production rates in marine sediments cores collected from the Harbor. The error bar on measured values represents the standard deviation on the mean of triplicates. ....	50
<b>Figure 18.</b> Pictures of permafrost cores collected in the polygonal patterned ground of Reindeer Point. Active layer section not shown. Panel a) is RP01, b) is RP02 and c) is RP03. ....	56
<b>Figure 19.</b> Vertical distribution of (a) total organic carbon (TOC) and (b) δ <sup>13</sup> C of soils used in the incubation experiment of cores RP01 and RP02. Data for RP03 are not available. The black horizontal dotted line represents the active layer-permafrost interface. Active layer data for RP01 and RP02 were presented in the Chapter 1 of this manuscript. This color scheme is used consistently throughout the manuscript. ....	59
<b>Figure 20.</b> Depth profiles of geochemical analyses conducted on sub-sampled cores used for the incubation experiment. Panel (a) shows chloride concentrations and panel (b) shows sulfate concentrations results from the leaching process. Chloride and sulfate concentrations are expressed in mmol g <sup>-1</sup> wet-weight <sup>-1</sup> . This color scheme is used consistently throughout the manuscript. Data for core RP03 is not available. ....	60
<b>Figure 21.</b> CH <sub>4</sub> production rates in anoxic and water saturated incubations derived from soil collected in cores RP01, RP02 and RP03. Each datapoint represents the mean value of three incubations with the error bar representing the standard deviation on the triplicates. ....	62
<b>Figure 22.</b> Stable carbon isotopic composition of CH <sub>4</sub> produced in soil incubations of RP01 and RP02, collected at Reindeer Point. Each value corresponds to the mean value of two or three measurements done on one incubation, depending on the CH <sub>4</sub> headspace concentration. The error bar on each point represents the analytical uncertainty on the measured value. RP01 had null production in the thawed permafrost, but the incubations contained enough CH <sub>4</sub> to perform the stable carbon isotopes analyses. ....	63
<b>Figure 23.</b> Relationship between CH <sub>4</sub> production rates and TOC content from (a) the active layer and (b) the permafrost at RP01 and RP02. Red circles represent the data from the study conducted in Tuktoyaktuk from Lapham et al. (2020). ....	66



## LISTE DES ABRÉVIATIONS, DES SIGLES ET DES ACRONYMES

<b>AT</b>	Azote total
<b>C</b>	Carbone
<b>FIG</b>	Figure
<b>GC-FID</b>	Chromatographe à phase gazeuse et détecteur à ionisation de flamme <i>(Gas chromatograph Flame ionization detector)</i>
<b>GES</b>	Gaz à effet de serre
<b>MO</b>	Matière organique (OM pour <i>organic matter</i> )
<b>RP</b>	Reindeer Point
<b>SSIM</b>	<i>Small sample introduction module</i>
<b>TNO</b>	Territoires du Nord-Ouest (NWT pour <i>North-West Territories</i> )
<b>TOC</b>	Carbone organique total ( <i>Total organic carbon</i> )
<b>TP</b>	Toker Point
<b>VPDB</b>	Bélemnite de Pee Dee ( <i>Vienna Pee Dee Belemnite</i> )
<b>Wt</b>	<i>Weight</i>
<b>Wweight</b>	<i>Wet weight</i>
<b>XRF</b>	Spectrométrie de fluorescence des rayons X ( <i>X-ray fluorescence</i> )





## INTRODUCTION GÉNÉRALE

### *Environnement côtier dynamique de l'Arctique canadien*

Les côtes de l'océan Arctique canadien sont des milieux de vie importants pour les communautés humaines nordiques. Elles offrent des lieux de subsistance par les activités de chasse et de pêche, et sont également des espaces de transport, de culture et de rassemblement. Puis, en tant qu'écosystèmes naturels riches et diversifiés, elles fournissent des services écosystémiques inestimables (Burn et Kokelj, 2009). Cependant, les portions naturelles et anthropisées de cet écosystème subissent un remodelage accéléré dû aux impacts des changements climatiques actuels (Hjort et al., 2018).

Entre 1979 et 2021, les températures atmosphériques de l'Arctique se sont réchauffées quatre fois plus rapidement que celles du reste du globe (Rantanen et al., 2022). Les projections climatiques prévoient une amplification de ce réchauffement, mais il est complexe d'en déterminer l'impact en raison de la dispersion des données observationnelles, océanographiques et environnementales. Actuellement, la transformation de l'écosystème côtier naturel de l'océan Arctique en réponse à ces changements se manifeste par l'augmentation du niveau marin, par la subsidence du territoire et de la submersion de zones terrestres (Irrgang et al., 2022 ; Lim et al., 2020), par la réduction du couvert de glace hivernal et par l'augmentation des taux d'érosion côtière (AMAP, 2019 ; Irrgang et al., 2022).

La présence de pergélisol continu et discontinu caractérise les structures sédimentaires qui façonnent ces côtes. En effet, le pergélisol recouvre environ 30 à 34% des environnements côtiers du monde, et l'ensemble des côtes canadiennes de l'Arctique est recouvert de pergélisol (Fig 1) (Lantuit et al., 2013). La particularité de ces types de sols réside dans leur gel perpétuel depuis plusieurs milliers d'années (van Huissteden, 2020). La réponse du pergélisol aux changements environnementaux s'observe près de la surface par

l'épaississement de la couche active ; horizon qui dégèle et regèle au rythme des saisons (Fig 2) (Lapham et al., 2020). Le dégel progressif du pergélisol, combiné à l'amplification de l'érosion côtière, entraîne une modification des flux de matière organique (MO) et de la dynamique sédimentaire au sein du continuum continent-océan (Irrgang et al., 2022 ; Tanski et al., 2021). Les zones du littoral Arctique composées de sédiments non consolidés et riches en glace sont particulièrement vulnérables à la dégradation (Are et al., 2008), surtout en saison des eaux libres, où les taux d'érosion varient entre 0,57 m/an et 25 m/an dans certains des endroits les plus vulnérables (Günther et al., 2015 ; Jones et al., 2018 ; Lantuit et al., 2012). La subsidence du territoire et la submersion par l'océan (Lim et al., 2020 ; O'Neill et al., 2023) sont également des mécanismes qui contribuent aux taux de recul des côtes de l'océan Arctique. Lorsque combiné à l'augmentation du niveau marin, l'intrusion d'eau salée dans les sols peut contribuer à la dégradation du pergélisol et à l'amplification des taux d'érosion côtière par dégel latéral (Guimond et al., 2021 ; Irrgang et al., 2022).





**Figure 1.** Distribution des zones de pergélisol et leurs côtes. Les côtes canadiennes bordant l’océan Arctique sont entièrement constituées de pergélisol (Tirée de Lantuit et al., 2013).

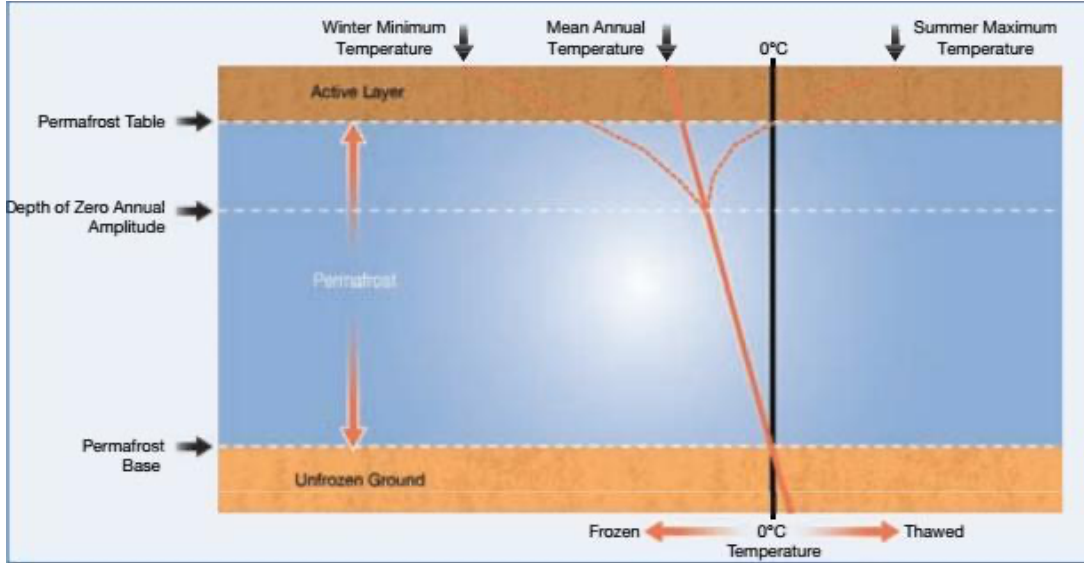


**Figure 2.** Profil vertical du pergélisol défini par la température (tirée de Palangi et Abyaneh, 2017).

Le remodelage actuel de la dynamique sédimentaire côtière de l'Arctique en réponse au réchauffement accéléré des températures atmosphériques entraîne des impacts notoires sur les écosystèmes, sur les cycles biogéochimiques de la région (AMAP, 2017) ainsi que sur les divers processus de dégradation de la MO (Tanski et al., 2021). Les sols pergélisolés de l'hémisphère nord stockent une vaste quantité de carbone organique, estimée à environ 1000 Pg (Mishra et al., 2021). Avec le réchauffement actuel des températures atmosphériques qui mène à l'épaississement de la couche active en saison estivale (Bonnaventure and Lamoureux, 2013), une plus grande portion de ce carbone est dégelée et disponible pour le transport et la décomposition par les microorganismes. Cette décomposition de MO mène à la production de CO<sub>2</sub> et de CH<sub>4</sub>, deux gaz à effet de serre importants, qui participe à l'amplification du réchauffement global des températures atmosphériques (Koven et al., 2011 ; MacDougall et al., 2012). Ainsi, le contexte dynamique actuel et futur des côtes pergélisolées de l'océan Arctique implique une modification des processus entrants et sortants du cycle biogéochimique du carbone, dont certains compartiments restent mal compris.

### ***Décomposition de MO et production de CH<sub>4</sub> en milieu côtier Arctique***

La quantité potentielle de carbone relâchée vers l'atmosphère en réponse au dégel du pergélisol est surtout influencée par la labilité de la MO (Khury et al., 2020). La labilité de la MO terrestre issue du pergélisol se définit par son potentiel intrinsèque à être transformée, décomposée et minéralisée par les communautés microbiennes présentes dans les sols suivant le dégel et le réchauffement de celle-ci (Haugk et al., 2022 ; van Huissteden, 2022). La MO labile se fait dégrader plus facilement et rapidement que celle qualifiée de réfractaire. La MO qualifiée de réfractaire est dite non accessible ou résistante à la dégradation microbienne rapide, mais elle n'est pas considérée inerte puisqu'elle peut être dégradée et reminéralisée par des processus plus lents (Baltar et al., 2021)

La labilité de la MO est influencée par les conditions climatiques et sédimentaires de l'environnement où le carbone s'est accumulé avant le développement des conditions de pergélisol subséquentes (Holm et al., 2020). Les variables climatiques, telles que les températures atmosphériques et les précipitations, affectent les conditions hydrologiques des sols et le couvert végétal, d'où provient la MO terrestre. Une étude menée par Holm et al. (2020) a mis en évidence l'importance de l'environnement de déposition du carbone organique sur les taux de production de CH<sub>4</sub> du pergélisol nouvellement dégelé. La production de CH<sub>4</sub> était significativement plus élevée dans les échantillons de pergélisol contenant du carbone accumulé lors de stades interglaciaires et interstadaux, caractérisés par des climats avec des températures plus chaudes et des précipitations plus abondantes. Ces conditions climatiques peuvent induire des conditions anoxiques dans les sols, favorisant l'établissement de communautés microbiennes capables de dégrader la MO par processus anaérobiques. Les conditions de gel perpétuel du pergélisol permettent la conservation des substrats organiques et des communautés microbiennes, qui peuvent reprendre leur activité métabolique dans des conditions de dégel et de saturation en eau. L'étude démontre que les taux de production de CH<sub>4</sub> sont fortement corrélés aux conditions paléo-environnementales lors de l'accumulation du carbone organique, qui sont intrinsèques à la labilité de la MO,

plutôt qu'à la quantité de carbone organique et d'azote présente dans les sols (Holm et al., 2020).

Les basses températures moyennes aux hautes latitudes favorisent une plus lente dégradation de la MO contenue dans les sols et une accumulation de MO plus récente (Ping et al., 2015). Conséquemment, plusieurs études ont démontré le caractère labile de la MO contenue dans le pergélisol, ce qui implique qu'elle soit hautement disponible à la dégradation par les microorganismes lors du dégel (Mueller et al., 2015 ; Walter et al., 2006 ; Walter et al., 2007 ; Zimov et al., 2006). En effet, la MO nouvellement dégelée peut être convertie en méthane (CH<sub>4</sub>) et en dioxyde de carbone (CO<sub>2</sub>) par l'entremise des processus de minéralisation de la MO (Van Huissteden, 2020). Cependant, le type de végétation de l'environnement de déposition de la MO peut jouer un rôle crucial sur sa qualité (Van Huissteden, 2020). Par exemple, il est démontré que la MO dérivée de plantes graminoides est plus labile que celle dérivée de plantes arbustives et de sphaignes (Hobbie, 1996 ; Szajdak et al., 2019 ; Van Huissteden, 2020). Les plantes arbustives produisent de la MO riche en composés phénoliques et pauvre en azote, favorisant un recyclage lent des nutriments (Eskelinen et al., 2009).

Dans les eaux océaniques, le réservoir de carbone organique dissous se compose également de portions labiles et réfractaires. Bien que la quantité de carbone organique dissous labile dans les eaux de surface soit relativement faible par rapport à la portion réfractaire, elle est transformée en CO<sub>2</sub> dix fois plus rapidement (Hansell, 2013). Ainsi, dans un contexte de subsidence et de submersion océanique ou d'érosion côtière, lorsque les eaux de surface entrent en contact avec la MO d'origine terrestre et que les communautés microbiennes de ces milieux se mélangent, les processus de dégradation de la MO se complexifient.

Les paramètres qui régulent la production de ces gaz dans les sols terrestres et les sédiments côtiers sont complexes et font intervenir la géochimie locale des environnements concernés (Pellerin et al., 2022). Dans les sédiments marins et côtiers, la respiration microbienne ainsi que la réoxydation d'espèces réduites (Fe<sup>2+</sup>, Mn<sup>2+</sup>, etc.) consomment

rapidement l'oxygène dans les premières couches de la colonne sédimentaire. Puis, en absence d'oxygène, certains accepteurs d'électrons alternatifs à l'oxygène peuvent être utilisés préférentiellement par les microorganismes selon une séquence dictée par le rendement énergétique de la réaction. Suivant la consommation totale d'oxygène, les nitrates ( $\text{NO}_3^-$ ) sont les premières espèces à être consommées. Les oxydes de fer ( $\text{FeOH}_3$ ) et de manganèse ( $\text{MnO}_2$ ) sont les suivantes et finalement les sulfates ( $\text{SO}_4^{2-}$ ) (Hesse et Schacht, 2011). Lorsque toutes ces espèces sont consommées, les MO complexes (ex : cellulose, pectine, chitine) subissent une fermentation qui libèrent une variété d'acides organiques et d'alcools, ainsi que du  $\text{CO}_2$  et du  $\text{H}_2$ . Ces métabolites peuvent ensuite être convertis en  $\text{CH}_4$  (Tableau 1 ; réactions 6 et 7). La méthanogénèse est le seul processus qui assure la décomposition complète de la MO dans l'absence d'oxydants inorganiques (ex :  $\text{O}_2$ ,  $\text{NO}_3^-$ ,  $\text{SO}_4^{2-}$ ,  $\text{Fe}^{3+}$ , etc.) (Conrad, 2020). Selon leur gradient de concentration, les composés réduits produits dans la séquence de minéralisation de la MO advectent dans les sédiments peu profonds ou diffusent dans la colonne sédimentaire profonde. Les composés se font alors réoxyder ou atteignent l'interface eau-sédiment (Seidel et al., 2012).

**Table 1.** Séquence des réactions de minéralisation de la MO associées à l'enthalpie libre respective. La méthanogénèse est décrite par deux réactions à substrats distincts. Selon Canfield, 1993 et Leclerc et al., 1995.

Réaction	DG° (KJ mol <sup>-1</sup> de CH <sub>2</sub> O)
<b>Respiration aérobie (1)</b>	
$\text{CH}_2\text{O} + \text{O}_2 \rightarrow \text{CO}_2 + \text{H}_2\text{O}$	-475
<b>Dénitrification (2)</b>	
$5\text{CH}_2\text{O} + 4\text{NO}_3^- \rightarrow 4\text{HCO}_3^- + \text{CO}_2 + 3\text{H}_2\text{O}$	-448
<b>Réduction des oxydes de manganèse (3)</b>	
$\text{CH}_2\text{O} + 3\text{CO}_2 + \text{H}_2\text{O} + 2\text{MnO}_2 \rightarrow 2\text{Mn}^{2+} + 4\text{HCO}_3^-$	-349
<b>Réduction des oxydes de fer (4)</b>	
$\text{CH}_2\text{O} + 7\text{CO}_2 + 4\text{Fe}(\text{OH})_3 \rightarrow 4\text{Fe}^{2+} + 8\text{HCO}_3^- + 3\text{H}_2\text{O}$	-114
<b>Réduction des sulfates (5)</b>	
$2\text{CH}_2\text{O} + \text{SO}_4^{2-} \rightarrow \text{H}_2\text{S} + 2\text{HCO}_3^-$	-77
<b>Méthanogénèse</b>	
$\text{CH}_3\text{COOH} \rightarrow \text{CH}_4 + \text{CO}_2$ (6)	-31
$4\text{H}_2 + \text{CO}_2 \rightarrow \text{CH}_4 + 2\text{H}_2\text{O}$ (7)	

En contexte de submersion océanique, qui favorise l'intrusion d'eau salée dans les sols (Irrgang et al., 2022), la présence de sulfates ( $\text{SO}_4^{2-}$ ) dans l'eau de mer peut modifier la séquence de consommation des accepteurs d'électrons. Même en faibles concentrations, les sulfates peuvent réduire significativement les processus de méthanogénèse et les repousser plus creux dans la colonne sédimentaire (Oremland et Polcin, 1982). Ainsi, les sulfates introduits dans les sols côtiers peuvent faciliter la production de  $\text{CO}_2$  via la respiration anaérobie (Whelan, 1974). Ces interactions dynamiques sont cruciales dans le contexte du cycle du carbone Arctique, où les émissions de gaz à effet de serre (GES) d'origine biogénique jouent un rôle essentiel. Cependant, la compréhension de ces processus à

l'interface continent-océan demeure incomplète, notamment dans les écosystèmes côtiers des hautes latitudes, où les études sont encore limitées (Tanski et al., 2017). Cette lacune souligne l'importance de recherches approfondies pour quantifier précisément les impacts des changements environnementaux sur les émissions de carbone dans ces régions dynamiques.

La méthanogénèse, processus exclusifs aux archées méthanogènes, utilise principalement deux substrats : l'acétate et le  $H_2/CO_2$  (Conrad, 1999 ; Flanagan et al., 2005 ; Whiticar et al., 1986). La disponibilité de ces substrats, conjuguée à la composition de la communauté microbienne et au type de MO présente dans les sols, détermine les réactions par lesquelles le  $CH_4$  est produit (Heffernan et al., 2022 ; Hodgkins et al., 2014). La méthanogénèse acétoclastique est le processus du clivage de l'acétate (réaction 6, tableau 1), alors que la méthanogénèse hydrogénotrophe est le processus de réduction du  $CO_2$  à l'aide de l'hydrogène (réaction 7, tableau 1) (Conrad, 1999). Les isotopes stables du carbone qui composent le  $CH_4$  produit par ces deux principaux mécanismes biogéniques sont distinctes : la méthanogénèse acétoclastique est associée à des valeurs de  $\delta^{13}C$  situées entre -65‰ et -50‰ alors que la méthanogénèse hydrogénotrophe produit du  $CH_4$  plus appauvri en  $^{13}C$ , avec des valeurs entre -110‰ et -60‰ (Horbibrook et al., 1997). Une proportion plus élevée de méthanogénèse acétoclastique est généralement corrélée à une plus grande labilité et à des apports plus importants de MO fraîche. À l'inverse, une proportion plus élevée de méthanogénèse hydrogénotrophe est liée à des écosystèmes plus anciens qui supporte de la MO plus réfractaire, ou elle peut être observée à des profondeurs plus importantes où l'acétate est présent en moins grandes concentrations (Duddleston et al., 2002 ; Heffernan et al., 2022 ; Prater et al., 2007). La distinction entre les signatures isotopiques associées à la méthanogénèse acétoclastique et hydrogénotrophe permet de mieux comprendre les mécanismes complexes qui régissent la production de  $CH_4$  dans l'optique d'augmenter la précision des modèles mécanistiques (Conrad, 2020). Cependant, certains méthanogènes sont capables de produire du méthane via des voies alternatives, telles que la méthanogénèse méthylotrophe, qui utilise le méthanol comme substrat. Ce processus est associé à des valeurs de  $\delta^{13}C$  qui se situent entre -83‰ et -72‰ (Penger et al., 2012). La plupart des études sur la production de méthane dans les environnements naturels ne prennent en considération que

les processus acétoclastiques et hydrogénotrophes puisque typiquement, la méthanogénèse méthylootrophe ne constituerait que 5 à 10% de la méthanogénèse totale (Penger et al., 2012).

Avant d'atteindre l'atmosphère, le CH<sub>4</sub> produit dans les sols et les sédiments peut être consommé par un amalgame de microorganismes spécifiques via des processus de méthanotrophie aérobie et/ou anaérobie (Fig 3). L'oxydation aérobie du CH<sub>4</sub>, réalisée par des bactéries méthanotrophes, est un processus qui se produit principalement dans les zones oxiqes de la colonne sédimentaire et des sols (Lee et al., 2023 ; Steinsdottir et al., 2022), transformant le CH<sub>4</sub> en CO<sub>2</sub> (Hanson et Hanson, 1996). Dans les sols des hautes latitudes, l'oxydation du CH<sub>4</sub> est fortement influencée par la dynamique de la couche active et du pergélisol. Les variations saisonnières de la température et de l'humidité du sol ainsi que la disponibilité en O<sub>2</sub> et en CH<sub>4</sub> modulent l'activité des méthanotrophes (Kip et al., 2010 ; Lee et al., 2023 ; Knoblauch et al., 2008). Des études et des modèles ont démontré que l'oxydation aérobie du CH<sub>4</sub> pouvait consommer plus de la moitié du CH<sub>4</sub> produit dans les sols (Oh et al., 2020 ; Zheng et al., 2018), réduisant significativement les concentrations de CH<sub>4</sub> émises vers l'atmosphère. En conditions anoxiques, l'oxydation du CH<sub>4</sub> peut également se faire par des consortia d'archées méthanotrophes anaérobiques et par des bactéries sulfato-réductrices, notamment dans les environnements côtiers riches en sulfates (Boetius et al., 2000). Cependant, l'oxydation anaérobie du CH<sub>4</sub> semble avoir un impact limité dans les sédiments de lacs thermokarstiques (Lotem et al., 2023). Les mécanismes d'oxydation comportent encore des incertitudes, alors leur étude approfondie est cruciale pour comprendre et modéliser les contributions nettes des écosystèmes Arctiques aux émissions de GES (Treat et al., 2015).



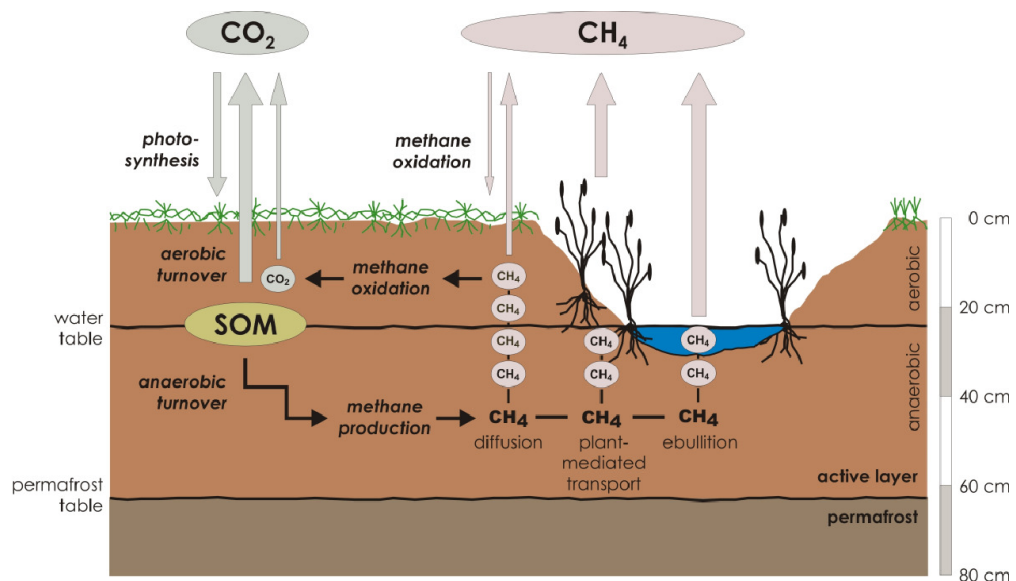


**Figure 3.** Cycle du carbone dans un environnement de pergélisol (tirée de Margesin, 2008).

Vu les implications globales du dégel du pergélisol sur le climat, le monitoring des émissions de  $\text{CH}_4$  et de  $\text{CO}_2$  dans l'Arctique suscite une attention particulière depuis les dernières décennies (Miner et al., 2022), qui implique des investissements et des développements technologiques considérables (Campbell et al., 2022). Bien que ces technologies permettent de mesurer les flux de GES dans les écosystèmes pergélisolés en dégradation (Engram et al., 2020), elles n'en permettent pas une compréhension fondamentale, lesquelles dépendent de caractéristiques locales et micro-topographiques spécifiques (Walter Anthony et al., 2018).

Récemment, des études biogéochimiques du cycle du carbone dans l'Arctique ont permis de quantifier les taux de production de  $\text{CH}_4$  en s'appuyant des paramètres géochimiques et biologiques simples (Pellerin et al., 2022 ; Treat et al., 2015 ; Knaubloch et al., 2021). Bien que les méthodologies varient selon les études, elles utilisent des techniques d'incubation qui consistent généralement à transférer des échantillons de sols prélevés dans des environnements de pergélisol dans des fioles de verre auxquels de l'eau y est ajoutée et l'air y est retirée (remplacée généralement par de l'azote). Ces incubations sont maintenues

à des températures prédéterminées pour une période définie, durant laquelle la production de CH<sub>4</sub> est mesurée. Des analyses géochimiques et parfois isotopiques sont effectuées afin de supporter les résultats de quantification de CH<sub>4</sub>. Ces études (1) offrent une méthode indépendante pour estimer les émissions de GES, (2) pourraient réduire significativement les coûts associés à l'estimation des flux de CH<sub>4</sub> et CO<sub>2</sub> en région Arctique et (3) améliorent la compréhension des processus biogéochimiques du cycle du carbone en liant ces mécanismes aux flux d'émissions de GES. Toutefois, deux problématiques principales subsistent : d'une part, les études d'incubations se concentrent principalement sur les milieux terrestres (Fig 4), introduisant un biais géographique puisque les écosystèmes côtiers présentent des conditions distinctes ; d'autre part, ces études d'incubations utilisent majoritairement de l'eau distillée, alors que l'eau de l'environnement d'échantillonnage contient son propre amalgame de nutriments, d'ions et de MO qui peut influencer les taux de production de CH<sub>4</sub> (Lehmann et Kleber, 2015), ce qui crée un biais méthodologique. Pour améliorer la précision de ces études et contribuer efficacement à l'amélioration des modèles mécanistiques d'estimation des gaz à effets de serre, il est crucial de réduire les biais actuels.

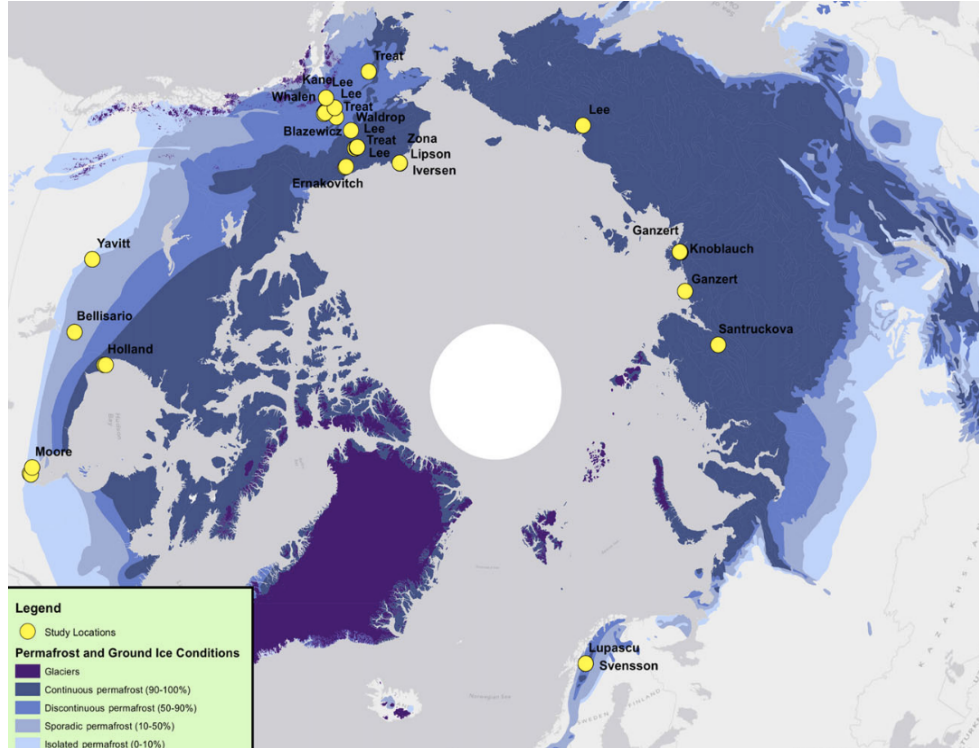


**Figure 4.** Sites d'études de la synthèse pan-Arctique de Treat et al. (2015) sur les études d'incubations anaérobiques dans les biomes boréal et toundra. Les points jaunes correspondent aux localisations géographiques des études (tirée de Treat et al., 2015).

### *Transition côtière de Tuktoyaktuk et décomposition de matière organique*

La péninsule de Tuktoyaktuk, bordée par l'océan Arctique dans les Territoires du Nord-Ouest et habitée par la communauté Inuvialuit de Tuktoyaktuk, est particulièrement affectée par le recul du trait de côte et par l'augmentation du niveau marin (Hansen et al., 2010 ; Hynes et al., 2014). Située dans la zone de pergélisol continue, l'épaisseur moyenne du pergélisol est d'environ 400 m (Hu et al., 2013). Les côtes se caractérisent par des dépôts sédimentaires glaciogéniques non lithifiées avec d'importantes structures de glace massive (Fig 5) (Burn et kokelj, 2009 ; Mackay et Dallimore, 1992 ; Rampton, 1988). Une caractéristique notable de la morphologie côtière de Tuktoyaktuk est la présence de sol

polygonaux et de plaines inondées (Coasta, 2022). Les sols polygonaux sont caractérisés par la présence de coins de glace. Ces sols se forment par la contraction et l'expansion thermique répétée des couches supérieures du pergélisol. Les températures hivernales froides provoquent la contraction du sol, alors que l'expansion estivale remplit les fissures avec de l'eau de fonte, créant des motifs polygonaux (Steedman et al., 2016). En surface, ces polygones apparaissent sous forme de caractéristiques micro-topographiques séparées par des canaux plus bas, souvent humides ou inondés. Les polygones peuvent être classés en deux principaux types : les polygones à bas centre (avec un centre bas et humide et des rebords surélevés) et les polygones à centres surélevés (avec des centres surélevés et des rebords inférieurs bien drainés). Ces formations morphologiques, typiques des environnements de pergélisol riches en glace, présentent de forts gradients thermiques, hydrologiques et géochimiques (Vaughn et al., 2016).

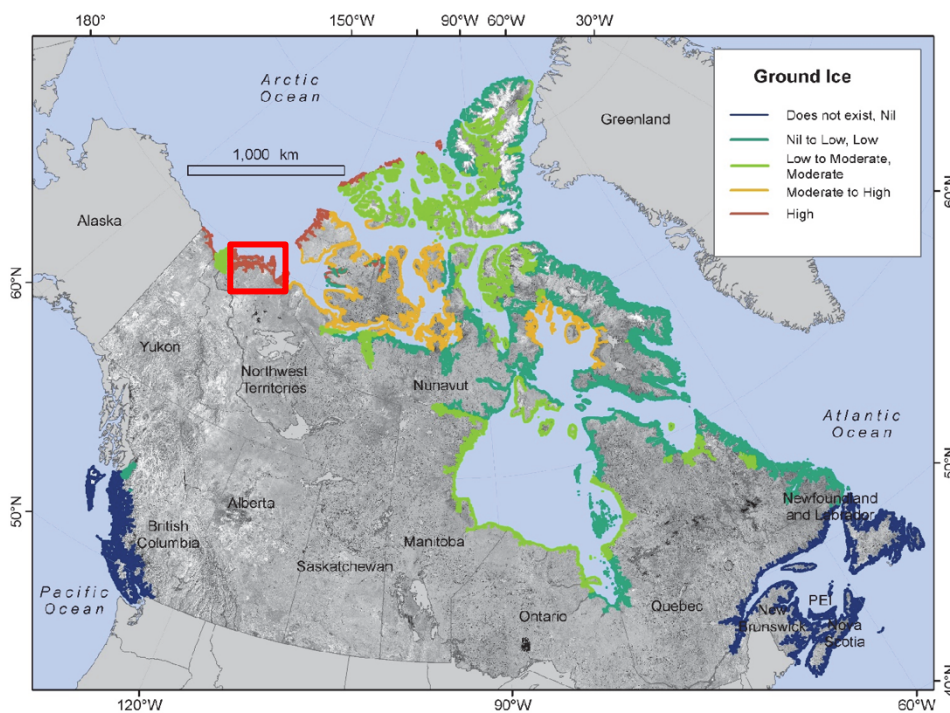


**Figure 5.** Distribution spatiale des structures de glace massive sur les côtes canadiennes. La péninsule de Tuktoyaktuk est située dans l'encadré rouge (modifiée de Manson et al., 2019).

La subsidence du territoire et la submersion par l'océan Arctique (Fig 6) entraînent des taux de recul de plus de 4 m/an dans le paysage côtier de Tuktoyaktuk (Costa, 2022). L'augmentation de la proportion des territoires submergés favorise l'établissement de conditions potentiellement anaérobiques dans les sols, favorisant la décomposition anaérobique de la MO. Cependant, cette dynamique reste peu étudiée dans la région. Une étude de Lapham et al. (2020) sur les processus microbiens de la production de GES biogénique a été menée à Tuktoyaktuk sur une carotte sédimentaire de 12 m récoltée sur une falaise en érosion. L'étude révèle de faibles concentrations de CH<sub>4</sub> *in situ*, avec une présence significative de sulfates et de chlorure dans les premiers 4 m. Les concentrations élevées de sulfates et de chlorure dans les sédiments confirment la connectivité avec la mer de Beaufort (Lapham et al., 2020). Cependant, de très faibles taux de production de CH<sub>4</sub> ont été mesurés lors des incubations, qui ont été réalisés sans ajout d'eau, ne répliquant pas les conditions naturelles d'érosion du territoire que l'étude met d'avant.



**Figure 6.** Variabilité spatiale des processus dominants du recul du trait de côte dans la péninsule de Tuktoyaktuk (tirée de Costa, 2022).

Les facteurs contrôlant la production biogénique de CH<sub>4</sub> dans les environnements de pergélisol de l'hémisphère nord sont multiples et leurs interactions sont complexes. Bien que les mécanismes soient relativement bien compris en milieu terrestre, ils restent encore en suspens en milieu côtier. L'influence du type de MO ainsi, de la composition de la communauté microbienne présente dans les sols, des conditions environnementales dans lesquelles le carbone s'y est accumulé ainsi que des conditions climatiques actuelles, puis la relation avec l'océan sont des facteurs à essentiel à considérer lors de l'évaluation des produits de décomposition de la MO en milieu côtier. Le contexte de transition sédimentaire côtière et le mélange des systèmes terrestres et océaniques soulèvent plusieurs questions : La connectivité continent-océan modifie-t-elle les patrons de production de CH<sub>4</sub> ? Existe-il un facteur principal qui contrôle la production de CH<sub>4</sub> dans le contexte de dégel du pergélisol ? Est-il possible d'établir un schéma général des produits de décomposition de la MO à l'échelle régionale ?

## **Objectifs**

L'objectif principal de l'étude est de proposer une approche expérimentale pragmatique à l'étude des flux de GES biogéniques en provenance de l'Arctique côtier. En utilisant des techniques d'incubations couplées à des mesures géochimiques et isotopiques, nous avons établi un système d'estimation de production de CH<sub>4</sub> biogéniques applicable à l'échelle locale. Plus spécifiquement, l'étude visait à i) identifier les impacts de la connectivité continent-océan sur les patrons de dégradation de la MO ii) identifier les processus biogéniques de la production de CH<sub>4</sub> par analyses isotopiques et lier ces processus aux conditions environnementales observées dans l'écosystème canadien de l'Arctique et iii) quantifier les taux de dégradation de la MO lors du dégel du pergélisol en contexte de submersion océanique.



**CHAPITRE 1 -  
L'ADDITION D'EAU SAUMÂTRE N'INHIBE PAS LA PRODUCTION  
DE MÉTHANE DANS LES SOLS DE LA TOUNDRA ARCTIQUE :  
IMPLICATIONS POUR LA SUBSIDENCE CÔTIÈRE**



## 1.1 RESUME EN FRANÇAIS DU PREMIER ARTICLE

Aux hautes latitudes, plus particulièrement à Tuktoyaktuk (TNO), la subsidence du territoire et la submersion par l'océan Arctique, combinées à l'augmentation de la fréquence des tempêtes, augmentent la surface des zones terrestres inondées. La MO contenue dans ces sols se fait dégrader par les communautés microbiennes par des processus encore incertains, à cause de la relation complexe entre la MO et l'eau de mer. La présence d'eau peut limiter considérablement les apports en oxygène, favorisant la dégradation anaérobie de la MO et produisant du CH<sub>4</sub>. Cependant, la présence de sulfate dans l'eau de mer peut inhiber la production de CH<sub>4</sub> dans les sols et les sédiments. Ainsi, il est encore difficile de déterminer précisément la contribution des écosystèmes côtiers de l'Arctique aux émissions de carbone atmosphériques. Nous présentons ici des taux de production de CH<sub>4</sub> ainsi que des analyses géochimiques et isotopiques issus de sols et de sédiments récoltés dans la péninsule de Tuktoyaktuk. Pour mieux cerner la dynamique de production de CH<sub>4</sub> sous influence marine, des profils de la couche active récoltés dans des sédiments marins, des sols côtiers et des sols non-côtiers ont été transférés dans des incubations anoxiques enrichies en eau saumâtre pour simuler une intrusion océanique. Les taux de production de CH<sub>4</sub> résultants ont été calculés en fonction de l'accumulation de CH<sub>4</sub> dans l'espace de tête des fioles d'incubation. La zone marine présentait des taux de production de CH<sub>4</sub> négligeables, alors que le site intérieur montrait des taux variables entre nuls et 35 nmol cm<sup>-3</sup> j<sup>-1</sup>. La zone côtière avait les taux les plus élevés atteignant 415 nmol cm<sup>-3</sup> j<sup>-1</sup>. L'une des découvertes majeures de cette étude a été la production de CH<sub>4</sub> en taux assez élevés dans les incubations des zones côtières et non-côtières malgré la présence de sulfates dans l'eau saumâtre et dans certains des sols. Les analyses des isotopes stables du carbone du CH<sub>4</sub> produit au cours de l'expérience d'incubation ont indiqué une plus grande acétotrophie. Ce résultat témoigne d'une labilité potentiellement plus élevée de la MO dans la zone côtière, contribuant probablement aux taux de production de CH<sub>4</sub> plus élevés mesurés à cet endroit. Cette étude met en évidence le potentiel d'émissions significatives de CH<sub>4</sub> même avec des concentrations de sulfate allant jusqu'à 17 mmol g<sup>-1</sup> wweight<sup>-1</sup>, suggérant que la salinité n'est pas un indicateur fiable de faible production de CH<sub>4</sub>.

## **1.2 ADDITION OF BRACKISH WATER TO TUNDRA SOILS DOES NOT INHIBIT METHANE PRODUCTION: IMPLICATIONS FOR COASTAL SUBSIDENCE IN THE ARCTIC**

**Roy-Lafontaine, A.<sup>1,3</sup>, Lee, R.<sup>2</sup>, Douglas, P.M.J.<sup>3,4</sup>, Whalen, D.<sup>2</sup>, Pellerin, A.<sup>1</sup>**

<sup>1</sup>Institut des Sciences de la Mer de Rimouski, Université du Québec à Rimouski, Rimouski, Québec, Canada et Centre de recherche Geotop

<sup>2</sup>Geological Survey of Canada, Natural Resources Canada, Halifax, Nova Scotia, Canada

<sup>3</sup>Department of Earth and Planetary Sciences and Geotop Research Centre, McGill University, Montréal, Québec, Canada

<sup>4</sup>Centre d'Études Nordiques, Université Laval, Québec, Québec, Canada

### **1.3 INTRODUCTION**

Arctic coastal ecosystems are impacted by sea level rise, coastal erosion, land submersion, higher frequency in storm events and permafrost degradation (AMAP 2019; Guimond et al., 2021; Irrgang et al., 2022; Lantuit et al., 2013; Lim et al., 2020). The amplification of coastal environmental changes has impacts on biogeochemical cycles (AMAP, 2017; Regnier et al., 2013) and on organic matter (OM) degradation processes and fluxes at the land-ocean continuum (Tanski et al., 2021). Furthermore, the progressive thawing of permafrost exposes long frozen organic matter to microbial decomposition (Lapham et al., 2020; Pellerin et al., 2022; Schuur et al., 2015), leading to the release of greenhouse gases like carbon dioxide (CO<sub>2</sub>) and methane (CH<sub>4</sub>). Inputs and outputs of the Arctic carbon biogeochemical cycle are known to be reshaped by rapid environmental changes (Couture et al., 2018), but processes in coastal settings are still poorly understood.

Rates of coastal change vary according to the morphology of coastal landscapes (Manson et al., 2005). The average rate of land retreat measured in the Tuktoyaktuk Coastlands (North-West Territories, Canada) between 1985 and 2020 was -1.06 m/yr, while processes of ground subsidence and submersion induced retreat rates higher than -4 m/yr

(Costa, 2022) which can inundate large swaths of land rapidly. Inundated tundra flats and polygons are widespread landforms in the landscape (Costa, 2022). Polygon tundra is characterized by ice-wedge polygons, which are formed by the repeated thermal contraction and expansion of the upper layers of the permafrost (Steedman et al., 2016). At the surface, the polygons are expressed as microtopographic features separated by lower-lying, often wet or inundated channels called troughs (Fig 7). Polygons can be classified as low-centered (with a low, wet center and raised rims) or as high-centered (with well-drained centers and lower well-drained rims) (Fig 7), exhibiting strong thermal, hydrological and geochemical gradients (Vaughn et al., 2016).

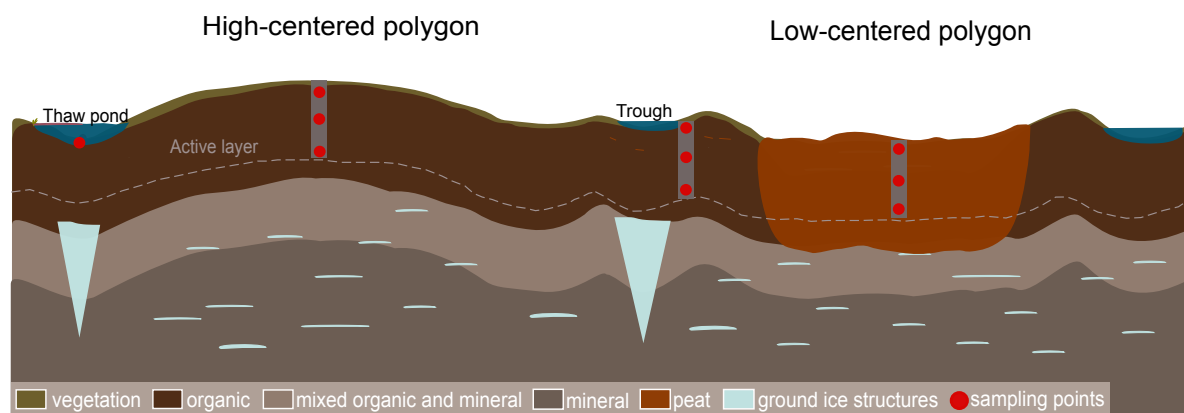


**Figure 7.** Schematic representation of polygonal tundra with peat accumulation as seen in continuous permafrost environments. High-centered polygons are associated with drier conditions, while low-centered polygons, troughs and pondlets are associated with humid or water-saturated conditions. Vegetation cover and OM reflect the hydrology of sites. Not to scale.

Hydrological conditions in polygons play a pivotal role in shaping the pathways of OM decomposition and consequently influence the resulting CO<sub>2</sub> and CH<sub>4</sub> production. Well drained oxic conditions allow microbes to decompose OM rapidly, leading to the production of CO<sub>2</sub> (Jones et al., 2020). Conversely, water saturation restricts oxygen availability, promoting anaerobic respiration and fermentation, thus inducing both CO<sub>2</sub> and CH<sub>4</sub> production (Lipson et al., 2012; Turetsky et al., 2008). Thus, coastal changes can swiftly alter

water saturation conditions in polygons, in many cases significantly enhancing fermentation and thus CH<sub>4</sub> production (Elberling et al., 2013; Holm et al., 2020; Treat et al., 2015).

Furthermore, coastal changes can also influence the chemistry of the water within soils which can affect OM degradation. In anaerobic conditions, OM degradation follows a sequence of electron acceptors of decreasing energetic yields with nitrate, manganese oxides, iron oxides and sulfate as the most abundant electron acceptors (Froelich et al., 1979). It is when all alternative electron acceptors are depleted that fermentation takes place, leading to the production of CH<sub>4</sub>; methanogenesis. For example, in beach, estuarine mudflats and marsh mudflats on the Brittany coast (France), OM degradation is dominated by sulfate reduction; the abundance sulfate from seawater inhibits methanogenesis through competitive inhibition (Winfrey and Ward, 1983). By contrast, OM degradation in sediments below thermokarst lakes, which are anoxic and devoid of alternative electron acceptors, is completely dominated by methanogenesis (Sepulveda-Jauregui et al., 2015). The aqueous chemistry therefore plays a critical role in determining OM degradation. CH<sub>4</sub> produced in soils or sediments can also be anaerobically oxidized by anaerobic methanotrophic archaea and sulfate-reducing bacteria (Boetius et al., 2003; La et al., 2022) present in the soils or sediment, contributing to lower CH<sub>4</sub> emissions in coastal environments. Thus, on or near the coast, the interaction with seawater, which contains electron acceptors such as sulfate, can shift the OM mineralization pathway and the resulting CO<sub>2</sub> and CH<sub>4</sub> productions. Consequently, a nuanced understanding of biogeochemical processes and their drivers is paramount in determining the magnitude of permafrost carbon emissions, especially from coastal environments.

Numerous CH<sub>4</sub> emissions monitoring programs are in operation, but remote-sensing methods lack the ability to comprehensively capture the microbial, biogeochemical and environmental processes involved. In specific regions, estimates of methane production from the breakdown of OM is possible by carefully studying degradation pathways and rates (Pellerin et al., 2022; Heslop et al., 2015; Knoblauch et al., 2018; Treat et al., 2014). To reduce the knowledge gap of CH<sub>4</sub> biogeochemistry in coastal permafrost settings, we collected material from the active layer for incubation experiments, which were coupled to

physical and chemical characterizations. The main objective of this study was to assess microbial CH<sub>4</sub> production dynamics in a coastal permafrost setting and apply it at the landscape level, since methane production is well documented in inland thermokarst but is not well understood in a land-ocean interaction context. We hypothesized that methanogenesis in coastal active layer incubations would be suppressed by the addition of sulfate. Consequently, we discuss the influence of environmental conditions on microbial CH<sub>4</sub> production with an emphasis on brackish water addition in coastal soils and sediments along with the microbial pathways involved. We then apply these results at the landscape level to provide a quantification estimate of CH<sub>4</sub> production in the polygonal patterned ground of the Tuktoyaktuk landscape.

## **1.4 METHODOLOGY**

### **1.4.1 Site description and sampling**

Tuktoyaktuk (69°26'24'' N, 133°01'52''W) is located in the Inuvik region of the North-West Territories, adjacent to the Arctic Ocean in the Kugmallit Bay, east of the Mackenzie Delta. The region experiences prolonged cold winters, short cool summers, and year-round low precipitation, fostering low-arctic tundra vegetation. Lying in the continuous permafrost zone, its coastal areas feature thick Quaternary and glaciogenic unconsolidated deposits (Rampton, 1988), where permafrost thickness averages 400 m (Hu et al., 2013) and is characterized by prevalent ground ice structures (Mackay and Dallimore, 1992; Martin et al., 2018; Murton, 1996; Rampton, 1988). The area has been ice-free for the past 13 000 years, with evidence indicating that early Holocene summer temperatures were up to 6°C warmer than today, fostering vegetation and peat accumulation (Dallimore et al., 1997; Vardy et al., 1997). During that same period, sea level was considerably lower than it is today and the Tuktoyaktuk area was located approximately 100 km inland (Vardy et al., 1997). Currently, ground subsidence and coastal erosion are major causes of rapid land retreat (Hynes et al., 2014; Lapham et al., 2020; Lim et al., 2020). Combined with sea level rise (Hill et al., 1993), it is projected that a substantial amount of terrestrial soil will become part of the

ocean seafloor either by erosion and deposition or by subsidence of land and submersion. Over the past 15 years, extensive studies on Tuktoyaktuk's coastal environment, driven by the region's vulnerability to climate change, highlighted challenges for the Inuvialuit population relying on hunting, fishing, trapping and harvesting (Andrachuk and Smit, 2012).

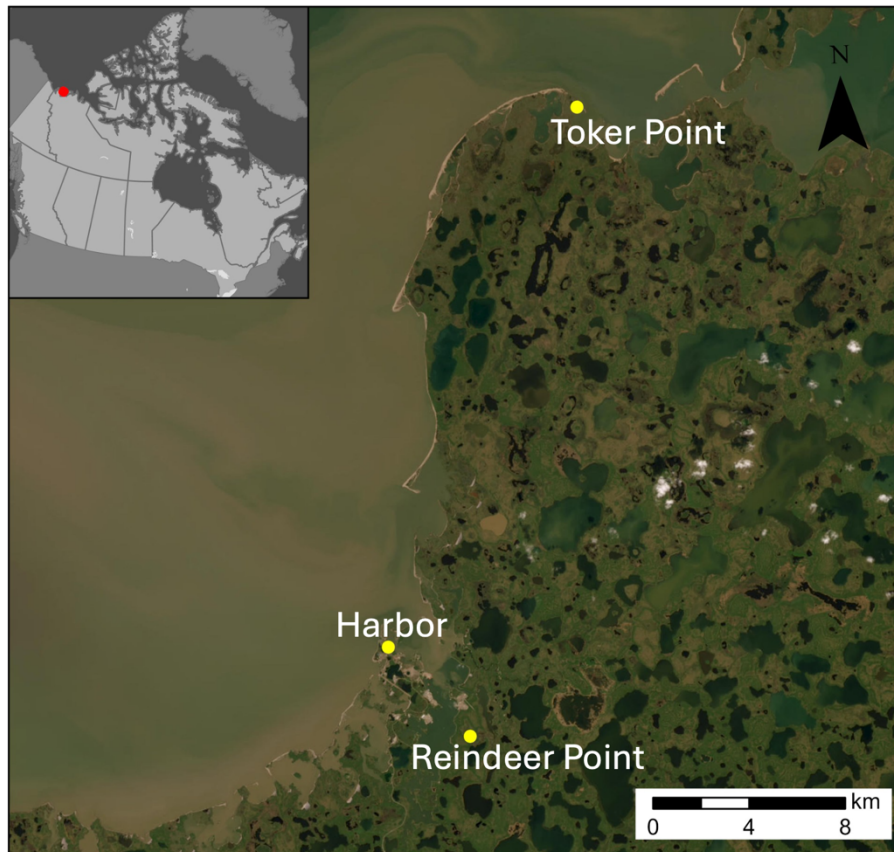


**Figure 8.** Map of study area indicating the sampled sites with yellow dots. Harbor site is located in the marine zone, Toker Point site is located in the coastal zone and Reindeer Point site is located in the inland zone.

Active layer samples were collected from three sites: an inland site, Reindeer Point (RP), a coastal site, Toker Point (TP) and a marine site, Harbor. RP was selected as the inland site because it features a polygonal patterned ground typical of the region, and is located in a stable region not affected by coastal processes such as storm surges, tides, seawater intrusion, erosion etc. The thermokarst lake margin about 300m south of RP has remain unchanged since aerial photos began recording the evolution of the landscape in 1947 (Fig

13). TP was selected as the coastal site because of the strong coastal processes such as tides, storm surge and seawater intrusion at play in this polygonal patterned ground, strongly influenced by ground subsidence. The Harbor site was selected about 400 m offshore in the Harbor of Tuktoyaktuk where cold marine bottom waters are overlain at about 10m depth by a surface brackish water layer. The water depth was 20 m. The sediment consisted of recently deposited silty sands originating from the strong erosional processes occurring in the region (Whalen et al., 2022). The site was accessible by small watercraft. At RP and TP sites, the soil profiles were extracted from the active layer using a shovel. To retain an intact stratigraphic relationship, samples were taken from the wall of the soil pit. At the Harbor site, sediments were collected using a UWITEC gravity corer. Biogenic ebullition gases were collected from pondlets at RP and TP. Pondlets were located within sampled polygonal patterned ground and are defined as small (1 to 3 m<sup>2</sup>) and shallow standing bodies of water, potentially draining seasonally. Samples were trapped using a plastic funnel attached to a 20 mL glass vial. Surface soil lying at the bottom of the pondlets (fig 7) were poked until the vial was filled with gas. Once full, vials were crimped with 20 mm butyl rubber stoppers and aluminum caps. Samples were kept frozen until the time of analyses.

The inland site, (RP), was located 750 m from the coast and 2 km East of Tuktoyaktuk in a polygonal patterned ground. This patterned ground is located in a depression, surrounded by elevated plateaus with observable ground water flowing into the valley. In this area, low-centered polygons exhibited higher moisture levels compared to high-centered polygons. High-centered polygons were colonized by shrubs and Ericaceae, while low-centered polygons were dominated by hydrophilic plants such as grasses and sedges. Wet troughs delimited the microtopographic forms, with vegetation reflecting waterlogged conditions. The mean active layer thickness across RP was about 35 cm. Profile 10A was collected from a trough and presented water-saturated conditions with brown OM. Profiles 10B and 10D were collected from high-centered polygons and characterized by unsaturated conditions with dark brown OM and presence of roots until 20 cm depth. Profile 10C was collected from a low-centered polygon and consisted of reddish-brown peat throughout. Profiles 10A, 10B and 10D did not consist of peat.

The coastal site (TP) is located 20 km NW of Tuktoyaktuk, featuring a polygonal patterned ground, largely colonized by *Carex sp.*, a type of graminoid plant common near Arctic coastlines. The mean active layer depth was 35 cm. The site's dynamics are influenced by the twice-daily ebb and flow of tides. Profile 07 was collected from a water-saturated low-centered polygon, located in the intertidal zone. The soil color was very dark greyish black. Profile 08 was collected from a water-saturated polygonal trough not immediately located in the intertidal zone, but which floods during storms. The soil was characterized by dark greyish-brown OM mixed with sand. Finally, profile 09, was collected from the center of a higher-centered polygon situated in the middle intertidal zone. The active layer appeared water unsaturated. The soil from this site consisted of a mixture of black organic-rich material and sand. The sand found in samples from TP appeared to be wind-deposited from nearby dunes.

#### **1.4.2 Methane production rates in incubations**

Long-term sediment and soil incubations under anoxic conditions were used to assess CH<sub>4</sub> production rates over several months by measuring CH<sub>4</sub> accumulation in the vials' headspace. The objective was to simulate the increased connectivity between the land and the ocean in the coastal environment of the Canadian Arctic, which represents an important aspect of the ongoing regional environmental transition. Collected sediments and soil profiles were immediately sub-sampled based on depth, at 5 or 10 cm intervals, according to shifts in sedimentary units. To prepare incubations, 4 mL of sediment and 2 mL of brackish water (collected from the coast) were immediately transferred into 20 mL glass vials. Incubation vials were crimped with 20 mm butyl rubber stoppers and aluminum caps. The bottles were flushed with nitrogen gas (Alpha Gaz 1) for 2 minutes in the field to remove air. Four incubations were prepared for each sampled depth; 3 were kept for measurements of methane production rates (triplicates) and one served for isotopic analyses. Incubations were kept at 4°C and incubated for 339 days total.



Analyses on incubations started 4 months after their preparation. They were performed on a gas chromatograph (Agilent 8900) equipped with a flame ionization detector (GC-FID) at UQAR facilities. The GC-FID is equipped with a 100  $\mu\text{l}$  injection loop to ensure a consistent volume of sample is transferred to the collector. To saturate the injection loop, 300  $\mu\text{l}$  taken from the headspace of the vials was injected with a gas-tight syringe. Prior to injection, samples were shaken for 30 seconds to equilibrate headspace and sediment gases. This procedure was done every two weeks to measure  $\text{CH}_4$  accumulation in the headspace. The resulting production rates were back calculated, and values are expressed in  $\text{nmol}$  of  $\text{CH}_4$  per cubic centimeters of wet material per day ( $\text{nmol cm}^{-3} \text{d}^{-1}$ ). The density of the collected samples varied widely, with some being organic deposits and peat, while others contained more mineral content. Consequently, the  $\text{CH}_4$  production rates were expressed volumetrically to account for these discrepancies which are more representative of the volume they occupy in the profiles and landscape. The limit of detection of the GC-FID is 0.3 ppm and all samples had higher concentrations. Each value represents the mean of triplicate measurements and the reported uncertainty on the measurement is the standard deviation on triplicates.

To estimate the potential total column methane production, the active layer samples were vertically integrated to obtain the total production for the active layer of each profile. Values are reported in  $\text{mol m}^{-2} \text{d}^{-1}$ . Using aerial photo imagery, the polygonal tundra at RP was mapped, allowing for the discrimination between high-centered polygons, low-centered polygons and throughs. The total area of each geomorphological form was calculated based on the map data (Fig 14). They were then coupled to the potential total column methane production to estimate the total  $\text{CH}_4$  produced in the polygonal tundra of RP over a day ( $\text{mol d}^{-1}$ ) (see S2 document for calculations).

### **1.4.3 Elemental and isotope composition of the sediment**

The total organic carbon (TOC) content of the sediments was measured by combustion using an elemental analyzer (ECS 8020, NC Technologies) combined with a gas chromatograph equipped with a thermal conductivity detector at ULaval facilities (The

International Research Laboratory Takuvik). A 100 mg aliquot of sediment was thawed and weighed for each sample. They were then dried in an oven at 60°C for 48 hours and reweighed to determine their water content. Sediments were then ground using a granite mortar pestle and homogenized using a 1.18 mm pore size sieve to remove roots and rootlets. Instruments were cleaned with ethanol between manipulations. Inorganic carbon was removed from sediments by adding 2.2 mL of 12M HCl in every sample. After fumigating for 24 hours, around 8 mg was encapsulated in tin foil capsules. Samples were kept in a desiccator until analyses. Values are expressed as % of carbon contained in the weighed sample (wt. %).

The organic carbon ( $\delta^{13}\text{C}$ -TOC) isotopic compositions were measured at UOttawa facilities (Jàn Veizer Stable Isotope Laboratory) using a continuous flow isotope ratio mass spectrometer (Delta Advantage, Thermo Germany) coupled to an elemental analyzer. The sample preparation method was the same used for elemental analyses.  $\delta^{13}\text{C}$ -TOC values are denoted as  $\delta\text{‰}=10^3 ((R_{\text{sample}}/R_{\text{standard}}) - 1)$ , where R is  $^{13}\text{C}/^{12}\text{C}$  and standards refer to the Vienna Pee Dee Belmnite (VPDP). Samples were kept in a desiccator until time of analyses.

#### **1.4.4 Stable carbon isotopic composition of methane**

One incubation vial was analyzed for stable carbon isotopic composition of headspace methane ( $\delta^{13}\text{C}$ -CH<sub>4</sub>). Stable carbon from methane ebullition samples collected from pondlets were also analyzed. Both types of samples were analyzed with a cavity ring-down spectrometer (PICARRO G2201-i isotopic CO<sub>2</sub>/CH<sub>4</sub>) equipped with a 16-port distribution manifold and small sample introduction module (SSIM) at McGill (McGill Isotope Biogeochemistry Laboratory). Incubations were kept at 4°C in the dark for 8 months to let the microbial community stabilize and produce sufficient CH<sub>4</sub> for analysis. To stay in the detection range of the analyzer (1.8-1000 ppm CH<sub>4</sub>), a small volume of the headspace, proportional to CH<sub>4</sub> concentration in sample, was drawn from the incubation vial (0.2-6 mL). The sample was introduced to the 16-port manifold with a 21G needle connected to a disposable luer lock plastic syringe. Samples were diluted with zero air by the SSIM to reach

a volume of 20 mL. Two or three measurements per sample were conducted depending on headspace concentration. Ebullition gases samples were analyzed following the same method. Measured values were corrected with internal certified methane standards (-59 ‰ and -42‰) from AirLiquide and stability of the analyzer was tested with injections of ambient air. Measured values were more precise than  $\pm 1.2\%$ . All  $\delta^{13}\text{C-CH}_4$  values are expressed relatively to VPDB.

#### **1.4.5 Sulfates and chlorine concentrations in sediments**

The extraction of  $\text{SO}_4^{2-}$  and  $\text{Cl}^-$  from sediments and soils pore-water was conducted through a leaching experiment following Lacelle (2015). Frozen aliquots of sediments and soils were thawed at 4°C overnight, then weighed, dried in the oven at 60°C for 24 hours and re-weighed to determine the densities. Aliquots of dried material were put in 50 mL falcon tubes with nanopure water following a 1:10 ratio. Tubes were then shaken for one hour to promote leaching of anions towards the aqueous phase of the solution. Once the leaching process was done, 2 mL of the aqueous solution was filtered using 0.2  $\mu\text{m}$  pore size Whatman 25 mm GD/X syringe filters and transferred in disposable microtubes. Concentrations of  $\text{SO}_4^{2-}$  and  $\text{Cl}^-$  were measured by ion chromatography using a Thermo Dionex Integrion at UQAR's Chemistry department facilities with a limit of detection of 0,01  $\mu\text{g/mL}$ . The measured concentrations are expressed in  $\text{mmol g}^{-1}$  wet-weight<sup>-1</sup> of material ( $\text{mmol g}^{-1}$  wweight<sup>-1</sup>). Only one measurement per sample was performed as stability tests revealed variability of less than 3% between measured samples. The error on each value was calculated by the least squares method (Skoog et al., 2014).

### **1.5 RESULTS**

#### **1.5.1 Soil description and composition**

TOC content in the sampled soils ranged from 2 to 47 wt. %, with no clear trend in relation to depth (Fig 9, a, c). The RP polygonal patterned ground featured organic soils with

TOC content ranging from 14 to 47 wt. % (Fig 9, c). The TP coastal polygonal patterned ground also featured organic soils with TOC content ranging from 2 to 37 wt. % (Fig 9, a).

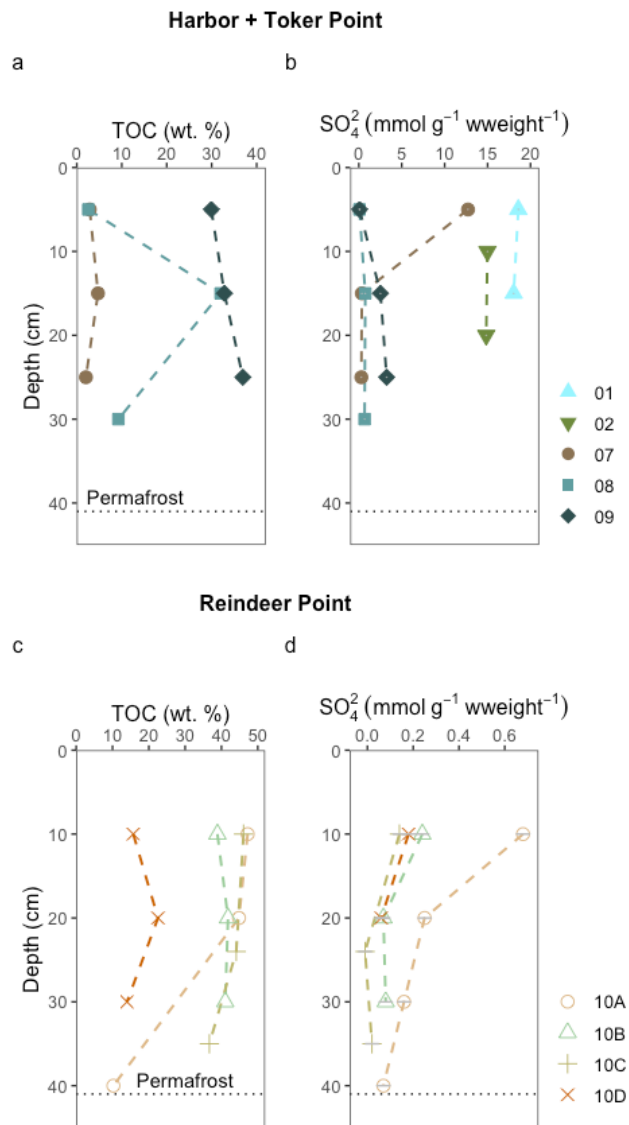


**Figure 9.** Total organic carbon and sulfate concentration in sediment or soil from the active layer of different sites in this study. The datasets are separated into two for clarity. The upper part of the figure (panels A and B) displays the data of the marine site Harbor (profile 01 and 02), and the coastal site, Toker Point (profile 07, 08 and 09). The lower part of the figure (panel C and D) displays the data from the inland site Reindeer Point (profile 10A, 10B, 10C and 10D). The black horizontal dotted line in each graph represents the permafrost-active

layer interface except for the Harbor site, where the active layer is much deeper but not measured. TOC data from Harbor site is not available. A uniform color pattern is used throughout this article.

RP, the inland site, had low sulfate and chloride concentrations relative to TP, the coastal site (Fig 9 (b), (d) and S2). Sulfates at RP ranged from null concentrations to  $0.68 \pm 0.03 \text{ mmol g}^{-1} \text{ wweight}^{-1}$ , while at TP, profiles exhibited varying concentrations and patterns in relation to depth. Sulfate concentrations, ranged from  $0.07 \pm 0.03$  to  $12.72 \pm 0.03 \text{ mmol g}^{-1} \text{ wweight}^{-1}$ . Profile 07, the low-centered polygon, exhibited the highest  $\text{SO}_4^{2-}$  concentrations of all TP site at its surface ( $12.72 \pm 0.03 \text{ mmol g}^{-1} \text{ wweight}^{-1}$ ), with concentrations decreasing drastically with depth, reaching  $0.29 \pm 0.03 \text{ mmol g}^{-1} \text{ wweight}^{-1}$  at 25 cm (Fig 9, a). In profile 09, the high-centered polygon, sulfate concentrations increased with depth ranging from  $0.09 \pm 0.03 \text{ mmol g}^{-1} \text{ wweight}^{-1}$  at 5 cm to  $3.2 \pm 0.03 \text{ mmol g}^{-1} \text{ wweight}^{-1}$  at 25 cm. Finally, profile 08, characterized as a polygonal trough, had sulfate concentrations ranging from  $0.07 \pm 0.03$  to  $0.75 \pm 0.03 \text{ mmol g}^{-1} \text{ wweight}^{-1}$ . The highest sulfate concentrations measured in this study were found in the sediments of the Harbor site, with a mean value of  $16.6 \text{ mmol g}^{-1} \text{ wweight}^{-1}$  (Fig 9, a).

## 1.5.2 Methane production

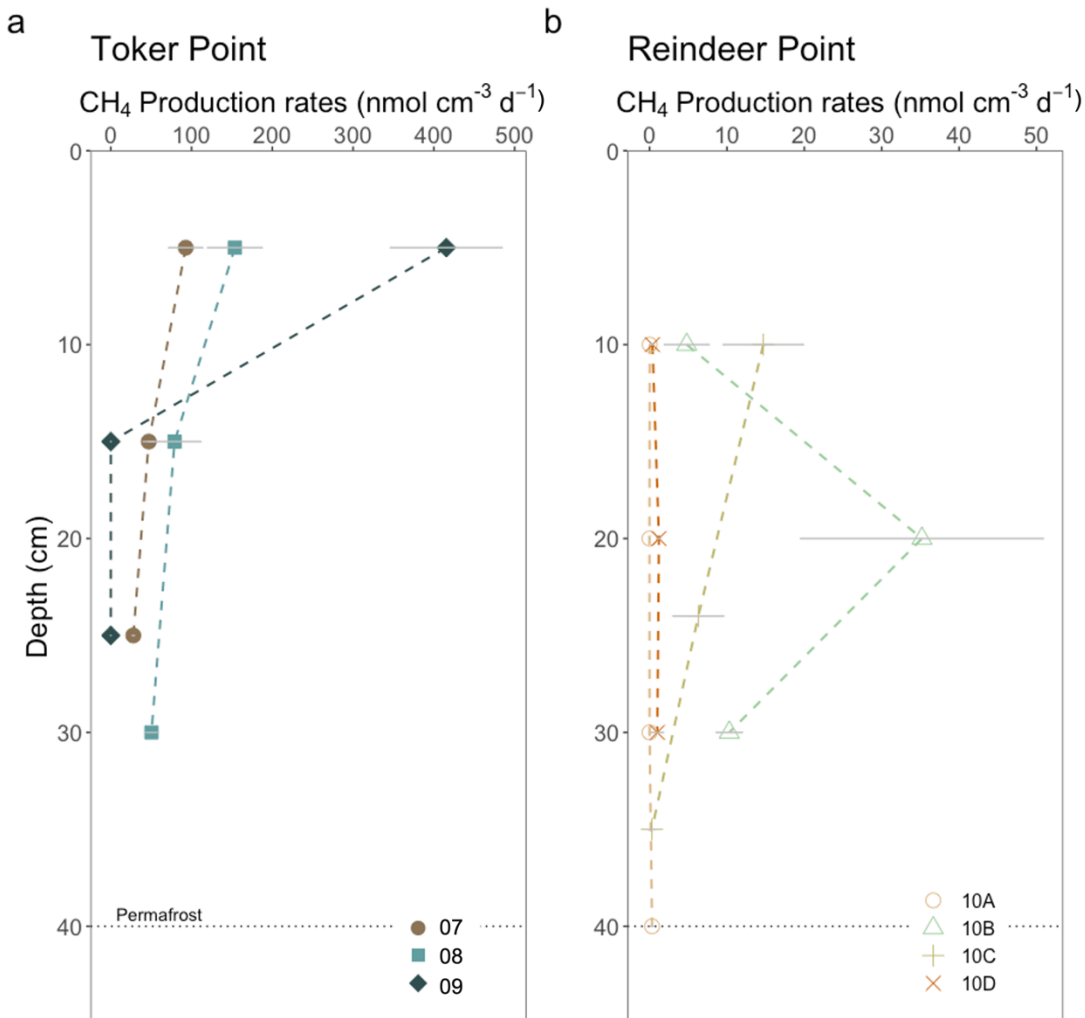


**Figure 10.** CH<sub>4</sub> production in incubations of soil and sediment with brackish water from (a) TP and (b) RP. Each datapoint represent the mean value of three incubations. The error bars equal to the standard deviation of the three separate incubations. Each profile corresponds to a specific landform. At Toker Point (panel A), profile 07 is from a low-centered polygon, profile 08 is from a trough and profile 09 is from a high-centered polygon. At Reindeer point (panel B), profile 10A is from a high-centered polygon, profile 10B is from a trough, profile 10C is from a low-centered polygon and profile 10D is from a high-centered polygon.

Rates of CH<sub>4</sub> production in incubations of sediment and soil with brackish water were undertaken at the three studied sites: RP, TP and Harbor. The brackish water added to all

incubations contained  $5.7 \pm 0.0 \text{ mmol g}^{-1} \text{ wweight}^{-1}$  of sulfates and  $28.7 \pm 0.5 \text{ mmol g}^{-1} \text{ wweight}^{-1}$  of Cl<sup>-</sup>. Production rates ranged from null to  $415.4 \pm 69.2 \text{ nmol cm}^{-3} \text{ d}^{-1}$  (Fig 10) throughout all samples in this study. At RP, the maximum CH<sub>4</sub> production rate of  $35.2 \pm 15.7 \text{ nmol cm}^{-3} \text{ d}^{-1}$  was measured in the trough profile (10B) at a depth of 20 cm. Lower values were obtained for the surface and at the active layer-permafrost interface. The low-centered polygon (10C) had its maximum CH<sub>4</sub> production rate in the surface, decreasing with depth. High-centered polygons (10A and 10D) both had very low production rates along their depth profiles ranging between null to  $1.2 \pm 0.2 \text{ nmol cm}^{-3} \text{ d}^{-1}$ . Both water-saturated microtopographic features (10B,10C) had relatively high CH<sub>4</sub> production rate compared with the high centered polygon profiles (10A, 10D), which were water-unsaturated.

At TP, a maximum CH<sub>4</sub> production rate was recorded in profile 09, the high-centered polygon at  $415.4 \pm 69.2 \text{ nmol cm}^{-3} \text{ d}^{-1}$  at the uppermost depth but it quickly decreased in the subsurface. Profile 08, the trough, and profile 07, the low-centered polygon, had lower subsurface CH<sub>4</sub> production rates, but rates decreased less drastically with depth with values being relatively high at the permafrost-active layer interface. Profile 07 had values ranging from  $27.9 \pm 1.5 \text{ nmol cm}^{-3} \text{ d}^{-1}$  to  $92.8 \pm 21.2 \text{ nmol cm}^{-3} \text{ d}^{-1}$  and profile 08 had values ranging from  $50.4 \pm 7.2 \text{ nmol cm}^{-3} \text{ d}^{-1}$  and  $153.7 \pm 33.9 \text{ nmol cm}^{-3} \text{ d}^{-1}$  (Fig 10). In general, at TP, the coastal site, much higher CH<sub>4</sub> production rates were measured than at RP, the inland site (Fig 10). The mean CH<sub>4</sub> production rate measured in the active layer of RP was  $5.7 \text{ nmol cm}^{-3} \text{ d}^{-1}$ , while at TP it was  $96.2 \text{ nmol cm}^{-3} \text{ d}^{-1}$ . The incubations with silty-clay Harbor sediments did not have measurable CH<sub>4</sub> production rates (Fig 16).

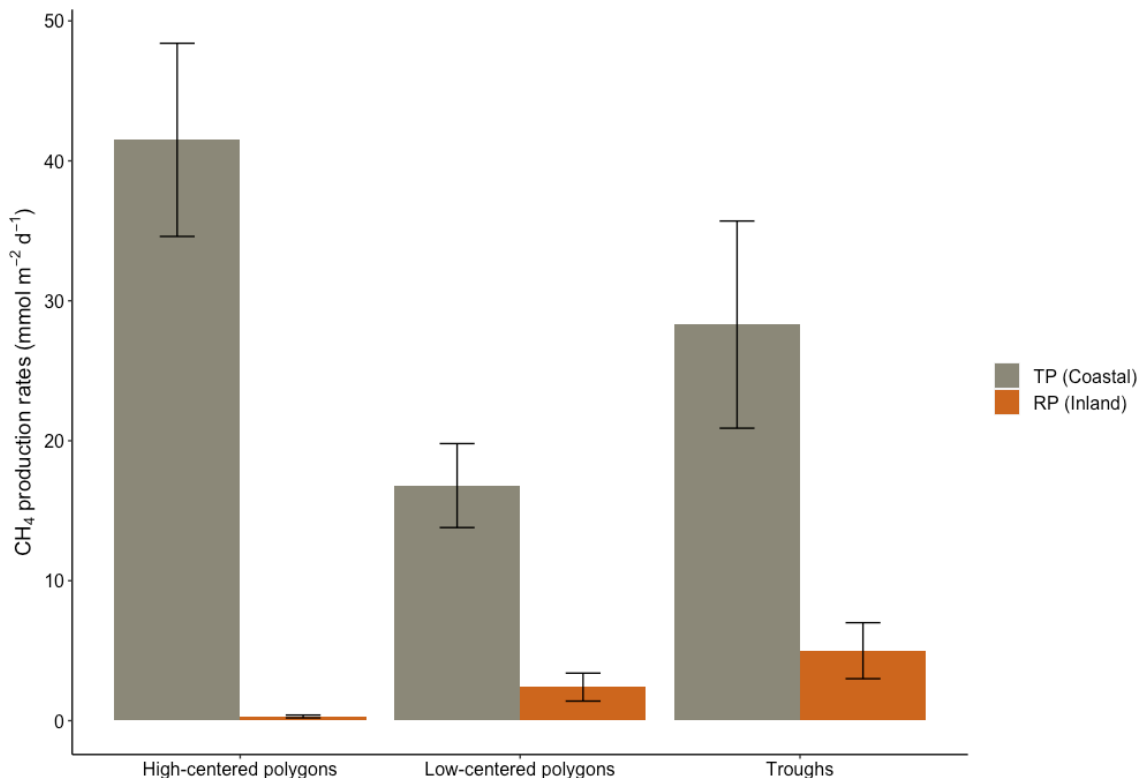


**Figure 11.** Total active layer production rates at Toker Point (Coastal) and Reindeer Point (Inland) organized by geomorphological forms of high-centered polygons, low-centered polygons and troughs. High-centered polygons at RP is the mean of two profiles. All other landforms at RP and TP are one profile. The uncertainty on total active layer production rate is propagated from the uncertainty of individual CH<sub>4</sub> production rates, not averages from replicate sites.

Estimated total active layer CH<sub>4</sub> production rates were calculated for each geomorphological landforms of RP and TP sites. At RP, the total CH<sub>4</sub> production estimated for the high-centered polygons (profile 10A and 10D), low-centered polygon (profile 10C) and trough (profile 10B) were  $0.3 \pm 0.1$  mmol m<sup>-2</sup> d<sup>-1</sup>,  $2.4 \pm 1.0$  mmol m<sup>-2</sup> d<sup>-1</sup> and  $5 \pm 2$  mmol m<sup>-2</sup> d<sup>-1</sup>, respectively (Fig 11). At TP, the total CH<sub>4</sub> production estimated for the high-centered polygon (profile 09), the low-centered polygon (profile 07) and the through (profile 08) were  $41.5 \pm 6.9$  mmol m<sup>-2</sup> d<sup>-1</sup>,  $16.8 \pm 3.0$  mmol m<sup>-2</sup> d<sup>-1</sup> and  $28.3 \pm 7.4$  mmol m<sup>-2</sup> d<sup>-1</sup>, respectively (Fig 11). In all landforms, the active layer CH<sub>4</sub> production rates were higher in the coastal site, TP, than the inland site, RP.



### 1.5.3 Isotopic composition of $^{13}\text{C}\text{-CH}_4$

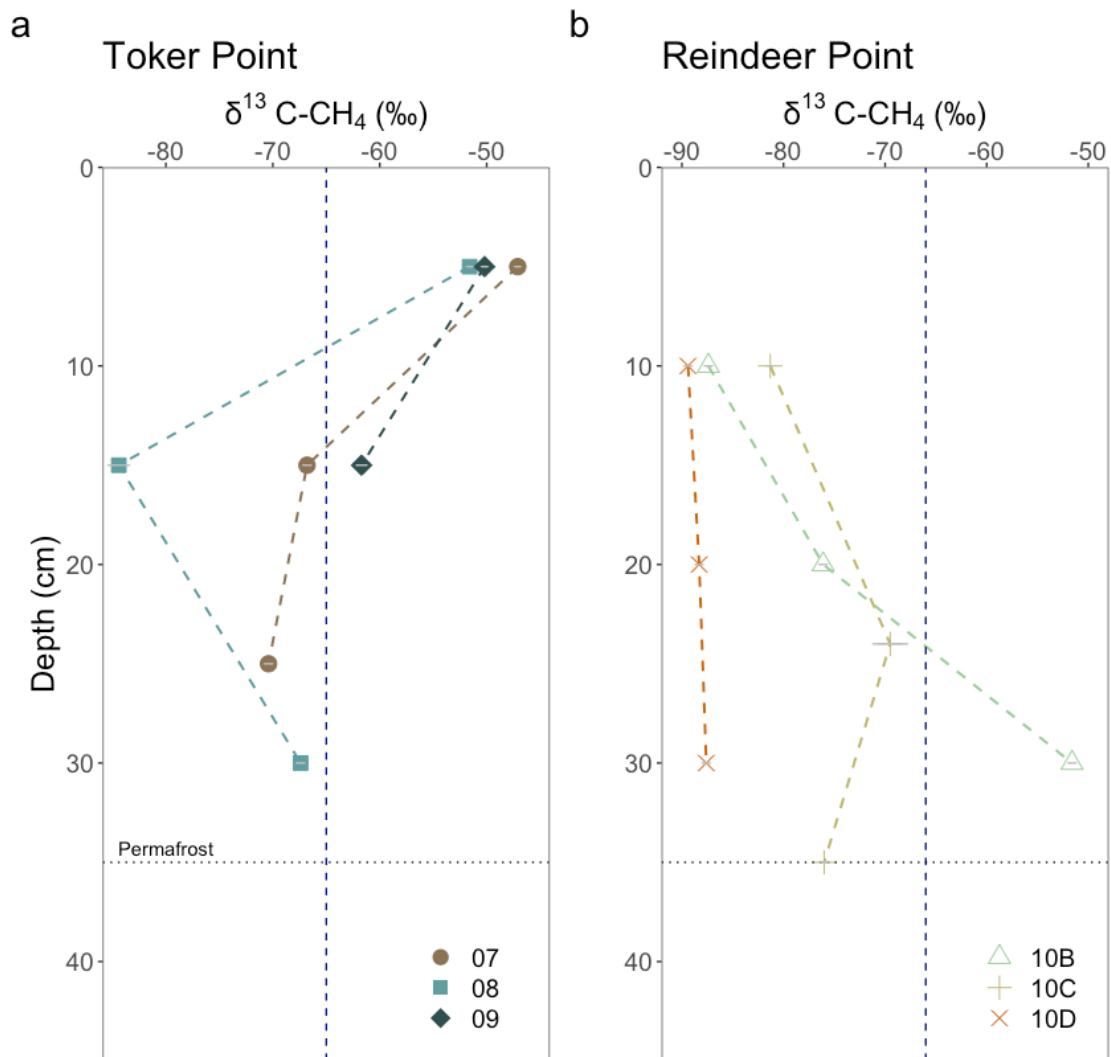


**Figure 12.** Isotopic composition of  $\text{CH}_4$  produced in brackish water incubations from (a) TP and (b) RP. Each datapoint corresponds to the mean value of two or three measurements done on one incubation, depending on the headspace concentration. The dashed vertical lines correspond to in situ ebullition  $\text{CH}_4$  collected in pondlets at each sampling site ( $n=1$ ). These values give information on the pathways used by the soil microbes to produce  $\text{CH}_4$ .  $\delta^{13}\text{C}$  between  $-65\text{‰}$  and  $-50\text{‰}$  is typically associated with acetoclastic methanogenesis, while  $\delta^{13}\text{C}$  between  $-110\text{‰}$  and  $-60\text{‰}$  is associated with hydrogenotrophic methanogenesis

(Hornibrook et al., 1997, 2000). The error bar on each point represents the analytical uncertainty on the measured value.

In parallel with CH<sub>4</sub> production rates, one incubation vial per depth was used to measure the stable carbon isotopic composition of the CH<sub>4</sub> produced. At RP, the  $\delta^{13}\text{C-CH}_4$  of the first sampled depth (10 cm) ranged from -81.3‰ to -89.4‰. At TP, the coastal site, the  $\delta^{13}\text{C-CH}_4$  signature of the first sampled depth (5 cm) ranged from -47.1‰ and -51.6‰. The values cluster together based on site, suggesting surface OM degradation processes are most similar within sites than between sites (Fig 12). Profiles at RP became progressively enriched in <sup>13</sup>C with depth, except for profile 10C where a more depleted value was observed at 35 cm. Conversely, at TP, profiles became depleted in <sup>13</sup>C with depth, except for profile 08 where an enrichment was measured between 15 and 30 cm.

Ebullition samples from pondlets were also measured for stable isotopes. The ebullition samples represent the net  $\delta^{13}\text{C}$  signature of methane produced in the sediments of pondlets at RP and TP. At RP, CH<sub>4</sub> ebullition from a sampled thaw pond had a  $\delta^{13}\text{C}$  of -66.1‰. At TP, CH<sub>4</sub> ebullition from a sampled pondlet had a  $\delta^{13}\text{C-CH}_4$  of -65.0‰.

## 1.6 DISCUSSION

### 1.6.1 Addition of brackish water to anoxic incubations did not strongly suppress methanogenesis

Despite the addition of brackish waters to incubations, the range of CH<sub>4</sub> production rates measured in this study are consistent with reports for anaerobic incubations of recently thawed permafrost soils. For example, in the talik of Big Trail Lake, a young thermokarst lake in the interior of Alaska, CH<sub>4</sub> production rates of incubations ranged between 4.7 and 16.1 nmol cm<sup>-3</sup> d<sup>-1</sup> (Pellerin et al., 2022), while in incubations from Vault Lake, another thermokarst lake in the interior of Alaska, CH<sub>4</sub> production rates varied between 11.1 and 275 nmol cm<sup>-3</sup> d<sup>-1</sup> (Heslop et al., 2015). In active layer incubations from the Yamal Peninsula in NW Siberia (Russia), CH<sub>4</sub> production rates of incubations varied between 0.1 and 33.8 nmol cm<sup>-3</sup> d<sup>-1</sup> (Heyer et al., 2002). This indicates that overall, the CH<sub>4</sub> production rates measured

at both TP and RP are within the range observed in typical ice-rich permafrost settings and reasonable for the environment studied (Fig 10).

The novel aspect of this study is that it attempts to understand marine influences on OM degradation by addition of brackish water in anoxic active layer sediment and soil incubations between a site that is submerged by the sea (Harbor), periodically submerged (TP) and never submerged (RP). This simulates the input of seawater to the active layer of tundra soils. We hypothesized that the addition of locally obtained brackish water, which contained sulfate ( $5.7 \text{ mmol L}^{-1}$ ), to the incubations, would suppress  $\text{CH}_4$  production in RP, the inland site and potentially also at TP, the coastal site. This reasoning is because supplying sulfate to low sulfate organic-rich sediment would promote sulfate reduction, which is thermodynamically more favorable than methanogenesis, thereby competitively inhibiting it (Lovely and Klug, 1983; Oremland and Polcin, 1982). RP had low sulfate concentrations before addition of the brackish water but so did many of the profiles from TP (Fig 9). In the harbor sediments, no methane production was observed (Fig 16). This is consistent with the competitive inhibition of methanogenesis by energetically favorable redox reactions with electron acceptors like oxygen, nitrate, iron oxides or sulfate that is typical of marine systems e.g. (Martens and Burner, 1974) as well as the potential anaerobic oxidation of methane (AOM). Given that the harbor sediments already had high sulfate concentrations, the lack of methane production with addition of brackish water was expected. However, strong  $\text{CH}_4$  production was observed in the incubations of both the coastal site TP and the inland site RP, indicating that  $\text{CH}_4$  production was not strongly inhibited by the addition of sulfate via the brackish water addition at those sites. While sulfate reduction rates were not measured, a strong sulfide smell was recorded when opening most of the incubations at the end of the experiment, likely indicating the coexistence of sulfate reduction and methanogenesis during the incubations. Sulfate was abundant throughout the experiments.

Coexistence of sulfate and methanogenesis within complex sediment systems such as estuarine, coastal and salt marsh sediments has been widely reported (Lovely et al., 1982; Oremland and Taylor, 1978; Sela-Adler et al., 2017). Two main mechanisms are invoked to

explain this co-existence in our incubation experiment: (1) noncompetitive methanogenesis (i.e. methylotrophic methanogenesis) and (2) syntrophic methanogenesis. (1) Noncompetitive substrates are substrates like methanol and methylamines that are used by methanogens alone and cannot be used with electron acceptors like sulfate (Lovley and Klug, 1983; Oremland et al., 1982). Noncompetitive substrates are thus microbially converted to methane, even in sediments with high sulfate concentrations (Maltby et al., 2018; Yuan et al., 2019). For example, in salt marshes, where high sulfate concentrations are often found, elevated CH<sub>4</sub> emissions are suggested to mainly stem from noncompetitive methanogenesis (Comer-Warner et al., 2022; Poffenbarger et al., 2011; Yuan et al., 2019). In the sulfate reducing zone of sediments from the Baltic Sea, where ample sulfate is found in the porewaters, seasonal methanogenesis rates were measured up to 1.3 nmol cm<sup>-3</sup> d<sup>-1</sup> due to noncompetitive substrates (Maltby et al., 2018). In permafrost soils, methanol, methylamines and the microorganisms capable of degrading them have been observed but their concentrations are typically low (Coolen and Orsi, 2015; Kramshoj et al., 2018). However, our study sites are on a coast undergoing a rapid transgression which may be driving imbalances between substrate supply and microbial abundances. The rates of methane production observed at RP and TP of up to 154 nmol cm<sup>-3</sup> d<sup>-1</sup> contrast with reported values for methylotrophic methanogenesis (Maltby et al., 2018). Based on these numbers, noncompetitive substrates likely play a small role in the total methane production at our study sites but further investigation into methylotrophic methane production in coastal environments will allow to document the overall role of methylotrophic methane production in coastal permafrost settings.

(2) Syntrophic methanogenesis occurs when molecular hydrogen produced by acetoclastic sulfate-reducing bacteria is used by hydrogenotrophic methanogens. In this syntrophy, the chemical energy is shared via interspecies hydrogen transfer (Ozuolmez et al., 2015). For instance, in permafrost soils of Sweden, it was demonstrated that syntrophic methanogenesis was favored in anoxic and water-saturated soils by an elevated abundance in methanogens and their syntrophic partners (Keuschnig et al., 2022). As the incubation experiment in our study at RP and TP featured water-saturated and anoxic environments,

syntrophic methanogenesis could participate in the co-occurrence of sulfate-reduction and methanogenesis. This mechanism is consistent with most incubations producing methane with a  $\delta^{13}\text{C}$  value in the range of hydrogenotrophic methanogenesis (see below).

Measuring methane production through incubations inherently has limitations as they prevent continuous inputs of microorganisms, fresh OM and nutrients that would occur in the natural environment. This can create a “bottle effect”, which leads to restrictions in microbial community composition, limits the input of nutrients and leads to the accumulation of metabolites which would normally be degraded (Ionescu et al., 2015). Typically, overestimation of microbial processes rates is observed compared to *in situ* data (Sherr et al., 1999). The overestimation of  $\text{CH}_4$  production rates by incubations relative to the *in situ* rates are difficult to assess because of a lack of data in permafrost environments (Heslop et al., 2020). Furthermore, a lag time between the start of anaerobic incubations and maximum  $\text{CH}_4$  production rate is widely documented, which appears to be the case for both active layer and thawed permafrost incubations (Holm et al., 2020; Knoblauch et al., 2018; Knoblauch et al., 2012; Roy Chowdry et al., 2015). Drier or water-unsaturated conditions lead to a longer lag time before the onset of maximum  $\text{CH}_4$  production (Treat et al., 2015). Microbial community composition in the soil or sediment also exerts a strong control on the organic carbon degradation and has been shown to change throughout the incubations (Holm et al., 2020). Low initial methanogen population in soils can contribute to this lag time, but other factors such as disturbance of sediment during sampling, substrate availability and redox state can also contribute to the observed lag time in some incubations (Treat et al., 2015; Roy Chowdry et al., 2015).

Furthermore, it is also possible that a “priming effect” from the addition of brackish water in incubations could have supercharged OM degradation with marine organic carbon, nutrients and microorganisms (Bianchi, 2011), which may have favored methane production. However, this priming effect was not observed in the Harbor sediments which were amended with the same brackish water. Furthermore,  $\text{CH}_4$  ebullition samples collected from pondlets adjacent to RP and TP exhibited broadly similar  $\delta^{13}\text{C}$  values to methane produced in

incubations (Fig 12), suggesting a similitude in microbial degradation pathways to methane *in situ* and in the incubations. Despite these uncertainties, our dataset shows clear depth trends and landscape-level variations, indicating that even under brackish water addition, local conditions will strongly influence methane production.

### **1.6.2 CH<sub>4</sub> production pathways depend on hydrology and organic matter lability**

The addition of brackish water resulted in incubation conditions being water-saturated in all cases, but it appears that biological and hydrological conditions of the polygonal patterned grounds influenced the magnitude of CH<sub>4</sub> production, nonetheless.

In all landforms, the active layer CH<sub>4</sub> production rates were lower at the inland site, RP than at TP, the coastal site (Fig 10). Inland, low-centered polygons and troughs have typically higher methane fluxes than unsaturated landforms like high-centered polygons (Roy Chowdry et al., 2015; Martin et al., 2018; Zheng et al., 2018) which indicates they likely also have higher methane production rates. Within sites in our study, brackish water amended incubations of high-centered polygon soils had lower CH<sub>4</sub> production rates, while brackish water amended incubations of troughs and low-centered polygons had higher CH<sub>4</sub> production rates (Fig 10). This indicates that for the degradation of organic matter into methane in tundra soils, increasing seawater interactions through coastal processes, such as submersion due to subsidence or increased storm severity, resulting in the input of seawater in terrestrial soils, does not halt methane production. It also shows that landforms and local hydrology remain important in controlling the microbial communities which affects the resulting methane emissions.

Marine OM and nutrient inputs from tides and storm surges may contribute to the higher lability of OM and could fuel greater fermentation (Valdemarsen and Kristensen, 2010). It was reported that 8.7% of the organic carbon in nearshore sediments of Herschel Island, Beaufort Sea, came from marine sources (Couture et al., 2018). This is relevant for the TP site because while  $\delta^{13}\text{C}$  signature of soils showed that terrestrial OM is dominant (Fig 16), marine OM may get transported and deposited in coastal soils during high tides and

storm surges. Although our analyses could not detect the presence of marine OM in TP soils, the higher CH<sub>4</sub> production rates recorded in the incubations of TP, relatively to those of RP could in part be explained by marine OM and nutrient inputs. Interestingly, the high-centered polygon at TP, profile 09 (Fig 10), did not behave in a predictable manner since it had very high CH<sub>4</sub> production rates on the surface. This may be due to the presence of high levels of geese fecal matter on the surface at TP, profile 09, which may provide a significant source of labile organic carbon or nutrients like N and P and a different microbial community composition on surface sediments, capable of high CH<sub>4</sub> production rates immediately following the start of the incubations. Lower in the profile, methane production rates were very low, characteristic of the methane production rates observed in water-unsaturated high-centered polygons (Fig. 10). Therefore, in this instance, proximity with the coast may have influenced methane production through the presence of fauna.

Vegetation cover is also strongly influenced by local hydrology, microtopography and the presence of the coast, which may influence methane production (Vaughn et al., 2016). OM quality is typically highest closest to the surface, where the youngest and most labile organic matter is found (Nilsson and Oquist, 2009). In permafrost landscapes, sites dominated by hydrophilic vegetation like sedges and graminoids, often found in low-centered polygons have been observed to typically emit more methane than sites dominated by shrubs, often found in high-centered polygons (Hodgkins et al., 2014; Treat et al., 2015; Olefeldt et al., 2013). At RP, relatively recalcitrant OM produced by shrubs, mosses and sphagnum may throttle CH<sub>4</sub> production and produce a more uniform profile of CH<sub>4</sub> production rates (Fig 10). At TP, tidal inundation supports dominant *Carex sp.* vegetation, which may promote CH<sub>4</sub> production and a strong depth-dependence of CH<sub>4</sub> production rates.

Stable carbon isotopic signature of CH<sub>4</sub> provides insights on the microbial processes involved in methanogenesis and on substrates used.  $\delta^{13}\text{C-CH}_4$  between -65‰ and -50‰ is typically associated with acetoclastic methanogenesis, while  $\delta^{13}\text{C-CH}_4$  between -110‰ and -60‰ is associated with hydrogenotrophic methanogenesis (Hornibrook et al., 1997, 2000). The stable isotopic signature of methylotrophic methanogenesis is between -83‰ and -72‰

(Penger et al., 2012), which overlaps with the hydrogenotrophic interval, precluding us from separating these two metabolic pathways. At RP, except for profile 10B,  $\delta^{13}\text{C-CH}_4$  had more negative values, consistent with the processing of recalcitrant organic matter through the hydrogenotrophic production pathway (Heffernan et al., 2022; Hodgkins et al., 2014). Profile 10B, a polygonal trough, had less negative  $^{13}\text{C-CH}_4$  values more consistent with acetoclastic methanogenesis (Hornibrook et al., 1997). At TP, the coastal polygonal tundra,  $\delta^{13}\text{C-CH}_4$  at 5 cm depth is less negative, consistent with methanogenesis with more labile organic carbon and the acetoclastic production pathway (Hodgkins et al., 2014), transitioning to more negative values, associated to hydrogenotrophic production with depth. This shift suggests an input of labile OM in TP surface and sub-surface soils. This may be due to the labile OM from abundant geese fecal matter that was observed in the surface. It is also possible that *Carex sp.*, the dominant plant species of the site, may be a source of labile fermentation precursors (Galand et al., 2010; Liebner et al., 2015).

By comparing the methane production rates from brackish water incubations from RP and TP we infer that the simple addition of brackish water is not the only parameter controlling methane production between inland and coastal sites. Other interactions from coastal processes must enhance methane production in the coastal site. Future research should investigate the potential role of additional marine organic matter inputs.

### **1.6.3 Active layer methane production rates are comparable to the net CH<sub>4</sub> fluxes measured in similar environments**

In a polygonal terrain of the Tuktoyaktuk Coastlands, net CH<sub>4</sub> fluxes from the center of high-centered polygons and troughs derived from flux chambers were measured to be  $1.9 \pm 20.4 \text{ mmol m}^{-2} \text{ d}^{-1}$  and  $13.0 \pm 20.4 \text{ mmol m}^{-2} \text{ d}^{-1}$  respectively (Martin et al., 2018). These overlap with values of estimated total CH<sub>4</sub> production derived from the brackish water amended incubation experiments (Fig. 11). It is clear from the large variations in measured CH<sub>4</sub> emissions from the study of Martin et al., (2018) that incubations to estimate total active layer CH<sub>4</sub> production rates can discern small differences due to local variations that stem



mostly from microtopography. For example, at RP a comparable polygonal terrain to the study of Martin et al., (2018), the active layer of high-centered polygons and trough, produced  $0.3 \pm 0.1 \text{ mmol m}^{-2} \text{ d}^{-1}$  and  $5.0 \pm 2.0 \text{ mmol m}^{-2} \text{ d}^{-1}$ , respectively which are significantly different. This indicates the role of microtopography in controlling the activity of microbial communities which controls methane production and the potential to scale more accurately methane production at the landscape level based on landform distributions.

Interestingly, TP, the coastal site, had an estimated total active layer  $\text{CH}_4$  production rate comparable to emissions of a St. Lawrence estuary salt marsh which had a  $\text{CH}_4$  flux of  $24 \pm 14.4 \text{ mmol m}^{-2} \text{ d}^{-1}$  (Comer-Warner et al., 2022). The St. Lawrence estuary salt marshes are affected by freeze-thaw cycles associated with seasons comparable to the freeze-thaw cycles observed in the active layer of Tuktoyaktuk coastlands despite lacking some characteristics features of our site like the presence of permafrost and rapid coastal erosion rates. Methane emission and production within areas of coastal influence thus appear of similar magnitude. By comparison, mangrove forests, which are a major global source of methane but a very different environmental conditions to our study of the coastal Arctic polygon terrain, had average  $\text{CH}_4$  fluxes to the atmosphere of  $0.3 \pm 0.1 \text{ mmol m}^{-2} \text{ d}^{-1}$  (Rosentreter et al., 2018). In another study, the average measured  $\text{CH}_4$  flux from a Yangtze Estuary (China) tidal salt marsh, with a subtropical monsoon climate, was  $2.4 \text{ mmol m}^{-2} \text{ d}^{-1}$  (Li et al., 2021). These reported values are similar to our values of  $\text{CH}_4$  production as well as other studies in the region and adds to the notion that Arctic coasts may be an underestimated source of methane emissions globally that warrant further investigation.

The calculated methane production rates from TP and RP do not take in account aerobic and anaerobic oxidation of  $\text{CH}_4$ , which will reduce fluxes of  $\text{CH}_4$  from these sites. Studies and models of Arctic soils emissions have highlighted that aerobic methanotrophy could consume more than half of the  $\text{CH}_4$  produced in soils, greatly limiting surface emissions (Oh et al., 2020; Zheng et al., 2018). Furthermore, AOM has been shown to play an important role in attenuating methane production in soils and sediments (Segarra et al., 2013; Winkel et al., 2019). However, AOM did not appear to influence significantly  $\text{CH}_4$  production in

incubations with thermokarst lake sediments (Lotem et al., 2023). While in this study, brackish water incubations are compared with methane emissions measured in similar landscapes, they should not be directly equated.

**Table 2.** Total methane active layer production in a context of marine submersion from high-centered polygons, low-centered polygons and troughs during growing season applied to the spatial scale of the polygonal landscape of RP. Two samples were taken for the the high-polygon form. The mean active layer depth of the region is 35 cm. The error represents the propagation of the analytical uncertainty.

Geomorphological form	Estimated Total CH <sub>4</sub> production in active layer (mol d <sup>-1</sup> )
High-centered polygons	20.7 ± 10.3
Low-centered polygons	284.1 ± 123.2
Troughs	182.3 ± 73.4

Total active layer CH<sub>4</sub> production, in a context of marine submersion, was extrapolated for the polygonal tundra of RP, which represents an area of 25 ha (Fig 14). This calculation simulates brackish water intrusion in the terrestrial polygonal landscape to quantify the potential total active layer CH<sub>4</sub> production rates that could take place in an event of submersion. Taking into consideration the distribution of the microtopography within RP and the relative areas of each landform, the CH<sub>4</sub> production rates in the active layer, excluding pondlets, is calculated to be 487 mol d<sup>-1</sup> (Table 1). This is roughly equivalent to the daily CH<sub>4</sub> emissions of 22 cows (Baceninaité et al., 2022). These results emphasize the substantial role of Arctic tundra in methane cycling and the need to better understand the drivers and controls of CH<sub>4</sub> production, especially in a context of marine submersion. More polygonal tundra in various settings should be investigated as a comparison to the studied region. Further research on aerobic and anaerobic methane oxidation is necessary to provide a more

precise estimate of the methane cycle inputs and outputs in a scope of the evaluation of its impacts on the greenhouse gas feedback loop.

## 1.7 CONCLUSIONS

The primary hypothesis for this study was that an increase in waterlogged environments due to coastal flooding and inundation processes would not enhance CH<sub>4</sub> production because of sulfates present in coastal waters. However, the incubation experiments revealed the highest CH<sub>4</sub> production rates at TP, the coastal site. Notable CH<sub>4</sub> production rates (40 nmol cm<sup>-3</sup>d<sup>-1</sup>) in the presence of SO<sub>4</sub><sup>2-</sup> at concentrations ranging between 5 and 18 mM were measured at TP. Additionally, waterlogged conditions attributed to the ebb and flow of tides, seems to favor anoxic OM degradation and may potentially provide inputs of fresh OM and nutrients from marine sources, contributing to the elevated CH<sub>4</sub> production rates measured in the coastal setting of TP. However, no conclusive explanation for the co-occurrence of sulfate-reduction and methanogenesis in our brackish water incubations was identified, but based on evidence, we suggest syntrophic methanogenesis could support this co-occurrence. However, more investigation on methylotrophic methanogenesis in the coastal soils of Tuktoyaktuk is needed as it can be an important process in saline environments (Conrad, 2020). This experiment suggests that despite addition of brackish water to soils, CH<sub>4</sub> production may not be suppressed in surface sediments of the Tuktoyaktuk coastlands, and other Arctic coastlines. Future studies should investigate CH<sub>4</sub> oxidation processes in greater detail, as they could provide crucial insights into Arctic coastal carbon cycling in sediments and soils dynamically affected by changing sea level.

## 1.8 ACKNOWLEDGEMENTS

We thank Santiago Mareque for assistance during field sampling. Mathieu Babin and Thi Hao Bui are acknowledged for assisting with the laboratory work performed at Université du Québec à Rimouski and at McGill University, respectively. Takuvik Laboratory is acknowledged for providing analyses and results on δ<sup>13</sup>C and TOC content of sediments. We

also thank the Tuktoyaktuk community for providing wildlife monitors with insightful information on the territory during field sampling. This research was funded by NSERC Discovery Grant with Northern Supplement to AP. ARL acknowledges financial support from the NSTP program. PMJD acknowledges support from the NSERC Discovery Grant and the Canadian Foundation for Innovation.

### 1.9 SUPPLEMENTAL INFORMATION

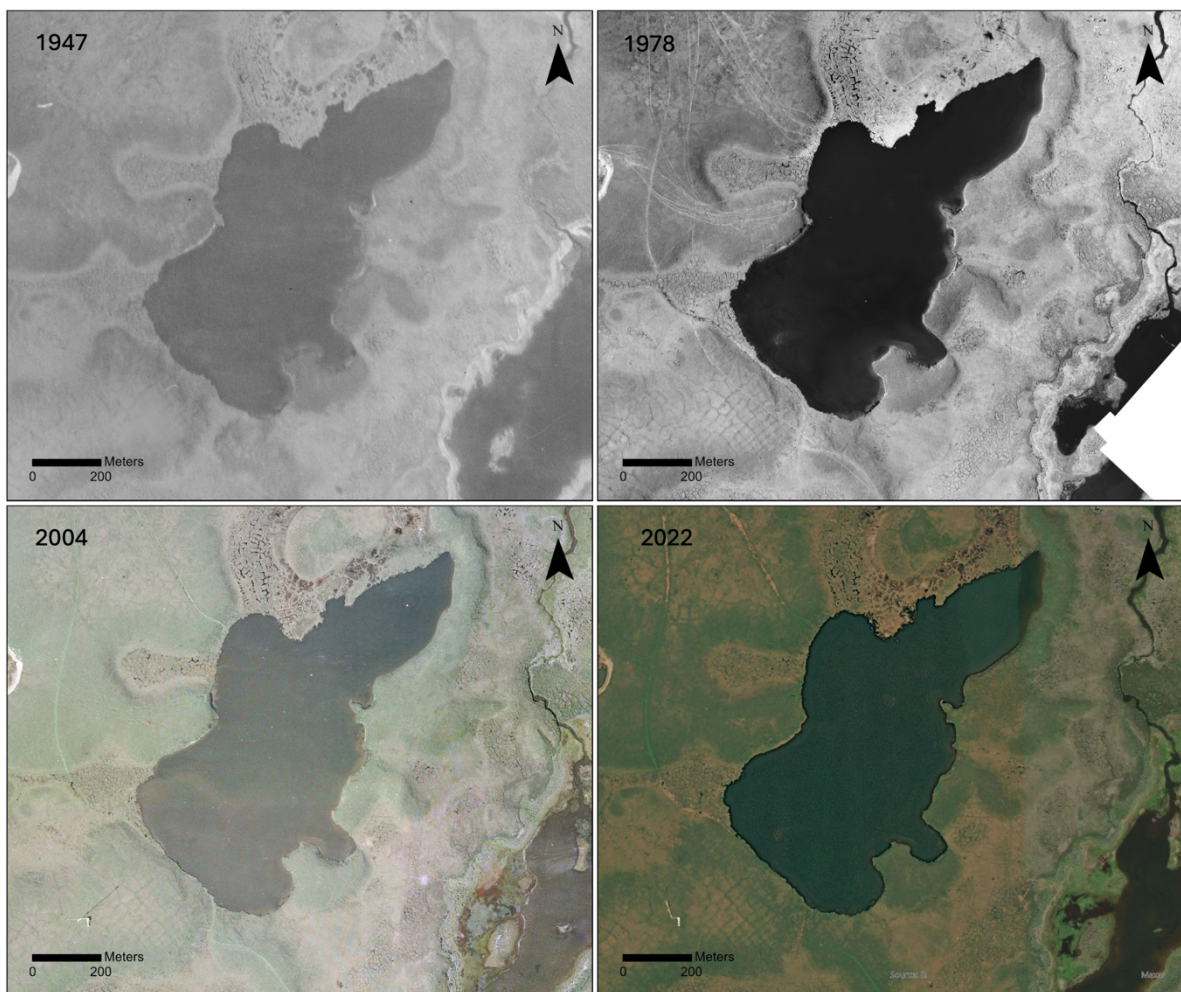


**Figure 13.** Temporal variability of the lake surrounding RP polygonal ground (North of lake), showcasing stability since 1947.

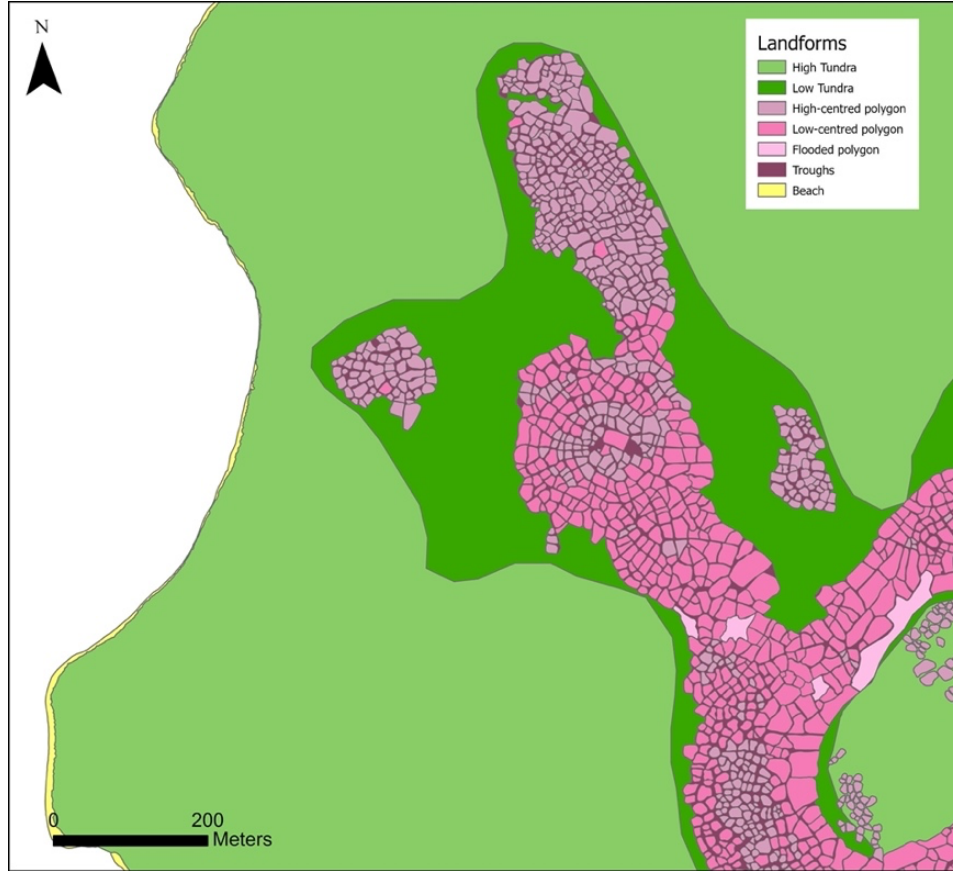


**Figure 14.** Map of Reindeer Point sampling site with delimitation of geomorphological polygonal forms. Forms were drawn based on aerial imagery from 2022.

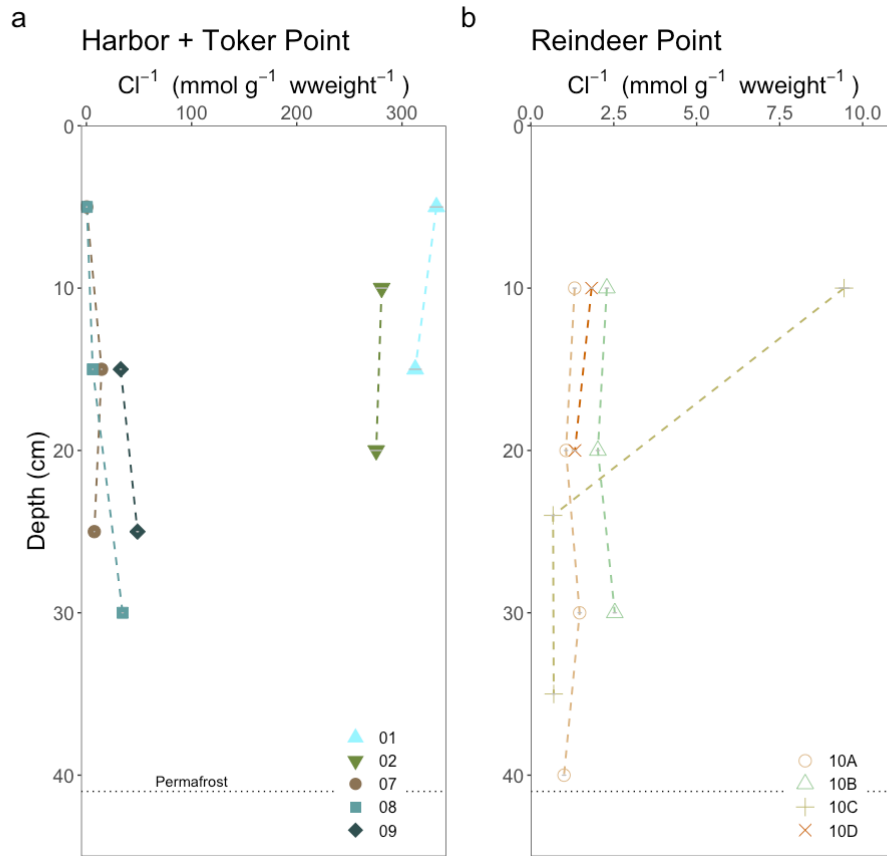


**Figure 15.** Cl<sup>-</sup> concentrations in (a) Harbor + Toker Point and (b) Reindeer Point sediments used in the incubation experiment.

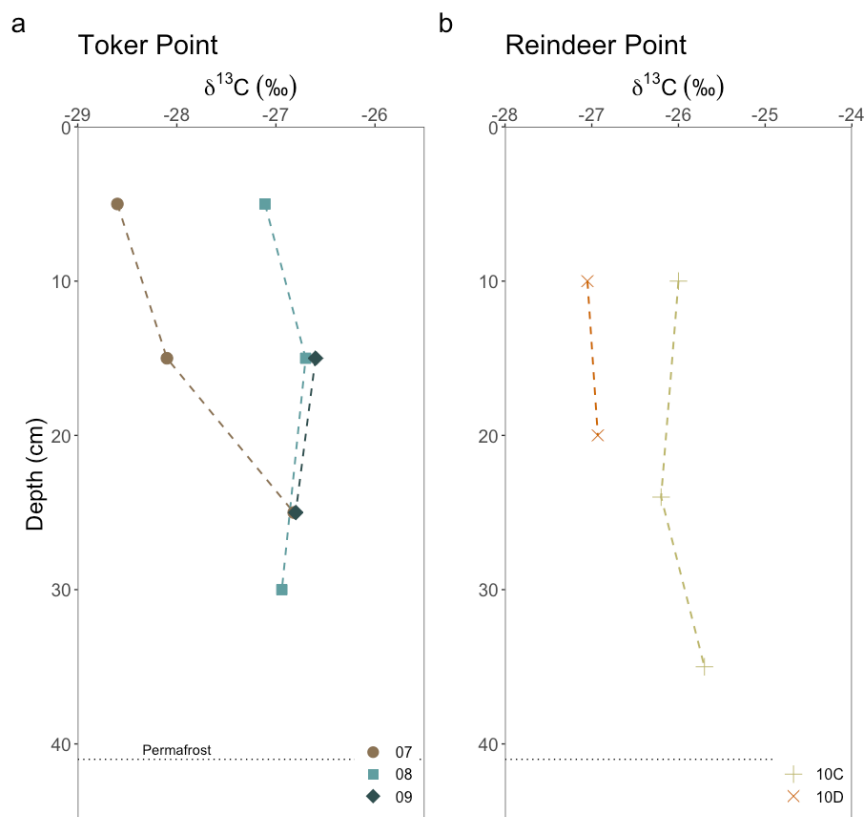


**Figure 16.**  $\delta^{13}\text{C}$  of (a) Harbor + Toker Point and (b) Reindeer Point sediments used in the incubation experiment. Values measured within the range of terrestrial OM (Fu et al., 1993).

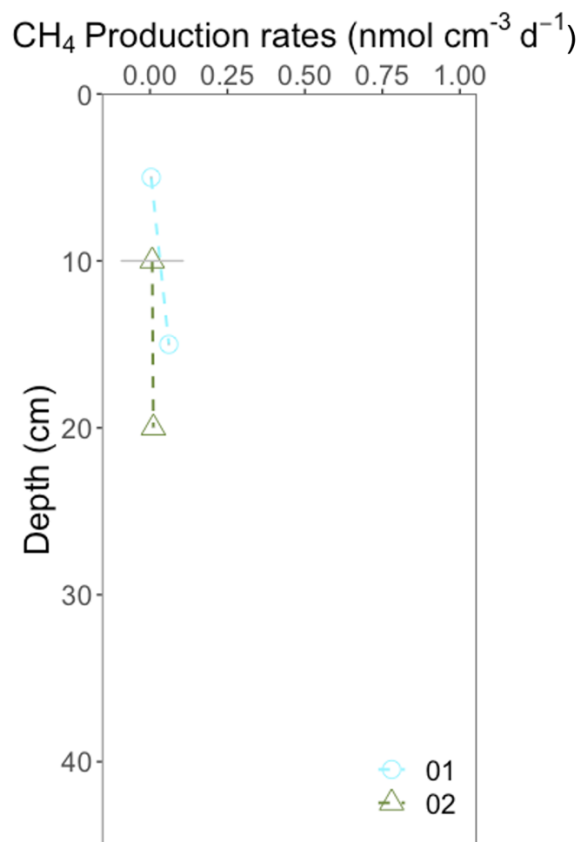


**Figure 17.** CH<sub>4</sub> production rates in marine sediments cores collected from the Harbor. The error bar on measured values represents the standard deviation on the mean of triplicates.



**CHAPITRE 2 – LA PRODUCTION DE MÉTHANE DANS LE PERGÉLISOL  
DÉGELÉ N’EST PAS INHIBÉE PAR L’AJOUT D’EAU SAUMÂTRE**

## 2.1 RESUME EN FRANÇAIS DU DEUXIEME ARTICLE

Le pergélisol stocke une grande quantité de carbone qui, une fois dégelé, peut être libéré dans l'atmosphère sous forme de GES par l'activité biologique et contribuer à l'amplification du réchauffement climatique. Les sols de pergélisol peuvent être hétérogènes et présenter des formes microtopographiques comme les polygones de coins de glace. Ces sols ont des conditions hydrologiques et géochimiques spécifiques qui influencent les processus de dégradation de la MO. Avec l'augmentation de la connectivité des sols terrestres avec l'océan, les interactions dans les processus de dégradation de MO se complexifient surtout due à l'apport d'accepteurs d'électrons alternatifs et de MO d'origine marine. À Tuktoyaktuk (TNO), 10% de la superficie du territoire est composé de sols polygonaux et les taux de subsidence côtière entraînent des taux de recul du territoire de plus de -4 m/an par endroits. Afin d'améliorer l'état des connaissances sur les processus de dégradation de la MO dans les sols polygonaux en contexte de submersion marine, trois carottes de pergélisol ont été récoltées à Tuktoyaktuk : une carotte dans une tourbière de polygone à centre bas, une autre récoltée dans un polygone à centre haut et une dans un sol de tundra qui borde la région de sol polygonal. Une expérience d'incubations de ces sols et d'eau saumâtre en conditions anoxique a permis de calculer des taux de production de CH<sub>4</sub> qui contrastent entre la couche active et le pergélisol, ainsi qu'entre sites. Bien qu'elle ne soit pas systémique, nous avons observé une tendance entre le contenu en TOC dans les sols et les taux de production de CH<sub>4</sub>. Les incubations de la couche active de la tourbière et du pergélisol dégelé du polygone à centre élevé ont exprimé une tendance positive entre les taux de production de CH<sub>4</sub> et le contenu en TOC. Cependant, les incubations de pergélisol dégelé de la tourbière n'ont pas produit de CH<sub>4</sub> malgré un contenu substantiel en TOC. Nos résultats démontrent que les conditions de submersion océanique n'inhibent pas la méthanogénèse dans les sols de la tundra Arctique malgré l'apport de sulfates par l'eau de mer, un accepteur d'électron alternatif. Les tendances de production de CH<sub>4</sub> semblent fortement dépendre de la préservation de la MO dans les conditions de pergélisol ainsi que des conditions géochimiques contenues par les sols.

## 2.2 ADDITION OF BRACKISH WATER TO THAWED PERMAFROST DOES NOT INHIBIT METHANE PRODUCTION

**Roy-Lafontaine, A.**<sup>1,3</sup>, Lee, R.<sup>2</sup>, Douglas, P.M.J.<sup>3,4</sup>, Whalen, D.<sup>2</sup>, Pellerin, A.<sup>1,3</sup>

<sup>1</sup>Institut des Sciences de la Mer de Rimouski, Université du Québec à Rimouski, Rimouski, Quebec, Canada

<sup>2</sup>Geological Survey of Canada, Natural Resources Canada, Halifax, Nova Scotia, Canada

<sup>3</sup>Department of Earth and Planetary Sciences and Geotop Research Centre, McGill University, Montreal, Quebec, Canada

<sup>4</sup>Centre d'Études Nordiques, Université Laval, Québec, Quebec, Canada

## 2.3 INTRODUCTION

Permafrost stores a vast amount of carbon, which once thawed, can be released into the atmosphere as greenhouse gases and contribute to the amplification of current global warming (Rantanen et al., 2022). In Arctic soils, freeze-thaw cycles lead to the development of microtopographic features (Black, 1982), such as polygonal tundra. Polygon tundra is characterized by ice-wedge polygons, which form by the repeated thermal contraction and expansion of the upper layers of the permafrost (Steedman et al., 2016). These features appear as raised rims with lower-lying, often wet channels called troughs. Polygons can be classified as low-centered (with wet centers and raised rims) or high-centered (with well-drained centers and lower rims). Due to the strong thermal, hydrological, and geochemical gradients in these landforms (Vaughn et al., 2016), organic matter (OM) mineralization processes are still not well understood.

Polygonal patterned grounds cover 10% of the Tuktoyaktuk Coastlands (North-West Territories) (Martin et al., 2018), a region affected by high coastal retreat rates due to erosion, ground subsidence and sea level rise (Hill et al, 1993; Hynes et al., 2014 Lim et al., 2020).

During the early Holocene, Tuktoyaktuk was located 100 km further inland as the sea level was considerably lower (Vardy, 1997). With ongoing and projected amplification of coastal retreat, important amount of terrestrial soil and sediments continues to become part of the ocean seafloor by transport and deposition (Whalen et al., 2022). Due to historical sea level rise, permafrost extends far offshore in the Beaufort Sea, composed of relict terrestrial permafrost (Erkens et al., 2024). Furthermore, intrusion of saltwater into soils and seafloor sediments could accelerate permafrost degradation by thickening the active layer (Irrgang et al., 2022), exposing long-term preserved frozen organic matter (Schuur et al., 2008) to microbial decomposition, which produces CO<sub>2</sub> and CH<sub>4</sub> (Lapham et al., 2020; Pellerin et al., 2022; Schuur et al., 2015). However, there is limited information available on the response of active layer and permafrost soils to saltwater intrusion. For example, under ocean submersion, such as occurs in subsea permafrost, and due to subsidence or storm events, CH<sub>4</sub> production might be inhibited by the presence of thermodynamically favored alternative electron acceptors such as sulfate contained in seawater, resulting in the predominance of CO<sub>2</sub> production through sulfate-reduction (Winfrey and Ward, 1983). Therefore, understanding the interplay between hydrological conditions, micrographic polygonal features and the presence of electron acceptors is crucial to elucidate how long-frozen OM is processed upon thawing (Jones et al., 2020) both on land and in the seafloor.

In the past years, numerous studies have attempted to quantify CH<sub>4</sub> production rates in permafrost soils because of the uncertainties related to the contribution of northern soils to the global carbon budget (Schuur et al., 2022). These incubation studies measured CH<sub>4</sub> production rates varying by 3 to 4 orders of magnitude between sites and studies (Treat et al., 2015). This highlights that controls on CH<sub>4</sub> production are still hardly constrain and that more work is needed to obtain a comprehensive portrait of methane dynamics in northern soils.

Methanogenesis, carried out by archaea, involves two primary pathways of decomposition (Conrad, 2020). Acetoclastic methanogenesis, the cleavage of acetate, is associated to ecosystems with higher OM lability (Hodgkins et al., 2014). Hydrogenotrophic methanogenesis, the reduction of CO<sub>2</sub> and H<sub>2</sub>, is mostly associated with older and more

recalcitrant plant material (Duddleston et al., 2002; Heffernan et al., 2022; Prater et al., 2007). It is possible to distinguish these two production pathways by the analysis of  $^{13}\text{C}$ - $\text{CH}_4$ . Acetoclastic methanogenesis produces  $^{13}\text{C}$  isotopic signatures typically in the range of -65‰ to -50‰, while hydrogenotrophic methanogenesis produces  $^{13}\text{C}$  in the range of -110‰ to -60‰ (Hornibrooke et al., 1997). Methane production in permafrost soils is contingent on multiple factors with complex interactions, but distinguishing between production pathways can provide insights into the controls of  $\text{CH}_4$  production as the microbial community present in soils is influenced by environmental conditions (Holm et al., 2020).

This study aims to (1) determine if OM degradation processes in a context of marine submersion differ between polygonal landforms and (2) identify potential subsea permafrost thaw OM degradation processes. To achieve this, soil samples from the active layer and permafrost were collected from a polygonal terrain of Tuktoyaktuk. They were incubated with brackish water under anoxic conditions to measure  $\text{CH}_4$  production rates. Soil geochemical analyses and stable carbon isotopic signature of  $\text{CH}_4$  were conducted to support the incubation experiment.

## **2.4 METHODOLOGY**

### **2.4.1 Site description and sampling**

Tuktoyaktuk (69°26'24'' N, 133°01'52''W) is located in the Inuvik region of the North-West Territories, adjacent to the Arctic Ocean. Its permafrost is characterized by prevalent ground ice structures (Mackay and Dallimore, 1992) and thick peat deposits (Martin et al., 2018). The region experiences prolonged cold winters, short cool summers, and year-round low precipitations, fostering low-arctic tundra vegetation. The selected site, Reindeer Point (RP), reflects the high-centered and low-centered polygonal patterned grounds found across the region.

Three cores were collected from RP, located 2 km east of Tuktoyaktuk. This patterned ground is located in a depression, surrounded by elevated plateaus. RP01 was retrieved from

the center of a low-centered polygon. The collected core measured 65 cm and was characterized by peat deposits and ice lenses (Fig 18, a). RP02 measured 95 cm and was retrieved from the center of a high-centered polygon with permafrost soils comprising dark grey decomposed organic matter with silt layers and ice lentils getting more abundant with depth (Fig 18, b). RP03 was retrieved from the middle of the slope of the plateau surrounding the patterned ground. The collected core measured 55 cm and was characterized by a mix of organic and mineral materials with low ground-ice content (Fig 18, c).



**Figure 18.** Pictures of permafrost cores collected in the polygonal patterned ground of Reindeer Point. Active layer section not shown. Panel a) is RP01, b) is RP02 and c) is RP03.

Samples were collected in August 2022 (RP01 and RP02) were merged with a supplemental core collected in August 2023 (RP03). The active layer samples were retrieved according to the sampling technique described by Roy-Lafontaine et al. (in submission). The

permafrost samples were collected with a SIPRE mechanical hand auger. The cores were immediately sub-sampled in the field every 10 cm using a saw and the core sections were transferred in whirl-pack bags. Water samples for the incubation experiment were collected from the coast in plastic bottles and were kept cool at 4°C.

#### **2.4.2 Methane production rates in incubation experiment**

Collected soil samples were transferred in 20 mL glass vials where brackish water was added for anoxic incubations. Soil samples from 2022 were put in brackish water incubations on field according to the method described by Roy-Lafontaine et al. (in submission). Four replicates per depth were prepared; three were kept for CH<sub>4</sub> production rates and one was kept for <sup>13</sup>C-CH<sub>4</sub> analyses. Samples from 2023 were brought back frozen and incubations were prepared in the laboratory where they were thawed overnight at 4°C and transferred in incubation vials according to Roy-Lafontaine et al. (in submission). Three replicates per depth were prepared for the measurements of CH<sub>4</sub> production rates. The samples were incubated at 4°C. Incubations from 2022 lasted 339 days while incubations from 2023 lasted 269 days. Active layer incubations from RP01 and RP02 were presented in Chapter 1 of this thesis, while all other incubations are presented for the first time in this chapter. CH<sub>4</sub> production rates were calculated by measuring the change in headspace concentrations of CH<sub>4</sub> over time following Roy-Lafontaine et al. (in submission). Values are expressed in nmol cm<sup>-3</sup> d<sup>-1</sup> and the error represents the standard deviation on the mean of triplicate vials.

#### **2.4.3 Geochemical analyses on soil samples**

The total organic carbon (TOC) content and the δ<sup>13</sup>C-TOC of the soils from cores RP01 and RP02 was determined following the method described by Roy-Lafontaine et al. (in submission). Results for TOC are expressed as % wt. C. and results for δ<sup>13</sup>C-TOC are expressed in ‰ relative to Vienna Pee Dee Belemnite (VPDB). Core RP03 was not analyzed for TOC. Chloride (Cl<sup>-</sup>) and sulfate (SO<sub>4</sub><sup>2-</sup>) in soil were measured following Roy-Lafontaine

et al. (in submission), with results expressed in  $\text{mmol g}^{-1}$  wet-weight<sup>-1</sup>. The uncertainty was estimated by a least squares method (Skoog et al., 2014).

#### **2.4.4 Stable carbon isotopic composition of methane**

One replicate vial from each sampled depth in cores RP01 and RP02 was retained for the analysis of the stable carbon isotopic composition of headspace methane ( $\delta^{13}\text{C-CH}_4$ ) following Roy-Lafontaine et al. (in submission). All  $\delta^{13}\text{C-CH}_4$  values are expressed relative to Vienna Pee Dee Belemnite (VPDB). Values were more precise than  $\pm 1.2\%$ .

### **2.5 RESULTS**

#### **2.5.1 Soil characterization and geochemical composition**

Soils retrieved from Reindeer Point exhibited relatively high TOC content, with values ranging from 8.9% to 46.1% (Fig 19). Distinct variations were observed between RP01 and RP02, with TOC content ranging from 35.1% to 46.1% and 8.9% to 22.5% respectively. In the active layer, the TOC content from RP01 decreased with depth, starting at 46.1% at 10 cm and reaching 36.7% at the permafrost interface (35 cm). Within the permafrost, TOC increased with depth, peaking at 45.0% at the base of the core (60 cm). Conversely, in RP02, TOC content increased from 15.7% to 22.5% between 10 to 25 cm depth, followed by a decline to 14.0% at the active layer-permafrost interface. In the permafrost, TOC content decreased slightly to 8.9% at 50 cm depth, then increased to 10.8% at 95 cm depth. The  $\delta^{13}\text{C-TOC}$  values of both cores were similar and remained constant with depth, ranging from -24.6‰ and -27.0‰.



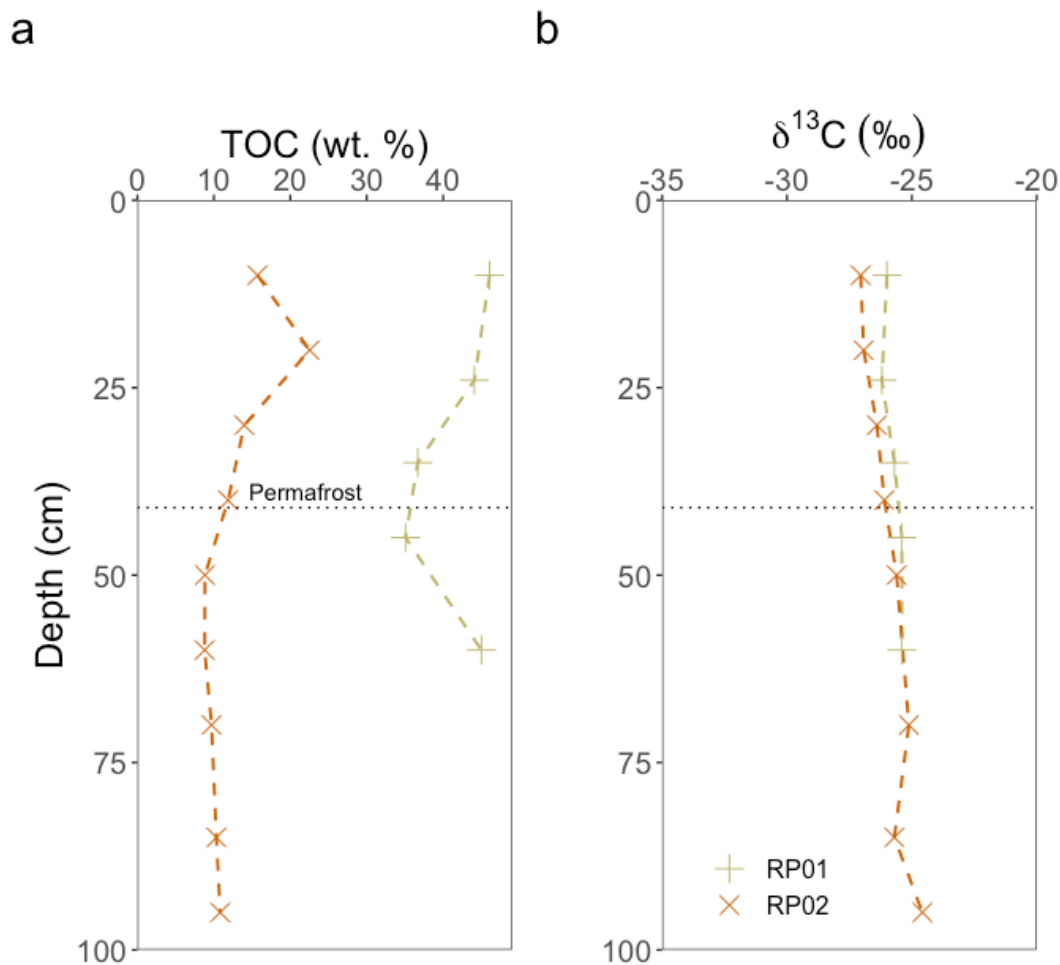


**Figure 19.** Vertical distribution of (a) total organic carbon (TOC) and (b)  $\delta^{13}\text{C}$  of soils used in the incubation experiment of cores RP01 and RP02. Data for RP03 are not available. The black horizontal dotted line represents the active layer-permafrost interface. Active layer data for RP01 and RP02 were presented in the Chapter 1 of this manuscript. This color scheme is used consistently throughout the manuscript.

$\text{Cl}^-$  concentrations were very low in each sampled core with values ranging from  $0.4 \pm 0.1 \text{ mmol g}^{-1} \text{ wweight}^{-1}$  to  $1.8 \pm 0.1 \text{ mmol g}^{-1} \text{ wweight}^{-1}$  (Fig 20, a). Sulfate concentrations were close to the detection limit throughout the active layer of sampled cores and stayed null in the permafrost horizon of core RP01 (Fig 20, a). However, at the active layer-permafrost interface of core RP02, sulfate concentrations peaked to  $2.50 \pm 0.03 \text{ mmol g}^{-1} \text{ wweight}^{-1}$ . Concentrations then gradually decreased to  $0.30 \pm 0.03 \text{ mmol g}^{-1} \text{ wweight}^{-1}$  at 70 cm.

Following a see-saw pattern, they increased back to  $1.40 \pm 0.03 \text{ mmol g}^{-1} \text{ wweight}^{-1}$  at 85 cm depth and finally decreased again to reach  $0.40 \pm 0.03 \text{ mmol g}^{-1} \text{ wweight}^{-1}$  at 95 cm, the base of the core.

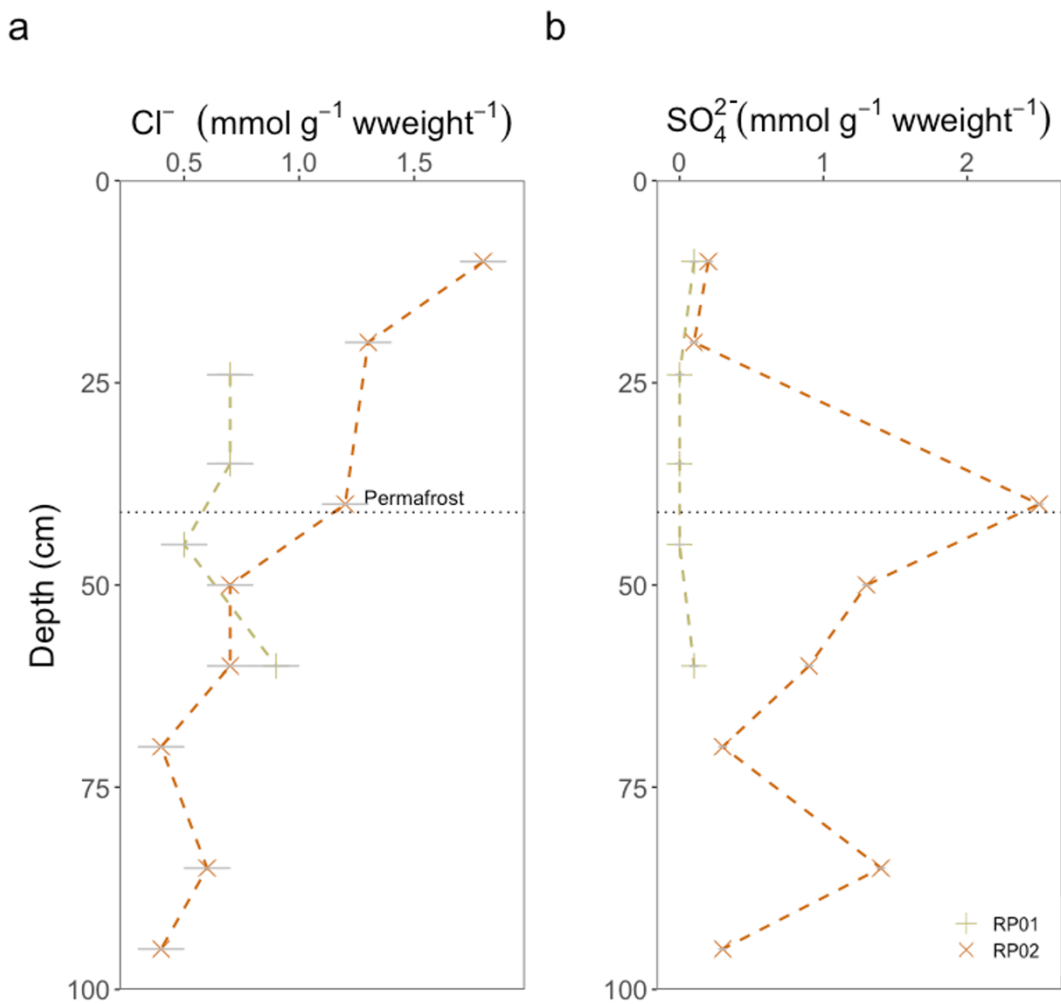


**Figure 20.** Depth profiles of geochemical analyses conducted on sub-sampled cores used for the incubation experiment. Panel (a) shows chloride concentrations and panel (b) shows sulfate concentrations results from the leaching process. Chloride and sulfate concentrations

are expressed in  $\text{mmol g}^{-1}$  wet-weight<sup>-1</sup>. This color scheme is used consistently throughout the manuscript. Data for core RP03 is not available.

### **2.5.2 Incubations methane production rates**

Incubations were amended with brackish water, containing  $5.7 \text{ mmol g}^{-1}$  wweight<sup>-1</sup> of sulfates and  $28.7 \pm 0.5 \text{ mmol g}^{-1}$  wweight<sup>-1</sup> of  $\text{Cl}^-$ . In the depth profiles of RP02 and RP03,  $\text{CH}_4$  production rates increased with depth. Conversely,  $\text{CH}_4$  production rates in profile of RP01 decreased with depth (Fig 21).

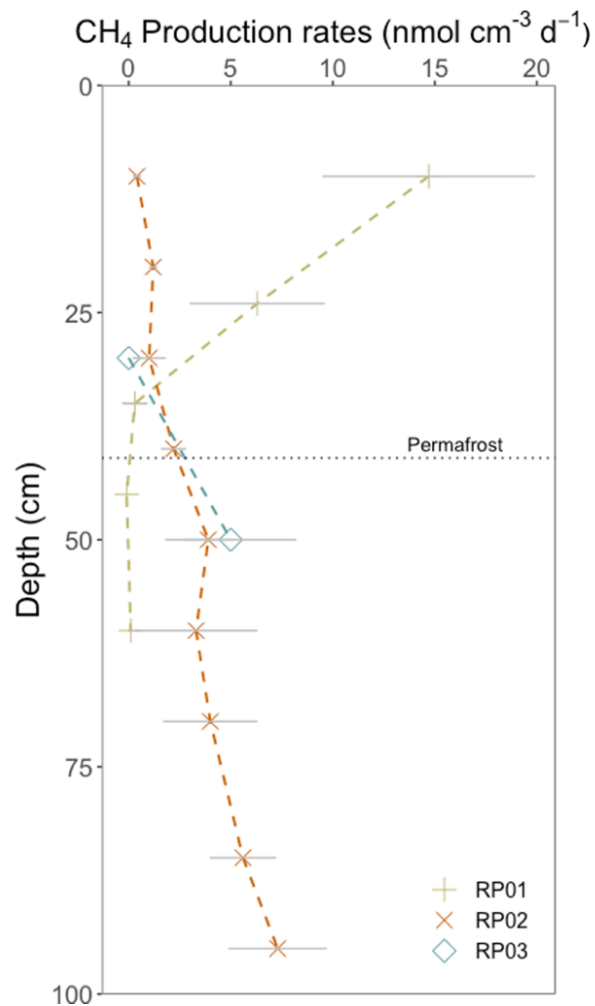


**Figure 21.** CH<sub>4</sub> production rates in anoxic and water saturated incubations derived from soil collected in cores RP01, RP02 and RP03. Each datapoint represents the mean value of three incubations with the error bar representing the standard deviation on the triplicates.

RP02 exhibited its lowest CH<sub>4</sub> production rates in the active layer, ranging between  $0.4 \pm 0.2$  nmol cm<sup>-3</sup> d<sup>-1</sup> and  $1.2 \pm 0.2$  nmol cm<sup>-3</sup> d<sup>-1</sup>. At 40 cm depth, marking the active layer-permafrost interface, CH<sub>4</sub> production rates doubled to  $2.2 \pm 0.6$  nmol cm<sup>-3</sup> d<sup>-1</sup> and continued to increase to reach  $7.3 \pm 2.4$  nmol cm<sup>-3</sup> d<sup>-1</sup> at 95 cm depth. A similar pattern is observed at RP03 where CH<sub>4</sub> production rates increase with depth. In the active layer, at 30 cm, the

calculated CH<sub>4</sub> production rate was null, while it increased to  $5.0 \pm 3.2$  nmol cm<sup>-3</sup> d<sup>-1</sup> in the permafrost horizon at 50 cm depth. RP01 had maximum CH<sub>4</sub> production rates closest to the surface at 10 cm, with  $14.7 \pm 5.2$  nmol cm<sup>-3</sup> d<sup>-1</sup> and decreased to  $0.3 \pm 0.6$  nmol cm<sup>-3</sup> d<sup>-1</sup> at 35 cm depth, just above the active layer-permafrost interface. Along the permafrost horizon, CH<sub>4</sub> production rates were null.

### 2.5.3 Isotopic composition of <sup>13</sup>C-CH<sub>4</sub> produced in incubations

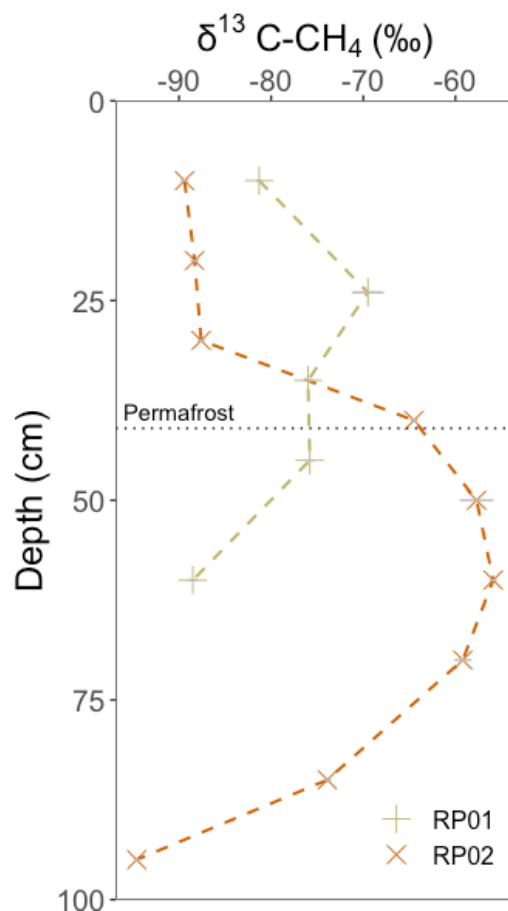


**Figure 22.** Stable carbon isotopic composition of CH<sub>4</sub> produced in soil incubations of RP01 and RP02, collected at Reindeer Point. Each value corresponds to the mean value of two or three measurements done on one incubation, depending on the CH<sub>4</sub> headspace concentration.

The error bar on each point represents the analytical uncertainty on the measured value. RP01 had null production in the thawed permafrost, but the incubations contained enough CH<sub>4</sub> to perform the stable carbon isotopes analyses.

$\delta^{13}\text{C-CH}_4$  values in the active layer of RP01 increased with depth, ranging from -81.3‰ to -69.5‰ and stayed consistent through the transition with the permafrost horizon at -75.8‰ until 45 cm (Fig 22). In the lowest part of the permafrost, values became more depleted in <sup>13</sup>C, reaching -88.5‰ at 60 cm depth. In the active layer of core RP02,  $\delta^{13}\text{C-CH}_4$  was stable with increasing depth, ranging from -89.4‰ to -87.6‰. However, at the active layer-permafrost interface,  $\delta^{13}\text{C-CH}_4$  was measured at -64.5‰, marking a great enrichment in <sup>13</sup>C relatively to the active layer (Fig 22). This enrichment continued, peaking at -55.9‰ at 60 cm. In the lower part of the permafrost, measured values became progressively depleted, reaching -94.6‰ at 95 cm depth.

## **2.6 DISCUSSION**

### **2.6.1 Addition of brackish water to incubations**

This study attempts to evaluate how brackish water intrusion in terrestrial soils could influence CH<sub>4</sub> production rates in the thawed permafrost tundra soils of Tuktoyaktuk. Soil incubations were amended with brackish water containing 5.7 mmol g<sup>-1</sup> wweight<sup>-1</sup> of sulfate, a substrate used for sulfate-reduction which is thermodynamically more favorable than methanogenesis (Oremland and Polcin, 1982). Thus, supplying sulfate, a higher yielding electron acceptor, to sulfate-poor, organic-rich soils could promote microbial sulfate-reduction, potentially slowing or inhibiting methanogenesis. However, our results demonstrated that this is not the case, as production was detected in most incubations of both the active layer and permafrost. This non-inhibition of methanogenesis suggests that saltwater intrusion in terrestrial tundra soils could potentially support methane production despite ample availability of electron acceptors. This was unexpected and perplexing. In the following sections, we tried to identify the main controls on methane production in thawed

permafrost and the control of local depositional, hydrological, geochemical and microbial conditions that could explain these unexpected observations.

CH<sub>4</sub> production rates measured in incubations of this study ranged from null to 15.7 nmol cm<sup>-3</sup> d<sup>-1</sup>, while CH<sub>4</sub> production rates recorded in active layer incubations of the Yamal Peninsula in Northwest Siberia ranged between 0.1 and 33.8 nmol cm<sup>-3</sup> d<sup>-1</sup> (Heyer et al., 2002). Furthermore, a study on a 12m core of permafrost sampled in Tuktoyaktuk and composed of fluvio-glacial sediment deposits showed methane production rates in incubations between zero and 13 nmol cm<sup>-3</sup> d<sup>-1</sup> (Lapham et al., 2020). While incubations from Heyer (2002) and from Lapham (2020) were performed without addition of water, our measured CH<sub>4</sub> production rates are comparable.

### **2.6.2 A contrasting correlation between TOC and CH<sub>4</sub> production rates**

While a correlation between TOC content and CH<sub>4</sub> production rates was observed (Fig 23), the patterns differed between active layer and permafrost sites. In both RP01 and RP02, the pattern observed in the active layer was not replicated in the permafrost. In the brackish water incubations of the active layer of RP01, the low-centered polygon composed exclusively of peat, CH<sub>4</sub> production rates appeared positively correlated with TOC (Fig 23). Conversely, in the thawed permafrost brackish water incubations of the same profile, RP01, a lack of CH<sub>4</sub> production was measured despite being in the highest TOC range (Fig 23). Furthermore, the very negative  $\delta^{13}\text{C-CH}_4$  (-90‰) values along the depth profile of RP01 are associated with the degradation of more recalcitrant OM compounds and the less energy favorable process of hydrogenotrophic methanogenesis (Heffernan et al., 2022). This may indicate that the thawed peat provides low quality OM for the microbial community to degrade, leading to slowed CH<sub>4</sub> production (Heffernan et al., 2022). This suggests that some more favored biogeochemical processes might be inhibiting CH<sub>4</sub> production.

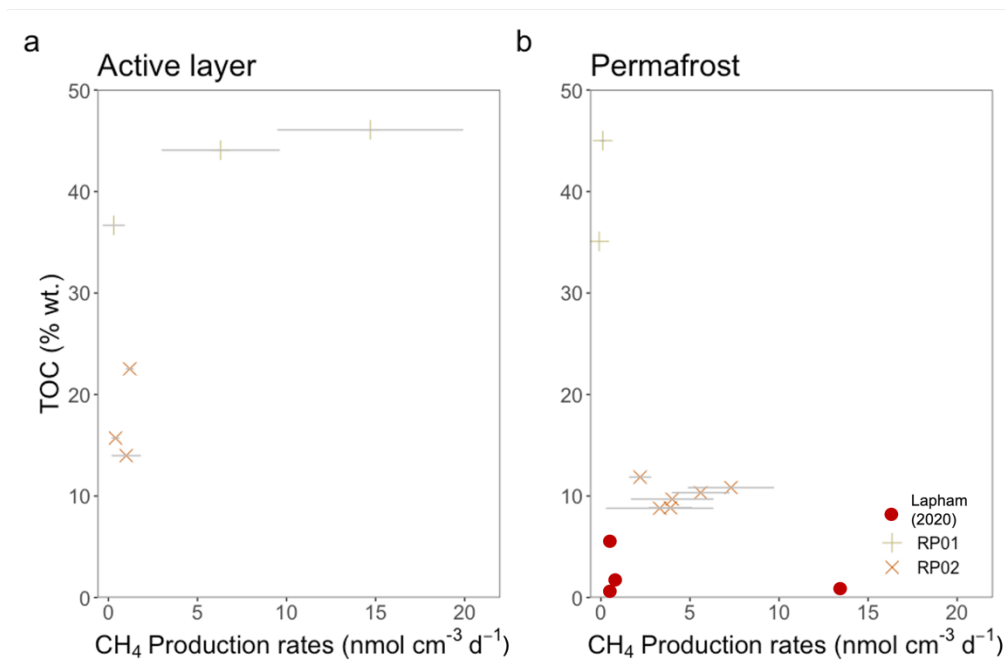


**Figure 23.** Relationship between CH<sub>4</sub> production rates and TOC content from (a) the active layer and (b) the permafrost at RP01 and RP02. Red circles represent the data from the study conducted in Tuktoyaktuk from Lapham et al. (2020).

In the brackish water incubations of the active layer of RP02, the high-centered polygon, no clear trend between TOC and CH<sub>4</sub> production was observed (Fig 23). However, in the brackish water incubations of the thawed permafrost, a positive relationship between TOC and CH<sub>4</sub> production rates was observed, where increasing TOC content led to increased CH<sub>4</sub> production rates (Fig 23). This may be explained by the preservation of organic substrates in perennially frozen permafrost where they may have not been actively degraded by microbial activity (Dutta et al., 2006; Knoblauch et al., 2018). While CH<sub>4</sub> production rates remained relatively low, they more than doubled in the permafrost horizon relative to the active layer, suggesting that the thawing of permafrost OM supplies substrates for microbial communities to degrade.

This is further supported by an observed shift in  $\delta^{13}\text{C}\text{-CH}_4$  from very negative values, typically associated with hydrogenotrophic methanogenesis, in the active layer to less



negative values associated with the degradation of more labile OM through acetoclastic methanogenesis in the upper part of the permafrost (fig 22, RP02) (Heffernan et al., 2022; Hodgkins et al., 2014). When thawed, these more labile compounds become available for microbial communities which can process these substrates more easily, leading to higher CH<sub>4</sub> production (Hodgkins et al., 2014). However, in the lower part of the permafrost,  $\delta^{13}\text{C-CH}_4$  values returned to those associated with hydrogenotrophic methanogenesis, but still with increasing CH<sub>4</sub> production rates likely a consequence of the increasing TOC (Fig 22). The same trend of increased CH<sub>4</sub> production in the permafrost relative to the active layer was observed in the brackish water incubations of RP03, a well-drained tundra site comparable to RP02. Although TOC and  $\delta^{13}\text{C-CH}_4$  data are unavailable for RP03, the increased CH<sub>4</sub> production in the permafrost compared to the active layer is likely driven by the same process. Consequently, in this type of permafrost environment, our results suggest that submersion by brackish water could support methanogenesis upon thaw regardless of the electron acceptor availabilities.

RP01 and RP02 were located only 20 m apart but the trends observed between TOC content and CH<sub>4</sub> production rates in this set of brackish water incubations varied spatially. A positive relationship between TOC and CH<sub>4</sub> production rates was observed in the active layer of RP01, but not RP02 (Fig 23). Conversely, a positive correlation between TOC and CH<sub>4</sub> production rates was observed in the permafrost horizon of RP02 but not RP01 (Fig 23). RP01, a low-centered polygon and RP02, a high-centered polygon, have different microtopography which influences OM degradation processes (Vaughn et al., 2016). Furthermore, although Lapham et al. (2020) found a similar range of CH<sub>4</sub> production rates in their sediments incubations carried out on a core collected in Tuktoyaktuk, no trend between TOC and CH<sub>4</sub> production rates was observed (Fig 23). As these results contrast with ours, their study was carried out between 60 cm and 12 m depth, where sediments were mainly composed of glaciofluvial deposits with low TOC content (Lapham et al., 2020), whereas our study focused on the first meter of organic rich soils. While we were able to demonstrate a relationship between CH<sub>4</sub> production rates and TOC in this set of brackish

water incubations, several questions remain unanswered to identify the controls on methane production.

Future studies should look further into the nature of the OM that drives methane production between the active layer and the permafrost. This could be done by Rock-Eval pyrolysis which can identify the different fractions of labile compounds responsible for driving biogeochemical cycles (Sanei et al., 2012). Ramped pyrolysis oxidation could also be used to further analyze the labile fraction of OM (Gillespie et al., 2014). These techniques could give insights in degradation of organic substrates between permafrost and active layer. Furthermore, iron (Fe(III)) concentrations in peatland soils, like RP01, should be investigated. Fe(III) is an electron acceptor that has a clear role in slowing and inhibiting methanogenesis in northern peatland ecosystems (Lipson et al., 2010 ; Van Bodegom et al., 2004; Ye et al., 2016). This could be done by applying the citrate-dithionite iron reduction method where all reactive solid iron phases and the organic carbon associated with these minerals into solution are dissolved and released (Lalonde et al., 2012; Mehra et al., 1958; Mu et al., 2016; Patzner et al., 2020). With this method, we can quantify (1) iron reactive species and (2) the amount of organic carbon that is bonded to the reactive iron species.

Furthermore, a set of control incubations drawn out with distilled water, could be helpful in precisely determining how the addition of brackish water in incubations affected CH<sub>4</sub> production. Additionally, soil samples from 2023 were frozen before incubation, while 2022 samples were incubated directly. Although this might affect microbial communities, no significant difference in CH<sub>4</sub> production rates was observed, suggesting the process did not bias the results. Accurately assessing the controlling factors of CH<sub>4</sub> production, especially in the context of terrestrial soils and brackish water interactions where studies are lacking, is crucial for estimating CH<sub>4</sub> dynamics of the rapidly changing Arctic. This experiment provides insights into OM degradation processes occurring through ocean submersion of terrestrial soils and on processes occurring in subsea permafrost, a dynamic that is hard to study because of the often-deep location of permafrost in the seafloor (Erkens et al., 2024).

## 2.7 CONCLUSION

Our incubation experiment highlights that CH<sub>4</sub> production in active layer and permafrost terrestrial soils in relation with brackish water is contingent on total organic carbon content, with evidence that *in situ* geochemical conditions held by soils can also play a significant role. Possible preservation of organic substrates in permafrost led to enhanced CH<sub>4</sub> production in thawed permafrost incubations of high-centered polygon and dry tundra soils. Conversely, very low CH<sub>4</sub> production was measured in the incubations conducted from a thawed permafrost peatland. We could not elucidate why we observed very low production with our dataset. It may be that the presence of humic acids and/or Fe(III), prevalent compounds in northern peatlands, which, when thawed, could act as alternative electron acceptor and be preferentially processed by microbial communities, limiting CH<sub>4</sub> production. This will need to be further investigated in subsequent studies. Thus, the observed production trends have implications in the event of ground subsidence and marine submersion observed in the Tuktoyaktuk landscape, but it also gives insights on OM degradation processes in subsea permafrost. Future research should aim to further elucidate the interactions between soil chemistry, microbial communities, and seawater which is essential to better constrain future methane emissions from the Arctic.

## 2.8 ACKNOWLEDGEMENTS

We thank Santiago Mareque for assistance during field sampling. Mathieu Babin and Thi Hao Bui are acknowledged for assisting with the laboratory work performed at Université du Québec à Rimouski and at McGill University, respectively. Takuvik Laboratory is acknowledged for providing analyses and results on  $\delta^{13}\text{C}$  and TOC content of sediments. We also thank the Tuktoyaktuk community for providing wildlife monitors with insightful information on the territory during field sampling. This research was funded by NSERC Discovery Grant with Northern Supplement to AP. ARL acknowledges financial support

from the NSTP program. PMJD acknowledges support from the NSERC Discovery Grant and the Canadian Foundation for Innovation.

## CONCLUSION GÉNÉRALE

Le travail de recherche présenté dans ce mémoire a permis de quantifier les taux de production de CH<sub>4</sub> ainsi que d'étudier les dynamiques de cette production à l'interface continent-océan dans une région de pergélisol continue particulièrement affectée par l'amplification du recul du trait de côte (Tuktoyaktuk, TNO). La quantification des taux de production de CH<sub>4</sub> a été possible grâce à l'utilisation de techniques d'incubations anaérobiques de sols et de sédiments ainsi d'eau récoltée à la région d'étude. Des analyses géochimiques sur les échantillons de sols et d'eau ainsi que les analyses isotopiques sur le CH<sub>4</sub> produit dans les incubations ont supporté les résultats des taux de production. L'originalité de cette étude résidait dans l'ajout d'eau de l'environnement aux incubations, qui permet d'obtenir des observations plus réalistes des processus *in situ* de dégradation de la MO. Avant cette étude, la majorité des études d'incubations n'ajoutaient pas d'eau ou ajoutaient de l'eau distillée (ex : Heyer et al., 2002 ; Knoblauch et al., 2018 ; Lapham et al., 2020 ; Lipson et al., 2012 ; Pellerin et al., 2022), qui impose un biais méthodologique puisque les eaux de fonte des coins de glace et des étangs de dégel des régions d'études comportent leurs propres amalgames de MO, de nutriments, d'accepteurs alternatifs d'électrons et de microorganismes qui influencent les processus de dégradation de MO (Bianchi et al., 2011).

L'hypothèse posée en amont du projet était l'inhibition de la production de CH<sub>4</sub> dans les sols pergélisolés de Tuktoyaktuk par l'addition inhérente de sulfates contenus dans l'eau de mer, un accepteur d'électrons qui favorise la sulfato-réduction, processus thermodynamiquement favorable à la méthanogénèse. Les résultats d'incubations ont infirmé l'hypothèse posée. Malgré des concentrations en sulfates relativement élevées (5–14 mmol g<sup>-1</sup> wweight<sup>-1</sup>) dans les sols de Toker Point, le site côtier, des taux de production de CH<sub>4</sub> supérieurs à ceux mesurés à Reindeer Point, le site non-côtier, ont été mesurés. Bien que les résultats ne permettent pas d'isoler les causes exactes de cette dynamique, les résultats des

analyses du  $\delta^{13}\text{C}-\text{CH}_4$  produit dans les incubations révèlent une dominance de la méthanogénèse acétoclastique dans les échantillons de surface de Toker Point, processus de production typiquement associé à de la MO plus labile. Ainsi, il est supposé que la connectivité du site avec la mer Beaufort ainsi que la présence abondante de matière fécale d'oiseaux favoriserait la méthanogénèse à cause d'apports en nutriments et en MO fraîche. Dans une perspective d'augmentation des taux de subsidence et d'érosion côtière de la région (Costa, 2022), cette découverte révèle que la production de  $\text{CH}_4$  pourrait être favorisée dans l'environnement côtier de la mer de Beaufort. Dans les sédiments marins récoltés, aucune production de  $\text{CH}_4$  n'a été détectée. Cependant, le projet se limite à l'étude des processus de production de  $\text{CH}_4$ , qui ne représente qu'une importante portion du cycle du carbone. En effet, les processus d'oxydation du  $\text{CH}_4$  dans les couches d'eau sus-jacentes en contexte de submersion par l'océan, pourraient limiter les concentrations de  $\text{CH}_4$  émises vers l'atmosphère (Li et al., 2022).

La deuxième portion de l'étude s'est penchée sur les processus de production de  $\text{CH}_4$  dans le pergélisol dégelé à partir d'échantillons de sols polygonaux, en simulant une submersion côtière. Cette étude apporte également un regard sur les processus de dégradation de la MO dans le pergélisol sous-marin, qui sont difficiles à étudier en raison de la profondeur significative à laquelle il peut se trouver dans le plancher océanique (Erkens et al., 2024). La détection de la méthanogénèse dans les incubations de pergélisol dégelé réfute encore une fois l'hypothèse selon laquelle l'ajout de sulfates, présents dans l'eau saumâtre utilisée, inhiberait la méthanogénèse.

Cependant, des résultats contrastants ont été observés : dans deux des trois sites, les taux de production de  $\text{CH}_4$  ont augmenté dans les incubations de pergélisol dégelé par rapport à la couche active. L'augmentation des taux de production de  $\text{CH}_4$  dans l'horizon de pergélisol a été mesurée à des sites similaires constitués de toundra bien drainée, alors qu'aucune production n'a été mesurée dans les incubations de pergélisol dégelé de la tourbière saturée en eau. Bien qu'elle ne fût pas systémique, il y avait une tendance entre les taux de production de  $\text{CH}_4$  et le contenu en TOC dans les sols. Dans le profil du pergélisol

dégelé du polygone à centre élevé, une augmentation des taux de production avec une augmentation du TOC a été observée, alors que le profil de pergélisol dégelé de la tourbière n'a produit aucun CH<sub>4</sub> malgré un contenu important en TOC (35-45%). Nos résultats ne permettent pas de cerner les mécanismes précis des différentes tendances de production de CH<sub>4</sub> observées dans l'étude. Cependant, ils soulignent l'importance de l'influence des conditions géochimiques locales dans les processus de production de CH<sub>4</sub>, même en contexte de simulation de submersion océanique. Il est suggéré que les conditions de pergélisol préservent la qualité des substrats organiques, lesquels sont favorables à la dégradation par les microorganismes à la suite du dégel. Ce principe pourrait expliquer l'augmentation des taux de production de CH<sub>4</sub> dans les échantillons de pergélisol dégelé du polygone à centre élevé avec l'augmentation du contenu en TOC des sols, supporté par l'acétotrophie mesurée dans la portion supérieure de l'horizon de pergélisol. À l'inverse, ce principe ne peut pas expliquer le manque de production de CH<sub>4</sub> dans la tourbière de pergélisol dégelée du polygone à centre bas. Les tourbières sont des écosystèmes qui peuvent être riches en fer, qui sont des accepteurs d'électrons qui favorisent la respiration anaérobie, relativement à la méthanogénèse. Ainsi, ces espèces pourraient être consommées en priorité de la méthanogénèse lors du dégel, favorisant les processus de respiration anaérobie. Ce mécanisme est proposé comme piste, mais plusieurs questions restent en suspens. Nous pouvons conclure en avançant que la méthanogénèse dans les sols terrestres de pergélisol ne semble pas être inhibée par la présence de sulfates dans l'eau saumâtre de la mer de Beaufort (5,7 mmol g<sup>-1</sup> w-weight<sup>-1</sup>), qui est la plus grande découverte de cette étude et que les conditions géochimiques locales des sols sont des variables importantes à considérer dans les dynamiques de production de CH<sub>4</sub>.

## **PERSPECTIVES**

Cette étude a permis une compréhension des interactions entre les microorganismes, les formes microtopographiques du pergélisol et l'océan Arctique sur la minéralisation de la MO en contexte de submersion océanique. Dans les futures études, il serait pertinent d'ajouter une série d'incubations « contrôle », réalisées avec de l'eau distillée afin d'évaluer

de façon précise l'influence de l'eau de mer sur les taux de production de CH<sub>4</sub>. De plus, certaines analyses sont manquantes afin de pouvoir expliquer avec certitude les résultats observés. Par exemple, la caractérisation de la MO pourrait permettre d'évaluer plus précisément sa labilité intrinsèque ainsi que d'identifier la présence de MO marine dans les sols côtiers, s'il y a lieu. Par exemple, les techniques d'analyses par pyrolyse analytiques, comme l'oxydation par pyrolyse à température programmée, permettraient d'obtenir des informations précises sur la quantité et la qualité du carbone organique contenu dans des échantillons complexes (Gillespie et al., 2014), comme ceux récoltés dans la région de Tuktoyaktuk, et de lier ces résultats à ceux des taux de production de CH<sub>4</sub>. De plus, il a été tenté d'analyser la signature du d<sup>2</sup>H du CH<sub>4</sub> produit dans les incubations. Les tentatives ont échoué à cause des interactions entre le sulfure d'hydrogène présent dans les incubations et le CH<sub>4</sub>, faussant les résultats et affectant la répétabilité des mesures. Cependant, la combinaison des analyses du <sup>13</sup>C-CH<sub>4</sub> et du d<sup>2</sup>H pourrait permettre de confirmer ou d'infirmer l'hypothèse posée de l'occurrence de la méthanogénèse issue de substrats non-compétitifs dans le premier article présenté dans ce mémoire et d'isoler de façon plus précise les mécanismes microbiens responsable de la production de CH<sub>4</sub> dans les différents sols (Bueno de Mesquita et al., 2023). Afin de de brosser un portrait plus complet du cycle du CH<sub>4</sub> de la région, l'analyse des processus d'oxydation du CH<sub>4</sub> dans les incubations réalisées auraient pu être évalué. L'ajout de CH<sub>4</sub> à composition connue de <sup>13</sup>C permettrait de calculer la portion de CH<sub>4</sub> consommée par les microorganismes dans les incubations (Vigderovich et al., 2022), identifiant ainsi le potentiel d'oxydation anaérobique dans les sols et d'obtenir les taux bruts de production de CH<sub>4</sub>. Finalement, l'ajout des mesures des taux de production du CO<sub>2</sub> ainsi que de la signature isotopique du <sup>13</sup>C-CO<sub>2</sub> pourrait aider à identifier plus précisément les voies de décomposition de la MO et de quantifier la décomposition totale dans l'environnement étudié.

Dans un contexte de réchauffement rapide des températures de l'Arctique, il importe de mieux comprendre les processus de dégradation de la MO à l'interface continent-océan, qui peuvent contribuer à l'amplification de l'effet de serre global. En réponse à l'épaississement de la couche active, une plus grande quantité de MO se trouve disponible à



la dégradation par les microorganismes (Lapham et al., 2020) et couplé à l'augmentation des taux de retrait côtiers et de l'augmentation du niveau marin (Lim et al., 2020 ; Hill et al., 1993), les dynamiques de dégradation de MO se trouvent modifiées par les interactions avec l'eau de mer. Peu de données et d'études sont disponibles sur ces processus, alors que 65% des côtes de l'Arctique sont constituées de dépôts meubles (Irrgang et al., 2022). Les résultats de ce mémoire sont appliqués à l'échelle locale, mais il serait crucial de les intégrer à une échelle plus large, car leurs implications pourraient avoir un impact significatif sur le climat global.

**ANNEXE 1: METHANE PRODUCTION IN A COASTAL PERMAFROST  
REGION OF THE CANADIAN ARCTIC (TUKTOYAKTUK, NWT)**



## Methane production in a coastal permafrost region of the Canadian Arctic (Tuktoyaktuk, NWT)

Alexie Roy-Lafontaine<sup>1</sup>, Rebecca Lee<sup>2</sup>, Dustin Whalen<sup>2</sup>, Peter Douglas<sup>3</sup> & André Pellerin<sup>1</sup>

<sup>1</sup>Institut des sciences de la mer, Université du Québec à Rimouski, Rimouski, Québec, Canada

<sup>2</sup>Geological Survey of Canada, Natural Resources Canada, Dartmouth, Nova Scotia, Canada

<sup>3</sup>Department of Earth and Planetary Sciences, McGill University, Montréal, Québec, Canada

Arctic coastal ecosystems are affected by sea level rise, erosion and land submersion, which alters sediment dynamics and organic matter (OM) fluxes along the land-ocean continuum (Tanski et al. 2021). In the Tuktoyaktuk coastlands of the North-West Territories (Canada), retreat rates exceed -4 m/yr due to ground subsidence and submersion, resulting in waterlogged environments (Costa 2022). In waterlogged conditions, the progressive thawing of permafrost exposes long-frozen OM to microbial decomposition, releasing methane (CH<sub>4</sub>) (Lapham et al. 2020). The drivers of biogenic greenhouse gas production in sediments are relatively well understood in terrestrial environments but their controls in actively changing landscapes, remain uncertain. This is particularly true in coastal environments with continuous permafrost, where high erosion rates and interaction with seawater strongly influence biogeochemistry and organic matter degradation.

In the Tuktoyaktuk coastlands, inundated tundra flats and polygons dominate the 831 km of coastline (Costa 2022). Ice-wedge polygons are interspersed with lower-lying, wet channels (throughs), underlain by peat deposits and ground ice structures (Martin 2018). Polygons can be categorized as low-centered or as high-centered. These microtopographic formations exhibit significant thermal, hydrological and geochemical gradients (Vaughn et al. 2016). Land submersion by seawater can influence geochemistry, which in turn modifies the microbial communities and organic matter degradation rates. In particular, sulfate anions that are present in seawater cause sulfate reduction to competitively inhibit methanogenesis. This research investigated the impact of seawater on organic matter degradation in this terrain and explores the feasibility of quantifying CH<sub>4</sub> production. The aim was to apply these findings at the landscape level to bridge the knowledge gap in coastal CH<sub>4</sub> biogeochemistry.

### METHODS

The study was carried out on cores collected from the active layer of an intertidal zone (Toker Point (TP), n=3) and an inland area (Reindeer Point (RP), n=4, about 750 m from coast). Basic environmental

parameters such as vegetation type, active layer depth, and waterlogged conditions were assessed in the field.

The type of vegetation present can provide insights on the type of organic carbon inputs to soil microbial communities. Both TP and RP featured polygonal terrain, with one low-centered polygon and through sampled at each site. One high-centered polygon was sampled at TP, two were sampled at RP.

Cores were subsampled at intervals of 5 to 10 cm depth, according to shifts in sedimentary units. In the field, samples from each depth were distributed to four 20 mL glass vials with blue butyl rubber stoppers and flushed with N<sub>2</sub> gas to remove oxygen. Anoxic brackish water (collected from the coast) was added to each vial to simulate saltwater input in the coastal sediments. Three vials per depth were used to account for natural variability within each sample. Vials were kept at 4 °C. To understand the variability in CH<sub>4</sub> production within each depth of each site, CH<sub>4</sub> production rates were derived from the accumulation of CH<sub>4</sub> in the headspace over time (Pellerin et al. 2022). These were then integrated over the depth of the active layer. δ<sup>13</sup>C-CH<sub>4</sub> was measured in the incubation to identify the methanogenesis pathways used by the microbial communities. Geochemical analyses of organic carbon and anions in sediments supported the incubations.

### RESULTS AND DISCUSSION

Sediments from the active layer at the coastal site (TP), produced more CH<sub>4</sub> than the inland site (RP), despite this inland site having a higher concentration in organic carbon (Table 1). It may be due to more recalcitrant organic matter at RP. This is indicated by more negative isotopic signature of <sup>13</sup>C-CH<sub>4</sub> (Figure 1), which signals a preferentially hydrogenotrophic pathway for methanogenesis, characteristic of sites with recalcitrant organic carbon (Heffernan et al. 2014). Contrarily, at TP, the coastal site, lower amounts but more labile organic matter in the sediments enhanced CH<sub>4</sub> production. More labile organic matter is indicated by less negative <sup>13</sup>C-CH<sub>4</sub> which signals a preferentially acetoclastic pathway for methanogenesis, characteristic of sites with labile organic carbon (Heffernan et al. 2014).

Table 1. Intervals of organic carbon, sulfate concentrations and CH<sub>4</sub> production rates for the active layer of the sampled landforms.

Geomorphological forms	C <sub>org</sub> (% wt.)	SO <sub>4</sub> <sup>2-</sup> (mmol L <sup>-1</sup> )	CH <sub>4</sub> (mmol m <sup>-2</sup> yr <sup>-1</sup> )
<b>Toker Point (coastal)</b>			
Low-centered polygon (n=3)	2.9 – 4.7	0.3 – 12	17 ± 3.0
Through (n=3)	2.5 – 32	0.07 – 0.8	28 ± 7.4
High-centered polygon (n=3)	30 – 37	0.09 – 3.2	41.5 ± 6.9
<b>Reindeer Point (inland)</b>			
Low-centered polygon (n=3)	37 – 46	0 – 0.1	2.4 ± 1.0
Through (n=3)	39 – 42	0.07 – 0.3	5.0 ± 2.0
High-centered polygon (n=3)	10 – 47	0.07 – 0.2	0.2 ± 0.1

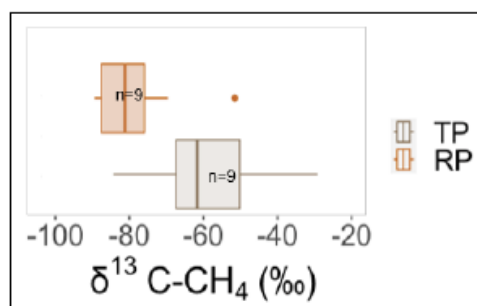


Figure 1. Active layer signature of <sup>13</sup>C-CH<sub>4</sub> produced in incubation at Toker Point (coastal) and Reindeer Point (RP).

Sites with a coastal influence thus may produce more CH<sub>4</sub> than inland sites because of more labile organic substrates. This could be due to the presence of a different flora of carex and sedges at TP, which degrade rapidly (Hobbie 1996). Alternatively, a marine input of organic matter from intermittent seawater immersion at the coastal site may also provide an unaccounted source of labile organic matter which could account for higher production rates at TP. However, stable carbon isotopic measurements of organic carbon at TP did not indicate a marine signature for bulk organic matter (data not shown).

Interestingly, CH<sub>4</sub> production did not seem inhibited by the presence of SO<sub>4</sub><sup>2-</sup> in the incubations. Samples contained a large range of SO<sub>4</sub><sup>2-</sup> concentrations (Table 1). However, brackish water with a SO<sub>4</sub><sup>2-</sup> concentration of 5.7 mmol/L was added to all incubations. High CH<sub>4</sub> production rates still occurred (Table 1). CH<sub>4</sub> production under sulfate-rich conditions may result from an imbalance in the microbial community (Adler et al. 2017) and may persist or even be enhanced in surface sediments of coastal systems despite significant interaction with seawater resulting from coastal ground subsidence and submersion.

## REFERENCES

- Costa, B. 2022. Remote Sensing Analysis of Recent Coastal Change and Controlling Factors in Tuktoyaktuk Peninsula (Beaufort Sea Coast, Canada). MSc thesis. University of Lisboa.
- Heffernan, L., Cavaco, M.A., Bhatia, M., Estop-Aragonés, C., Knorr, K-H., and Olefeldt, D. 2022. High peatland methane emissions following permafrost thaw: enhanced acetoclastic methanogenesis during early successional stages. *Biogeosciences*. 19, 3051–3071.
- Hobbie, S.E. 1996. Temperature and plant species control over litter decomposition in Alaskan tundra. *Ecological Monographs*, 66, 503–522.
- Lapham, L., Dallimore, S., Magen, C., Henderson, L., Powers, L., Gonsior, M., Clark, B., Côté, M., Fraser, P., and Orcutt, B. 2020. Microbial Greenhouse Gas Dynamics Associated With Warming Coastal Permafrost, Western Canadian Arctic. *Frontiers in Earth Science*. 8:582103.
- Pellerin, A., Lotem, N., Anthony, K., Russak, E., Hasson, N., Chanton, J., and Sivan, O. 2022. Methane production controls in a young thermokarst lake formed by abrupt permafrost thaw. *Global Change Biology*. 28(10), 3206–3221.
- Martin, A.F., Lantz, T.C., and Humphreys, E.R. 2018. Ice wedge degradation and CO<sub>2</sub> and CH<sub>4</sub> emissions in the Tuktoyaktuk Coastlands, Northwest Territories. *Arctic Science*, 4(1).
- Tanski, G., Bröder, L., Wagner, D., Knoblauch, C., Lantuit, H., Beer, C., Sachs, T., Fritz, M., Tesl, T., Koch, B., Haghpour N., Eglinton, T., Strauss, J., and Vonk, J. 2021. Permafrost Carbon and CO<sub>2</sub> Pathways Differ at Contrasting Coastal Erosion Sites in the Canadian Arctic. *Frontiers in Earth Science*. 9:630493.
- Vaughn, L.J.S., Conrad, M.E., Bill, M., and Torn, M.S. 2016. Isotopic insights into methane production, oxidation, and emissions in Arctic polygon tundra. *Global Change Biology*, 22, 3487–3502.



## RÉFÉRENCES BIBLIOGRAPHIQUES

- AMAP, 2019. AMAP Climate Change Update 2019: An Update to Key Findings of Snow, Water, Ice and Permafrost in the Arctic (SWIPA) 2017. Arctic Monitoring and Assessment Programme (AMAP), Oslo, Norway. 12 pp.
- AMAP, 2017. Snow, Water, Ice and Permafrost in the Arctic (SWIPA) 2017. Arctic Monitoring and Assessment Programme (AMAP), Oslo, Norway. xiv + 269 pp
- Andrachuk, M., & Smit, B. (2012). Community-based vulnerability assessment of Tuktoyaktuk, NWT, Canada to environmental and socio-economic changes. *Regional Environmental Change*, 12(4), 867–885. <https://doi.org/10.1007/s10113-012-0299-0>
- Are, F., Reimnitz, E., Grigoriev, M., Hubberten, H.-W., & Rachold, V. (2008). The influence of cryogenic processes on the erosional Arctic shoreface. *Journal of Coastal Research*, 24(1), 110–121. <https://doi.org/10.2112/05-0573.1>
- Bačėninaitė, D., Džermeikaitė, K., & Antanaitis, R. (2022). Global Warming and Dairy Cattle: How to Control and Reduce Methane Emission. *Animals*, 12(19), Article 19. <https://doi.org/10.3390/ani12192687>
- Baltar, F., Alvarez-Salgado, X. A., Arístegui, J., Benner, R., Hansell, D. A., Herndl, G. J., & Lønborg, C. (2021). What Is Refractory Organic Matter in the Ocean? *Frontiers in Marine Science*, 8. <https://doi.org/10.3389/fmars.2021.642637>
- Bianchi, T. S. (2011). The role of terrestrially derived organic carbon in the coastal ocean: A changing paradigm and the priming effect. *Proceedings of the National Academy of Sciences*, 108(49), 19473–19481. <https://doi.org/10.1073/pnas.1017982108>
- Black, R. F. (1982). Ice-Wedge Polygons of Northern Alaska. In D. R. Coates (Ed.), *Glacial Geomorphology* (pp. 247–275). Springer Netherlands. [https://doi.org/10.1007/978-94-011-6491-7\\_9](https://doi.org/10.1007/978-94-011-6491-7_9)
- Boetius, A., Ravenschlag, K., Schubert, C. J., Rickert, D., Widdel, F., Gieseke, A., Amann, R., Jørgensen, B. B., Witte, U., & Pfannkuche, O. (2000). A marine microbial consortium apparently mediating anaerobic oxidation of methane. *Nature*, 407(6804), 623–626. <https://doi.org/10.1038/35036572>

- Bonnaventure, P. P., & Lamoureux, S. F. (2013). The active layer: A conceptual review of monitoring, modelling techniques and changes in a warming climate. *Progress in Physical Geography: Earth and Environment*, 37(3), 352–376. <https://doi.org/10.1177/0309133313478314>
- Bueno de Mesquita, C. P., Wu, D., & Tringe, S. G. (2023). Methyl-Based Methanogenesis: An Ecological and Genomic Review. *Microbiology and Molecular Biology Reviews*, 87(1), e00024-22. <https://doi.org/10.1128/membr.00024-22>
- Burn, C. R., & Kokelj, S. V. (2009). The environment and permafrost of the Mackenzie Delta area. *Permafrost and Periglacial Processes*, 20(2), 83–105. <https://doi.org/10.1002/ppp.655>
- Campbell, A. D., Fatoyinbo, T., Charles, S. P., Bourgeau-Chavez, L. L., Goes, J., Gomes, H., Halabisky, M., Holmquist, J., Lohrenz, S., Mitchell, C., Moskal, L. M., Poulter, B., Qiu, H., Sousa, C. H. R. D., Sayers, M., Simard, M., Stewart, A. J., Singh, D., Trettin, C., ... Lagomasino, D. (2022). A review of carbon monitoring in wet carbon systems using remote sensing. *Environmental Research Letters*, 17(2), 025009. <https://doi.org/10.1088/1748-9326/ac4d4d>
- Canfield, D. E. (1993). Organic Matter Oxidation in Marine Sediments. In R. Wollast, F. T. Mackenzie, & L. Chou (Eds.), *Interactions of C, N, P and S Biogeochemical Cycles and Global Change* (pp. 333–363). Springer. [https://doi.org/10.1007/978-3-642-76064-8\\_14](https://doi.org/10.1007/978-3-642-76064-8_14)
- Comer-Warner, S. A., Ullah, S., Ampuero Reyes, W., Krause, S., & Chmura, G. L. (2022). *Spartina alterniflora* has the highest methane emissions in a St. Lawrence estuary salt marsh. *Environmental Research: Ecology*, 1(1), 011003. <https://doi.org/10.1088/2752-664X/ac706a>
- Conrad, R. (2020). Importance of hydrogenotrophic, acetoclastic and methylotrophic methanogenesis for methane production in terrestrial, aquatic and other anoxic environments: A mini review. *Pedosphere*, 30(1), 25–39. [https://doi.org/10.1016/s1002-0160\(18\)60052-9](https://doi.org/10.1016/s1002-0160(18)60052-9)
- Conrad, R. (1999). Contribution of hydrogen to methane production and control of hydrogen concentrations in methanogenic soils and sediments. *FEMS Microbiology Ecology*, 28(3), 193–202. <https://doi.org/10.1111/j.1574-6941.1999.tb00575.x>
- Coolen, M. J. L., & Orsi, W. D. (2015). The transcriptional response of microbial communities in thawing Alaskan permafrost soils. *Frontiers in Microbiology*, 6. <https://doi.org/10.3389/fmicb.2015.00197>
- Couture, N. J., Irrgang, A., Pollard, W., Lantuit, H., & Fritz, M. (2018). Coastal Erosion of Permafrost Soils Along the Yukon Coastal Plain and Fluxes of Organic Carbon to the

Canadian Beaufort Sea. *Journal of Geophysical Research: Biogeosciences*, 123(2), 406–422. <https://doi.org/10.1002/2017JG004166>

Dallimore, S. R., Wolfe, S. A., Matthews Jr., J. V., & Vincent, J.-S. (1997). Mid-Wisconsinan eolian deposits of the Kittigazuit Formation, Tuktoyaktuk Coastlands, Northwest Territories, Canada. *Canadian Journal of Earth Sciences*, 34(11), 1421–1441. <https://doi.org/10.1139/e17-116>

Duddleston, K. N., Kinney, M. A., Kiene, R. P., & Hines, M. E. (2002). Anaerobic microbial biogeochemistry in a northern bog: Acetate as a dominant metabolic end product. *Global Biogeochemical Cycles*, 16(4). <https://doi.org/10.1029/2001gb001402>

Dutta, K., Schuur, E. a. G., Neff, J. C., & Zimov, S. A. (2006). Potential carbon release from permafrost soils of Northeastern Siberia. *Global Change Biology*, 12(12), 2336–2351. <https://doi.org/10.1111/j.1365-2486.2006.01259.x>

Elberling, B., Michelsen, A., Schädel, C., Schuur, E. A. G., Christiansen, H. H., Berg, L., Tamstorf, M. P., & Sigsgaard, C. (2013). Long-term CO<sub>2</sub> production following permafrost thaw. *Nature Climate Change*, 3(10), 890–894. <https://doi.org/10.1038/nclimate1955>

Engram, M., Walter Anthony, K. M., Sachs, T., Kohnert, K., Serafimovich, A., Grosse, G., & Meyer, F. J. (2020). Remote sensing northern lake methane ebullition. *Nature Climate Change*, 10(6), 511–517. <https://doi.org/10.1038/s41558-020-0762-8>

Erkens, E., Angelopoulos, M., Tronicke, J., Dallimore, S. R., Whalen, D., Boike, J., & Overduin, P. P. (2024). *Mapping subsea permafrost around Tuktoyaktuk Island (NWT, Canada) using electrical resistivity tomography*. <https://doi.org/10.5194/egusphere-2024-1044>

Eskelinen, A., Stark, S., & Männistö, M. (2009). Links between plant community composition, soil organic matter quality and microbial communities in contrasting tundra habitats. *Oecologia*, 161(1), 113–123. <https://doi.org/10.1007/s00442-009-1362-5>

Flanagan, L. B. (2005). 1 - Introduction: Stable Isotopes and Earth System Science. In L. B. Flanagan, J. R. Ehleringer, & D. E. Pataki (Eds.), *Stable Isotopes and Biosphere Atmosphere Interactions* (pp. 1–5). Academic Press. <https://doi.org/10.1016/B978-012088447-6/50001-5>

Froelich, P., Klinkhammer, G., Bender, M., Luedtke, N., Heath, G., Cullen, D., Dauphin, P., Hammond, D., Hartman, B., & Maynard, V. (1979). Early oxidation of organic matter in pelagic sediments of the eastern equatorial Atlantic: suboxic diagenesis. *Geochimica Et Cosmochimica Acta*, 43(7), 1075–1090. [https://doi.org/10.1016/0016-7037\(79\)90095-4](https://doi.org/10.1016/0016-7037(79)90095-4)



- Fu, Q. A., Boutton, T. W., Ehleringer, J. R., & Flagler, R. B. (1993). Environmental and Developmental Effects on Carbon Isotope Discrimination by Two Species of *Phaseolus*. In *Stable Isotopes and Plant Carbon-water Relations* (pp. 297–309). Elsevier. <https://doi.org/10.1016/B978-0-08-091801-3.50028-3>
- Galand, P. E., Yrjälä, K., & Conrad, R. (2010). Stable carbon isotope fractionation during methanogenesis in three boreal peatland ecosystems. *Biogeosciences*, 7(11), 3893–3900. <https://doi.org/10.5194/bg-7-3893-2010>
- Gillespie, A. W., Sanei, H., Diochon, A., Ellert, B. H., Regier, T. Z., Chevrier, D., Dynes, J. J., Tarnocai, C., & Gregorich, E. G. (2014). Perennially and annually frozen soil carbon differ in their susceptibility to decomposition: Analysis of Subarctic earth hummocks by bioassay, XANES and pyrolysis. *Soil Biology and Biochemistry*, 68, 106–116. <https://doi.org/10.1016/j.soilbio.2013.09.021>
- Guimond, J. A., Mohammed, A. A., Walvoord, M. A., Bense, V. F., & Kurylyk, B. L. (2021). Saltwater Intrusion Intensifies Coastal Permafrost Thaw. *Geophysical Research Letters*, 48(19), e2021GL094776. <https://doi.org/10.1029/2021GL094776>
- Hansell, D. A. (2013). Recalcitrant Dissolved Organic Carbon Fractions. *Annual Review of Marine Science*, 5(1), 421–445. <https://doi.org/10.1146/annurev-marine-120710-100757>
- Hansen, J., Ruedy, R., Sato, M., & Lo, K. (2010). Global Surface Temperature Change. *Reviews of Geophysics*, 48(4). <https://doi.org/10.1029/2010RG000345>
- Hanson, R. S., & Hanson, T. E. (1996). Methanotrophic bacteria. *Microbiological Reviews*, 60(2), 439–471.
- Haugk, C., Jongejans, L. L., Mangelsdorf, K., Fuchs, M., Ogneva, O., Palmtag, J., Mollenhauer, G., Mann, P. J., Overduin, P. P., Grosse, G., Sanders, T., Tuerena, R. E., Schirrmeister, L., Wetterich, S., Kizyakov, A., Karger, C., & Strauss, J. (2022). Organic matter characteristics of a rapidly eroding permafrost cliff in NE Siberia (Lena Delta, Laptev Sea region). *Biogeosciences*, 19(7), 2079–2094. <https://doi.org/10.5194/bg-19-2079-2022>
- Heffernan, L., Cavaco, M. A., Bhatia, M. P., Estop-Aragónés, C., Knorr, K.-H., & Olefeldt, D. (2022). High peatland methane emissions following permafrost thaw: Enhanced acetoclastic methanogenesis during early successional stages. *Biogeosciences*, 19(12), 3051–3071. <https://doi.org/10.5194/bg-19-3051-2022>
- Herndon, E. M., Mann, B. F., Roy Chowdhury, T., Yang, Z., Wullschleger, S. D., Graham, D., Liang, L., & Gu, B. (2015). Pathways of anaerobic organic matter decomposition in tundra

soils from Barrow, Alaska. *Journal of Geophysical Research: Biogeosciences*, 120(11), 2345–2359. <https://doi.org/10.1002/2015JG003147>

Hershey, A. E., Northington, R. M., & Whalen, S. C. (2014). Substrate limitation of sediment methane flux, methane oxidation and use of stable isotopes for assessing methanogenesis pathways in a small arctic lake. *Biogeochemistry*, 117(2), 325–336. <https://doi.org/10.1007/s10533-013-9864-y>

Heslop, J. K., Walter Anthony, K. M., Sepulveda-Jauregui, A., Martinez-Cruz, K., Bondurant, A., Grosse, G., & Jones, M. C. (2015). Thermokarst lake methanogenesis along a complete talik profile. *Biogeosciences*, 12(14), 4317–4331. <https://doi.org/10.5194/bg-12-4317-2015>

Heslop, J. K., Walter Anthony, K. M., Winkel, M., Sepulveda-Jauregui, A., Martinez-Cruz, K., Bondurant, A., Grosse, G., & Liebner, S. (2020). A synthesis of methane dynamics in thermokarst lake environments. *Earth-Science Reviews*, 210, 103365. <https://doi.org/10.1016/j.earscirev.2020.103365>

Hesse, R., & Schacht, U. (2011). Chapter 9—Early Diagenesis of Deep-Sea Sediments. In H. HüNeke & T. Mulder (Eds.), *Developments in Sedimentology* (Vol. 63, pp. 557–713). Elsevier. <https://doi.org/10.1016/B978-0-444-53000-4.00009-3>

Heyer, J., Berger, U., Kuzin, I. L., & Yakovlev, O. N. (2002). Methane emissions from different ecosystem structures of the subarctic tundra in Western Siberia during midsummer and during the thawing period. *Tellus B*, 54(3), 231–249. <https://doi.org/10.1034/j.1600-0889.2002.01280.x>

Hill, P. R., Héquette, A., & Ruz, M.-H. (1993). Holocene sea-level history of the Canadian Beaufort shelf. *Canadian Journal of Earth Sciences*, 30(1), 103–108. <https://doi.org/10.1139/e93-009>

Hjort, J., Karjalainen, O., Aalto, J., Westermann, S., Romanovsky, V. E., Nelson, F. E., Etzelmüller, B., & Luoto, M. (2018). Degrading permafrost puts Arctic infrastructure at risk by mid-century. *Nature Communications*, 9(1), 5147. <https://doi.org/10.1038/s41467-018-07557-4>

Hobbie, S. E., & Chapin, F. S. (1996). Winter regulation of tundra litter carbon and nitrogen dynamics. *Biogeochemistry*, 35(2), 327–338. <https://doi.org/10.1007/BF02179958>

Hodgkins, S. B., Tfaily, M. M., McCalley, C. K., Logan, T. A., Crill, P. M., Saleska, S. R., Rich, V. I., & Chanton, J. P. (2014). Changes in peat chemistry associated with permafrost thaw

increase greenhouse gas production. *Proceedings of the National Academy of Sciences*, 111(16), 5819–5824. <https://doi.org/10.1073/pnas.1314641111>

Holm, S., Walz, J., Horn, F., Yang, S., Grigoriev, M. N., Wagner, D., Knoblauch, C., & Liebner, S. (2020). Methanogenic response to long-term permafrost thaw is determined by paleoenvironment. *FEMS Microbiology Ecology*, 96(3), fiae021. <https://doi.org/10.1093/femsec/fiae021>

Hornibrook, E. R. C., Longstaffe, F. J., & Fyfe, W. S. (2000). Evolution of stable carbon isotope compositions for methane and carbon dioxide in freshwater wetlands and other anaerobic environments. *Geochimica et Cosmochimica Acta*, 64(6), 1013–1027. [https://doi.org/10.1016/S0016-7037\(99\)00321-X](https://doi.org/10.1016/S0016-7037(99)00321-X)

Hornibrook, E. R., Longstaffe, F. J., & Fyfe, W. S. (1997). Spatial distribution of microbial methane production pathways in temperate zone wetland soils: Stable carbon and hydrogen isotope evidence. *Geochimica Et Cosmochimica Acta*, 61(4), 745–753. [https://doi.org/10.1016/s0016-7037\(96\)00368-7](https://doi.org/10.1016/s0016-7037(96)00368-7)

Hu, K., Issler, D., Chen, Z., & Brent, T. (2013). *Permafrost investigation by well logs, and seismic velocity and repeated shallow temperature surveys, Beaufort-Mackenzie Basin*. <https://doi.org/10.4095/293120>

Hynes, S., Solomon, S. M., & Whalen, D. (2014). *GIS compilation of coastline variability spanning 60 years in the Mackenzie Delta and Tuktoyaktuk in the Beaufort Sea* (7685; p. 7685). <https://doi.org/10.4095/295579>

Ionescu, D., Bizic-Ionescu, M., Khalili, A., Malekmohammadi, R., Morad, M. R., de Beer, D., & Grossart, H.-P. (2015). A new tool for long-term studies of POM-bacteria interactions: Overcoming the century-old Bottle Effect. *Scientific Reports*, 5(1), 14706. <https://doi.org/10.1038/srep14706>

Irrgang, A. M., Bendixen, M., Farquharson, L. M., Baranskaya, A. V., Erikson, L. H., Gibbs, A. E., Ogorodov, S. A., Overduin, P. P., Lantuit, H., Grigoriev, M. N., & Jones, B. M. (2022). Drivers, dynamics and impacts of changing Arctic coasts. *Nature Reviews Earth & Environment*, 3(1), 39–54. <https://doi.org/10.1038/s43017-021-00232-1>

Jones, B. M., Farquharson, L. M., Baughman, C. A., Buzard, R. M., Arp, C. D., Grosse, G., Bull, D. L., Günther, F., Nitze, I., Urban, F., Kasper, J. L., Frederick, J. M., Thomas, M., Jones, C., Mota, A., Dallimore, S., Tweedie, C., Maio, C., Mann, D. H., ... Romanovsky, V. E. (2018). A decade of remotely sensed observations highlight complex processes linked to

coastal permafrost bluff erosion in the Arctic. *Environmental Research Letters*, 13(11), 115001. <https://doi.org/10.1088/1748-9326/aae471>

Jones, E. L., Hodson, A. J., Thornton, S. F., Redeker, K. R., Rogers, J., Wynn, P. M., Dixon, T. J., Bottrell, S. H., & O'Neill, H. B. (2020). Biogeochemical Processes in the Active Layer and Permafrost of a High Arctic Fjord Valley. *Frontiers in Earth Science*, 8. <https://www.frontiersin.org/articles/10.3389/feart.2020.00342>

Keuschnig, C., Larose, C., Rudner, M., Pesqueda, A., Doleac, S., Elberling, B., Björk, R. G., Klemedtsson, L., & Björkman, M. P. (2022). Reduced methane emissions in former permafrost soils driven by vegetation and microbial changes following drainage. *Global Change Biology*, 28(10), 3411–3425. <https://doi.org/10.1111/gcb.16137>

Kip, N., van Winden, J. F., Pan, Y., Bodrossy, L., Reichart, G.-J., Smolders, A. J. P., Jetten, M. S. M., Damsté, J. S. S., & Op den Camp, H. J. M. (2010). Global prevalence of methane oxidation by symbiotic bacteria in peat-moss ecosystems. *Nature Geoscience*, 3(9), 617–621. <https://doi.org/10.1038/ngeo939>

Knoblauch, C., Beer, C., Liebner, S., Grigoriev, M. N., & Pfeiffer, E.-M. (2018). Methane production as key to the greenhouse gas budget of thawing permafrost. *Nature Climate Change*, 8(4), 309–312. <https://doi.org/10.1038/s41558-018-0095-z>

Knoblauch, C., Beer, C., Sosnin, A., Wagner, D., & Pfeiffer, E.-M. (2013). Predicting long-term carbon mineralization and trace gas production from thawing permafrost of Northeast Siberia. *Global Change Biology*, 19(4), 1160–1172. <https://doi.org/10.1111/gcb.12116>

Knoblauch, C., Zimmermann, U., Blumenberg, M., Michaelis, W., & Pfeiffer, E.-M. (2008). Methane turnover and temperature response of methane-oxidizing bacteria in permafrost-affected soils of northeast Siberia. *Soil Biology and Biochemistry*, 40(12), 3004–3013. <https://doi.org/10.1016/j.soilbio.2008.08.020>

Kotsyurbenko, O. R., Friedrich, M. W., Simankova, M. V., Nozhevnikova, A. N., Golyshin, P. N., Timmis, K. N., & Conrad, R. (2007). Shift from Acetoclastic to H<sub>2</sub>-Dependent Methanogenesis in a West Siberian Peat Bog at Low pH Values and Isolation of an Acidophilic Methanobacterium Strain. *Applied and Environmental Microbiology*, 73(7), 2344–2348. <https://doi.org/10.1128/AEM.02413-06>

Koven, C. D., Ringeval, B., Friedlingstein, P., Ciais, P., Cadule, P., Khvorostyanov, D., Krinner, G., & Tarnocai, C. (2011). Permafrost carbon-climate feedbacks accelerate global warming. *Proceedings of the National Academy of Sciences*, 108(36), 14769–14774. <https://doi.org/10.1073/pnas.1103910108>

- Kramshøj, M., Albers, C. N., Holst, T., Holzinger, R., Elberling, B., & Rinnan, R. (2018). Biogenic volatile release from permafrost thaw is determined by the soil microbial sink. *Nature Communications*, 9(1), 3412. <https://doi.org/10.1038/s41467-018-05824-y>
- Kuhry, P., Bárta, J., Blok, D., Elberling, B., Faucherre, S., Hugelius, G., Jørgensen, C. J., Richter, A., Šantrůčková, H., & Weiss, N. (2020). Lability classification of soil organic matter in the northern permafrost region. *Biogeosciences*, 17(2), 361–379. <https://doi.org/10.5194/bg-17-361-2020>
- La, W., Han, X., Liu, C.-Q., Ding, H., Liu, M., Sun, F., Li, S., & Lang, Y. (2022). Sulfate concentrations affect sulfate reduction pathways and methane consumption in coastal wetlands. *Water Research*, 217, 118441. <https://doi.org/10.1016/j.watres.2022.118441>
- Lacelle, D., Fontaine, M., & Kokelj, S. (2015). Geochemistry of the active layer and permafrost in northwestern Canada: From measurements to Quaternary stratigraphy. *GEOQuébec2015*.
- Lalonde, K., Mucci, A., Ouellet, A., & Gélinas, Y. (2012). Preservation of organic matter in sediments promoted by iron. *Nature*, 483(7388), 198–200. <https://doi.org/10.1038/nature10855>
- Lantuit, H., Overduin, P. P., Couture, N., Wetterich, S., Aré, F., Atkinson, D., Brown, J., Cherkashov, G., Drozdov, D., Forbes, D. L., Graves-Gaylord, A., Grigoriev, M., Hubberten, H.-W., Jordan, J., Jorgenson, T., Ødegård, R. S., Ogorodov, S., Pollard, W. H., Rachold, V., ... Vasiliev, A. (2012). The Arctic Coastal Dynamics Database: A New Classification Scheme and Statistics on Arctic Permafrost Coastlines. *Estuaries and Coasts*, 35(2), 383–400. <https://doi.org/10.1007/s12237-010-9362-6>
- Lapham, L. L., Dallimore, S. R., Magen, C., Henderson, L. C., Powers, L. C., Gonsior, M., Clark, B., Côté, M., Fraser, P., & Orcutt, B. N. (2020). Microbial Greenhouse Gas Dynamics Associated With Warming Coastal Permafrost, Western Canadian Arctic. *Frontiers in Earth Science*, 8. <https://www.frontiersin.org/articles/10.3389/feart.2020.582103>
- Leclerc, H., Gaillard, J., & Simonet, M. (1995). *Microbiologie générale: la bactérie et le monde bactérien*. Doin Editions.
- Lee, J., Yun, J., Yang, Y., Jung, J. Y., Lee, Y. K., Yuan, J., Ding, W., Freeman, C., & Kang, H. (2023). Attenuation of Methane Oxidation by Nitrogen Availability in Arctic Tundra Soils. *Environmental Science & Technology*, 57(6), 2647–2659. <https://doi.org/10.1021/acs.est.2c05228>

- Lehmann, J., & Kleber, M. (2015). The contentious nature of soil organic matter. *Nature*, 528(7580), 60–68. <https://doi.org/10.1038/nature16069>
- Li, Y., Wang, D., Chen, Z., Chen, J., Hu, H., & Wang, R. (2021). Methane Emissions during the Tide Cycle of a Yangtze Estuary Salt Marsh. *Atmosphere*, 12(2), 245. <https://doi.org/10.3390/atmos12020245>
- Liebner, S., Ganzert, L., Kiss, A., Yang, S., Wagner, D., & Svenning, M. M. (2015). Shifts in methanogenic community composition and methane fluxes along the degradation of discontinuous permafrost. *Frontiers in Microbiology*, 6. <https://doi.org/10.3389/fmicb.2015.00356>
- Lim, M., Whalen, D., Martin, J., Mann, P. J., Hayes, S., Fraser, P., Berry, H. B., & Ouellette, D. (2020). Massive Ice Control on Permafrost Coast Erosion and Sensitivity. *Geophysical Research Letters*, 47(17), e2020GL087917. <https://doi.org/10.1029/2020GL087917>
- Lipson, D. A., Zona, D., Raab, T. K., Bozzolo, F., Mauritz, M., & Oechel, W. C. (2012). Water-table height and microtopography control biogeochemical cycling in an Arctic coastal tundra ecosystem. *Biogeosciences*, 9(1), 577–591. <https://doi.org/10.5194/bg-9-577-2012>
- Lotem, N., Pellerin, A., Anthony, K. W., Gafni, A., Boyko, V., & Sivan, O. (2023). Anaerobic oxidation of methane does not attenuate methane emissions from thermokarst lakes. *Limnology and Oceanography*, 68(6), 1316–1330. <https://doi.org/10.1002/lno.12349>
- Lovley, D. R., Dwyer, D. F., & Klug, M. J. (1982). Kinetic analysis of competition between sulfate reducers and methanogens for hydrogen in sediments. *Applied and Environmental Microbiology*, 43(6), 1373–1379. <https://doi.org/10.1128/aem.43.6.1373-1379.1982>
- Lovley, D. R., & Klug, M. J. (1983). Sulfate reducers can outcompete methanogens at freshwater sulfate concentrations. *Applied and Environmental Microbiology*, 45(1), 187–192. <https://doi.org/10.1128/aem.45.1.187-192.1983>
- MacDougall, A. H., Avis, C. A., & Weaver, A. J. (2012). Significant contribution to climate warming from the permafrost carbon feedback. *Nature Geoscience*, 5(10), 719–721. <https://doi.org/10.1038/ngeo1573>
- Mackay, J. R., & Dallimore, S. R. (1992). Massive ice of the Tuktoyaktuk area, western Arctic coast, Canada. *Canadian Journal of Earth Sciences*, 29(6), 1235–1249. <https://doi.org/10.1139/e92-099>
- Maltby, J., Steinle, L., Löscher, C. R., Bange, H. W., Fischer, M. A., Schmidt, M., & Treude, T. (2018). Microbial methanogenesis in the sulfate-reducing zone of sediments in the

- Eckernförde Bay, SW Baltic Sea. *Biogeosciences*, 15(1), 137–157. <https://doi.org/10.5194/bg-15-137-2018>
- Martin, A. F., Lantz, T. C., & Humphreys, E. R. (2018). Ice wedge degradation and CO<sub>2</sub> and CH<sub>4</sub> emissions in the Tuktoyaktuk Coastlands, Northwest Territories. *Arctic Science*, 4(1), 130–145. <https://doi.org/10.1139/as-2016-0011>
- Manson, G. K., Couture, N. J., & James, T. S. (2019). *CanCoast 2.0: Data and indices to describe the sensitivity of Canada's marine coasts to changing climate* (8551; p. 8551). <https://doi.org/10.4095/314669>
- Margesin, R. (2008). Global Warming and Carbon Dynamics in Permafrost Soils: Methane Production and Oxidation. In: <https://www.semanticscholar.org/paper/Global-Warming-and-Carbon-Dynamics-in-Permafrost-%3A-Margesin/f9a0395ed1455a0806a1acacec9f6c19df5b4a6a>
- Mehra, O. P., & Jackson, M. L. (1958). Iron Oxide Removal from Soils and Clays by a Dithionite-Citrate System Buffered with Sodium Bicarbonate. *Clays and Clay Minerals (National Conference on Clays and Clay Minerals)*, 7, 317–327. <https://doi.org/10.1346/CCMN.1958.0070122>
- Miner, K. R., Turetsky, M. R., Malina, E., Bartsch, A., Tamminen, J., McGuire, A. D., Fix, A., Sweeney, C., Elder, C. D., & Miller, C. E. (2022). Permafrost carbon emissions in a changing Arctic. *Nature Reviews Earth & Environment*, 3(1), 55–67. <https://doi.org/10.1038/s43017-021-00230-3>
- Mishra, U., Hugelius, G., Shelef, E., Yang, Y., Strauss, J., Lupachev, A., Harden, J. W., Jastrow, J. D., Ping, C.-L., Riley, W. J., Schuur, E. A. G., Matamala, R., Siewert, M., Nave, L. E., Koven, C. D., Fuchs, M., Palmtag, J., Kuhry, P., Treat, C. C., ... Orr, A. (2021). Spatial heterogeneity and environmental predictors of permafrost region soil organic carbon stocks. *Science Advances*, 7(9), eaaz5236. <https://doi.org/10.1126/sciadv.aaz5236>
- Mu, C. C., Zhang, T. J., Zhao, Q., Guo, H., Zhong, W., Su, H., & Wu, Q. B. (2016). Soil organic carbon stabilization by iron in permafrost regions of the Qinghai-Tibet Plateau. *Geophysical Research Letters*, 43(19), 10,286–10,294. <https://doi.org/10.1002/2016GL070071>
- Mueller, C. W., Rethemeyer, J., Kao-Kniffin, J., Löppmann, S., Hinkel, K. M., & G. Bockheim, J. (2015). Large amounts of labile organic carbon in permafrost soils of northern Alaska. *Global Change Biology*, 21(7), 2804–2817. <https://doi.org/10.1111/gcb.12876>

- Oh, Y., Zhuang, Q., Liu, L., Welp, L. R., Lau, M. C. Y., Onstott, T. C., Medvigy, D., Bruhwiler, L., Dlugokencky, E. J., Hugelius, G., D'Imperio, L., & Elberling, B. (2020). Reduced net methane emissions due to microbial methane oxidation in a warmer Arctic. *Nature Climate Change*, *10*(4), 317–321. <https://doi.org/10.1038/s41558-020-0734-z>
- Olefeldt, D., Turetsky, M. R., Crill, P. M., & McGuire, A. D. (2013). Environmental and physical controls on northern terrestrial methane emissions across permafrost zones. *Global Change Biology*, *19*(2), 589–603. <https://doi.org/10.1111/gcb.12071>
- O'Neill, H. B., Smith, S. L., Burn, C. R., Duchesne, C., & Zhang, Y. (2023). Widespread permafrost degradation and thaw subsidence in northwest Canada. *Journal of Geophysical Research Earth Surface*, *128*(8). <https://doi.org/10.1029/2023jf007262>
- Oremland, R. S., & Polcin, S. (1982). Methanogenesis and Sulfate Reduction: Competitive and Noncompetitive Substrates in Estuarine Sediments. *Applied and Environmental Microbiology*, *44*(6), 1270–1276. <https://doi.org/10.1128/aem.44.6.1270-1276.1982>
- Ozuolmez, D., Na, H., Lever, M. A., Kjeldsen, K. U., Jørgensen, B. B., & Plugge, C. M. (2015). Methanogenic archaea and sulfate reducing bacteria co-cultured on acetate: Teamwork or coexistence? *Frontiers in Microbiology*, *6*, 492. <https://doi.org/10.3389/fmicb.2015.00492>
- Patzner, M. S., Mueller, C. W., Malusova, M., Baur, M., Nikeleit, V., Scholten, T., Hoeschen, C., Byrne, J. M., Borch, T., Kappler, A., & Bryce, C. (2020). Iron mineral dissolution releases iron and associated organic carbon during permafrost thaw. *Nature Communications*, *11*(1), 6329. <https://doi.org/10.1038/s41467-020-20102-6>
- Pellerin, A., Lotem, N., Walter Anthony, K., Eliani Russak, E., Hasson, N., Røy, H., Chanton, J. P., & Sivan, O. (2022). Methane production controls in a young thermokarst lake formed by abrupt permafrost thaw. *Global Change Biology*, *28*(10), 3206–3221. <https://doi.org/10.1111/gcb.16151>
- Penger, J., Conrad, R., & Blaser, M. (2012). Stable Carbon Isotope Fractionation by Methylophilic Methanogenic Archaea. *Applied and Environmental Microbiology*, *78*(21), 7596–7602. <https://doi.org/10.1128/AEM.01773-12>
- Ping, C. L., Jastrow, J. D., Jorgenson, M. T., Michaelson, G. J., & Shur, Y. L. (2015). Permafrost soils and carbon cycling. *SOIL*, *1*(1), 147–171. <https://doi.org/10.5194/soil-1-147-2015>
- Poffenbarger, H. J., Needelman, B. A., & Megonigal, J. P. (2011). Salinity Influence on Methane Emissions from Tidal Marshes. *Wetlands*, *31*(5), 831–842. <https://doi.org/10.1007/s13157-011-0197-0>



- Prater, J. L., Chanton, J. P., & Whiting, G. J. (2007). Variation in methane production pathways associated with permafrost decomposition in collapse scar bogs of Alberta, Canada. *Global Biogeochemical Cycles*, 21(4). <https://doi.org/10.1029/2006GB002866>
- Rampton, V. N. (1988). *Quaternary geology of the Tuktoyaktuk coastlands, Northwest Territories*. <https://www.osti.gov/etdeweb/biblio/6877609>
- Rantanen, M., Karpechko, A. Y., Lipponen, A., Nordling, K., Hyvärinen, O., Ruosteenoja, K., Vihma, T., & Laaksonen, A. (2022). The Arctic has warmed nearly four times faster than the globe since 1979. *Communications Earth & Environment*, 3(1), 1–10. <https://doi.org/10.1038/s43247-022-00498-3>
- Rosentreter, J. A., Maher, D. T., Erler, D. V., Murray, R. H., & Eyre, B. D. (2018). Methane emissions partially offset “blue carbon” burial in mangroves. *Science Advances*, 4(6). <https://doi.org/10.1126/sciadv.aao4985>
- Roy Chowdhury, T., Herndon, E. M., Phelps, T. J., Elias, D. A., Gu, B., Liang, L., Wullschleger, S. D., & Graham, D. E. (2015). Stoichiometry and temperature sensitivity of methanogenesis and CO<sub>2</sub> production from saturated polygonal tundra in Barrow, Alaska. *Global Change Biology*, 21(2), 722–737. <https://doi.org/10.1111/gcb.12762>
- Sanei, H., Stasiuk, L. D., & Goodarzi, F. (2005). Petrological changes occurring in organic matter from Recent lacustrine sediments during thermal alteration by Rock-Eval pyrolysis. *Organic Geochemistry*, 36(8), 1190–1203. <https://doi.org/10.1016/j.orggeochem.2005.02.009>
- Schuur, E. A. G., Abbott, B. W., Commane, R., Ernakovich, J., Euskirchen, E., Hugelius, G., Grosse, G., Jones, M., Koven, C., Leshyk, V., Lawrence, D., Loranty, M. M., Mauritz, M., Olefeldt, D., Natali, S., Rodenhizer, H., Salmon, V., Schädel, C., Strauss, J., ... Turetsky, M. (2022). Permafrost and Climate Change: Carbon Cycle Feedbacks From the Warming Arctic. *Annual Review of Environment and Resources*, 47(1), 343–371. <https://doi.org/10.1146/annurev-environ-012220-011847>
- Schuur, E. a. G., McGuire, A. D., Schädel, C., Grosse, G., Harden, J. W., Hayes, D. J., Hugelius, G., Koven, C. D., Kuhry, P., Lawrence, D. M., Natali, S. M., Olefeldt, D., Romanovsky, V. E., Schaefer, K., Turetsky, M. R., Treat, C. C., & Vonk, J. E. (2015). Climate change and the permafrost carbon feedback. *Nature*, 520(7546), 171–179. <https://doi.org/10.1038/nature14338>
- Schuur, E. A. G., Bockheim, J., Canadell, J. G., Euskirchen, E., Field, C. B., Goryachkin, S. V., Hagemann, S., Kuhry, P., Lafleur, P. M., Lee, H., Mazhitova, G., Nelson, F. E., Rinke, A., Romanovsky, V. E., Shiklomanov, N., Tarnocai, C., Venevsky, S., Vogel, J. G., & Zimov,

- S. A. (2008). Vulnerability of Permafrost Carbon to Climate Change: Implications for the Global Carbon Cycle. *BioScience*, 58(8), 701–714. <https://doi.org/10.1641/B580807>
- Segarra, K. E., Comerford, C., Slaughter, J., & Joye, S. B. (2013). Impact of electron acceptor availability on the anaerobic oxidation of methane in coastal freshwater and brackish wetland sediments. *Geochimica Et Cosmochimica Acta*, 115, 15–30. <https://doi.org/10.1016/j.gca.2013.03.029>
- Segulveda-Jauregui, A., Anthony, K. M. W., Martinez-Cruz, K., Martinez-Cruz, K., Greene, S., Thalasso, F., & Thalasso, F. (2015). Methane and carbon dioxide emissions from 40 lakes along a north–south latitudinal transect in Alaska. *Biogeosciences*, 12(11), 3197–3223. <https://doi.org/10.5194/bg-12-3197-2015>
- Seidel, M., Graue, J., Engelen, B., Köster, J., Sass, H., & Rullkötter, J. (2012). Advection and diffusion determine vertical distribution of microbial communities in intertidal sediments as revealed by combined biogeochemical and molecular biological analysis. *Organic Geochemistry*, 52, 114–129. <https://doi.org/10.1016/j.orggeochem.2012.08.015>
- Sela-Adler, M., Ronen, Z., Herut, B., Antler, G., Vigderovich, H., Eckert, W., & Sivan, O. (2017). Co-existence of Methanogenesis and Sulfate Reduction with Common Substrates in Sulfate-Rich Estuarine Sediments. *Frontiers in Microbiology*, 8. <https://www.frontiersin.org/articles/10.3389/fmicb.2017.00766>
- Sherr, E., Sherr, B., & Sigmon, C. (1999). Activity of marine bacteria under incubated and in situ conditions. *Aquatic Microbial Ecology*, 20, 213–223. <https://doi.org/10.3354/ame020213>
- Skoog, Douglas A., West, Donald M., Holler, F. James, Crouch, Stanley R.. (2014). *Fundamentals of Analytical Chemistry* (Ed. 9th). Singapore: Cengage Learning.
- Steedman, A. E., Lantz, T. C., & Kokelj, S. V. (2017). Spatio-Temporal Variation in High-Centre Polygons and Ice-Wedge Melt Ponds, Tuktoyaktuk Coastlands, Northwest Territories. *Permafrost and Periglacial Processes*, 28(1), 66–78. <https://doi.org/10.1002/ppp.1880>
- Steinsdóttir, H. G. R., Schaubberger, C., Mhatre, S., Thamdrup, B., & Bristow, L. A. (2022). Aerobic and anaerobic methane oxidation in a seasonally anoxic basin. *Limnology and Oceanography*, 67(6), 1257–1273. <https://doi.org/10.1002/lno.12074>
- Ström, L., Ekberg, A., Mastepanov, M., & Røjle Christensen, T. (2003). The effect of vascular plants on carbon turnover and methane emissions from a tundra wetland. *Global Change Biology*, 9(8), 1185–1192. <https://doi.org/10.1046/j.1365-2486.2003.00655.x>

- Szajdak, L. W., Meysner, T., Inisheva, L. I., Lapshina, E., Szczepański, M., & Gaca, W. (2019). Dynamics of organic matter and mineral components in Sphagnum- and Carex-dominated organic soils. *Mires and Peat*, 24, 1–15. <https://doi.org/10.19189/MaP.2019.BG.StA.1754>
- Tanski, G., Bröder, L., Wagner, D., Knoblauch, C., Lantuit, H., Beer, C., Sachs, T., Fritz, M., Tesi, T., Koch, B. P., Haghypour, N., Eglinton, T. I., Strauss, J., & Vonk, J. E. (2021). Permafrost Carbon and CO<sub>2</sub> Pathways Differ at Contrasting Coastal Erosion Sites in the Canadian Arctic. *Frontiers in Earth Science*, 9. <https://www.frontiersin.org/articles/10.3389/feart.2021.630493>
- Treat, C. C., Natali, S. M., Ernakovich, J., Iversen, C. M., Lupascu, M., McGuire, A. D., Norby, R. J., Roy Chowdhury, T., Richter, A., Šantrůčková, H., Schädel, C., Schuur, E. A. G., Sloan, V. L., Turetsky, M. R., & Waldrop, M. P. (2015). A pan-Arctic synthesis of CH<sub>4</sub> and CO<sub>2</sub> production from anoxic soil incubations. *Global Change Biology*, 21(7), 2787–2803. <https://doi.org/10.1111/gcb.12875>
- Treat, C. C., Wollheim, W. M., Varner, R. K., Grandy, A. S., Talbot, J., & Frohling, S. (2014). Temperature and peat type control CO<sub>2</sub> and CH<sub>4</sub> production in Alaskan permafrost peats. *Global Change Biology*, 20(8), 2674–2686. <https://doi.org/10.1111/gcb.12572>
- Turetsky, M. R., Treat, C. C., Waldrop, M. P., Waddington, J. M., Harden, J. W., & McGuire, A. D. (2008). Short-term response of methane fluxes and methanogen activity to water table and soil warming manipulations in an Alaskan peatland. *Journal of Geophysical Research: Biogeosciences*, 113(G3). <https://doi.org/10.1029/2007JG000496>
- Valdemarsen, T. B., & Kristensen, E. (2010). Degradation of dissolved organic monomers and short-chain fatty acids in sandy marine sediment by fermentation and sulfate reduction. *Geochimica Et Cosmochimica Acta*, 74(5), 1593–1605. <https://doi.org/10.1016/j.gca.2009.12.009>
- van Bodegom, P. M., Scholten, J. C. M., & Stams, A. J. M. (2004). Direct inhibition of methanogenesis by ferric iron. *FEMS Microbiology Ecology*, 49(2), 261–268. <https://doi.org/10.1016/j.femsec.2004.03.017>
- Van Huissteden, J. (2020). *Thawing Permafrost: Permafrost Carbon in a Warming Arctic*. Springer International Publishing. <https://doi.org/10.1007/978-3-030-31379-1>
- Vardy, S. R., Warner, B. G., & Aravena, R. (1997). Holocene Climate Effects on the Development of a Peatland on the Tuktoyaktuk Peninsula, Northwest Territories. *Quaternary Research*, 47(1), 90–104. <https://doi.org/10.1006/qres.1996.1869>

- Vaughn, L. J. S., Conrad, M. E., Bill, M., & Torn, M. S. (2016). Isotopic insights into methane production, oxidation, and emissions in Arctic polygon tundra. *Global Change Biology*, 22(10), 3487–3502. <https://doi.org/10.1111/gcb.13281>
- Vigderovich, H., Eckert, W., Elul, M., Rubin-Blum, M., Elvert, M., & Sivan, O. (2022). Long-term incubations provide insight into the mechanisms of anaerobic oxidation of methane in methanogenic lake sediments. *Biogeosciences*, 19(8), 2313–2331. <https://doi.org/10.5194/bg-19-2313-2022>
- Walter Anthony, K., Schneider von Deimling, T., Nitze, I., Frolking, S., Emond, A., Daanen, R., Anthony, P., Lindgren, P., Jones, B., & Grosse, G. (2018). 21st-century modeled permafrost carbon emissions accelerated by abrupt thaw beneath lakes. *Nature Communications*, 9(1), 3262. <https://doi.org/10.1038/s41467-018-05738-9>
- Walter, K. M., Zimov, S. A., Chanton, J. P., Verbyla, D., & Chapin, F. S. (2006). Methane bubbling from Siberian thaw lakes as a positive feedback to climate warming. *Nature*, 443(7107), 71–75. <https://doi.org/10.1038/nature05040>
- Walz, J., Knoblauch, C., Böhme, L., & Pfeiffer, E.-M. (2017). Regulation of soil organic matter decomposition in permafrost-affected Siberian tundra soils—Impact of oxygen availability, freezing and thawing, temperature, and labile organic matter. *Soil Biology and Biochemistry*, 110, 34–43. <https://doi.org/10.1016/j.soilbio.2017.03.001>
- Whalen, D., Forbes, D. L., Kostylev, V., Lim, M., Fraser, P., Nedimović, M. R., & Stuckey, S. (2022). Mechanisms, volumetric assessment, and prognosis for rapid coastal erosion of Tuktoyaktuk Island, an important natural barrier for the harbour and community. *Canadian Journal of Earth Sciences*, 59(11), 945–960. <https://doi.org/10.1139/cjes-2021-0101>
- Whelan, T. (1974). Methane, carbon dioxide and dissolved sulfate from interstitial water of coastal marsh sediments. *Estuarine and Coastal Marine Science*, 2(4), 407–415. [https://doi.org/10.1016/0302-3524\(74\)90008-5](https://doi.org/10.1016/0302-3524(74)90008-5)
- Whiticar, M. J., Faber, E., & Schoell, M. (1986). Biogenic methane formation in marine and freshwater environments: CO<sub>2</sub> reduction vs. acetate fermentation—Isotope evidence. *Geochimica et Cosmochimica Acta*, 50(5), 693–709. [https://doi.org/10.1016/0016-7037\(86\)90346-7](https://doi.org/10.1016/0016-7037(86)90346-7)
- Winfrey, M. R., & Ward, D. M. (1983). Substrates for Sulfate Reduction and Methane Production in Intertidal Sediments. *Applied and Environmental Microbiology*, 45(1), 193–199. <https://doi.org/10.1128/aem.45.1.193-199.1983>

- Winkel, M., Sepulveda-Jauregui, A., Martinez-Cruz, K., Heslop, J. K., Rijkers, R., Horn, F., Liebner, S., & Walter Anthony, K. M. (2019). First evidence for cold-adapted anaerobic oxidation of methane in deep sediments of thermokarst lakes. *Environmental Research Communications*, 1(2), 021002. <https://doi.org/10.1088/2515-7620/ab1042>
- Ye, R., Keller, J. K., Jin, Q., Bohannon, B. J., & Bridgman, S. D. (2016). Peatland types influence the inhibitory effects of a humic substance analog on methane production. *Geoderma*, 265, 131–140. <https://doi.org/10.1016/j.geoderma.2015.11.026>
- Yuan, J., Liu, D., Ji, Y., Xiang, J., Lin, Y., Wu, M., & Ding, W. (2019). *Spartina alterniflora* invasion drastically increases methane production potential by shifting methanogenesis from hydrogenotrophic to methylotrophic pathway in a coastal marsh. *Journal of Ecology*, 107(5), 2436–2450. <https://doi.org/10.1111/1365-2745.13164>
- Zheng, J., RoyChowdhury, T., Yang, Z., Gu, B., Wullschleger, S. D., & Graham, D. E. (2018). Impacts of temperature and soil characteristics on methane production and oxidation in Arctic tundra. *Biogeosciences*, 15(21), 6621–6635. <https://doi.org/10.5194/bg-15-6621-2018>
- Zimov, S. A., Davydov, S. P., Zimova, G. M., Davydova, A. I., Schuur, E. a. G., Dutta, K., & Chapin, F. S. (2006). Permafrost carbon: Stock and decomposability of a globally significant carbon pool. *Geophysical Research Letters*, 33(20). <https://doi.org/10.1029/2006gl027484>